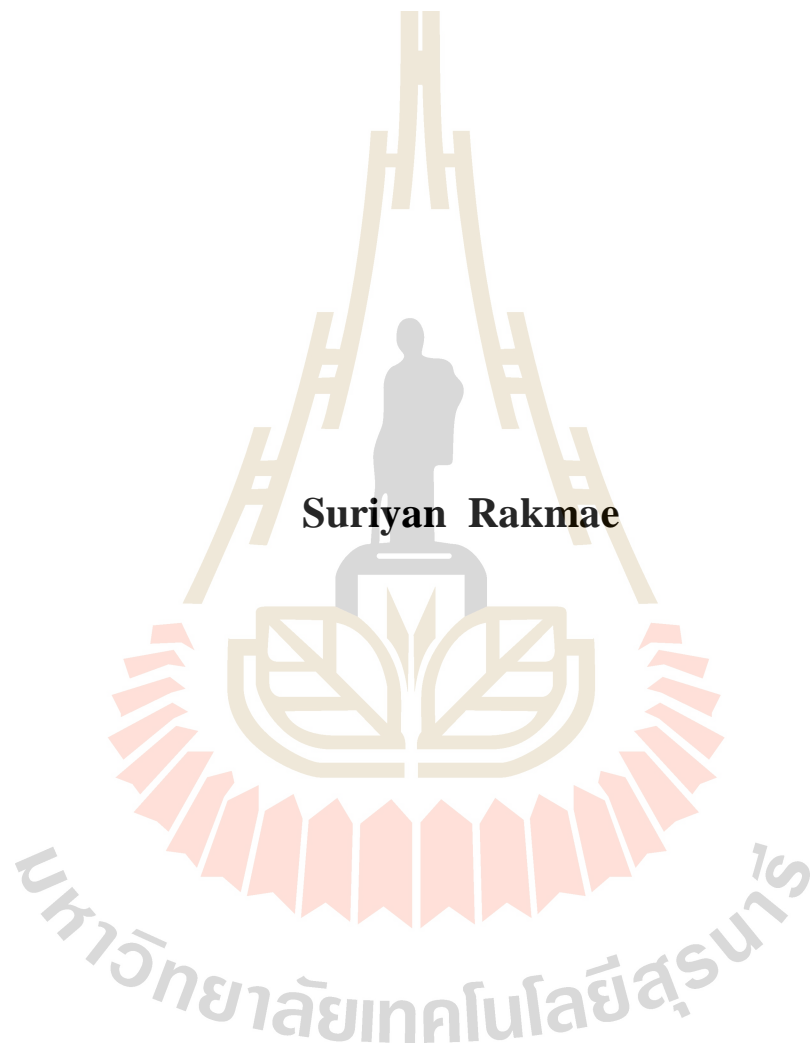# THE STUDY OF USING NATURAL HYDROXYAPATITE

AS A FILLER FOR POLY(LACTIC ACID) COMPOSITES

Suriyan Rakmae

A Thesis Submitted in Partial Fulfillment of Requirements for the

Degree of Master of Engineering in Polymer Engineering

Suranaree University of Technology

Academic year 2009

การศึกษาการใช้ไฮดรอกซีอะปาไทต์ธรรมชาติเพื่อเป็นสารตัวเติม
ในพอลิแลกติกแอซิดคอมโพสิท

สุริยัน รักแม่

THE STUDY OF USING NATURAL HYDROXYAPATITE AS
A FILLER FOR POLY(LACTIC ACID) COMPOSITES

Suranaree University of Technology has approved this thesis submitted in partial fulfillments of the requirement for a Master's Degree.

Thesis Examining Committee

_____
(Asst. Prof. Dr. Utai Meekum)

Chairperson

_____
(Asst. Prof. Dr. Nitinat Suppakarn)

Member (Thesis Advisor)

_____
(Asst. Prof. Dr. Wimonlak Sutapun)

Member

_____
(Asst. Prof. Dr. Yupaporn Ruksakulpiwat)

Member

_____
(Assoc. Prof. Dr. Jatuporn Wittayakun)

Member

_____
(Asst. Prof. Dr. Visit Vao-soongnern)

Member

_____
(Asst. Prof. Dr. Sirirat T. Rattanachan)

Member

_____
(Prof. Dr. Sukit Limpijumnong)

Vice Rector for Academic Affairs

_____
(Assoc. Prof. Dr. Vorapot Khompis)

Dean of Institute of Engineering

สุริยัน รักแม่ : การศึกษาการใช้ไฮดรอกซีอะปาไทต์ธรรมชาติเพื่อเป็นสารตัวเติมใน
พอลิแลกติกแอซิดคอมโพสิท (THE STUDY OF USING NATURAL
HYDROXYAPATITE AS A FILLER FOR POLY(LACTIC ACID) COMPOSITES)
อาจารย์ที่ปรึกษา : ผู้ช่วยศาสตราจารย์ ดร.นิธินาถ ศุภกาญจน์, 139 หน้า.

วิทยานิพนธ์นี้ศึกษาความเป็นไปได้ในการนำไฮดรอกซีอะปาไทต์ธรรมชาติมาใช้เป็นสาร
ตัวเติมในพอลิแลกติกแอซิดคอมโพสิท โดยไฮดรอกซีอะปาไทต์ธรรมชาติที่ใช้ในงานวิจัยนี้ได้มา
จากกระดูกวัวที่ผ่านการเผาและบด เมื่อนำผงกระดูกที่ได้มาวิเคราะห์ทางสัณฐานวิทยาด้วยกล้อง
จุลทรรศน์อิเล็กตรอนแบบส่องกราด (SEM) วิเคราะห์สารประกอบและความเป็นผลึกด้วยเครื่องวัด
การเลี้ยวเบนของรังสีเอกซ์ (XRD)   และวิเคราะห์หมู่ฟังก์ชันเครื่องอินฟราเรดสเปกโตรสโคปี
(FTIR) แล้วพบว่าผงกระดูกวัวที่ผ่านการเผาแล้วจะได้ผลึกของไฮดรอกซีอะปาไทต์ที่มีหมู่
คาร์บอเนตเป็นส่วนประกอบและเกาะกลุ่มกันแน่น
พอลิเมอร์คอมโพสิทระหว่างพอลิแลกติกแอซิดกับผงไฮดรอกซีอะปาไทต์ถูกเตรียมขึ้นโดย
วิธีผสมที่ต่างกันสองวิธีเพื่อเลือกวิธีการผสมที่ดีที่สุดในการผลิตชิ้นงานพอลิแลกติกแอซิด
คอมโพสิท ซึ่งวิธีแรกคือการใช้สารละลายคลอโรฟอร์มละลายพอลิแลกติกแอซิดก่อนที่จะผสมผง
ไฮดรอกซีอะปาไทต์ลงไป (solution-mixing technique) และวิธีที่สองคือการใช้ความร้อนเพื่อหลอม
พอลิแลกติกแอซิดก่อนที่จะผสมผงไฮดรอกซีอะปาไทต์ลงไป (melt-mixing technique) ซึ่งจากผล
การตรวจสอบสมบัติทางกลและสมบัติทางความร้อนของพอลิแลกติกแอซิดคอมโพสิทที่เตรียมจาก
กระบวนการผสมทั้งสองแบบ แสดงให้เห็นว่าคอมโพสิทที่ผ่านกระบวนการผสมแบบหลอมจะมี
การกระจายตัวของผงไฮดรอกซีอะปาไทต์ สมบัติทางกล และอุณหภูมิการสลายตัวที่สูงกว่า
กระบวนการผสมโดยใช้ตัวทำละลายคลอโรฟอร์ม ดังนั้นในการวิจัยนี้จึงเลือกวิธีการผสมแบบที่ใช้
ความร้อนเพื่อหลอมพอลิแลกติกแอซิดก่อนที่จะผสมผงไฮดรอกซีอะปาไทต์ลงไปเพื่อใช้ในการ
เตรียมคอมโพสิท แต่อย่างไรก็ตามคอมโพสิทที่ผ่านการผสมด้วยวิธีการผสมแบบนี้ยังคงมีสมบัติ
บางประการที่จำเป็นต้องได้รับการปรับปรุงให้ดีขึ้นคือความเข้ากันได้ระหว่างไฮดรอกซีอะปาไทต์
กับพอลิแลกติกแอซิดรวมถึงการสลายตัวของของพอลิแลกติกแอซิดที่เกิดขึ้นระหว่างการเตรียม
คอมโพสิท
การปรับปรุงพื้นผิวของไฮดรอกซีอะปาไทต์เพื่อเพิ่มความเข้ากันได้ระหว่างไฮดรอกซี
อะปาไทต์กับพอลิแลกติกแอซิดทำโดยการใช้สารคู่ควบไซเลน (silane coupling agents) 2 ชนิด คือ
3-อะมิโนโพรพิลไตรเอทอกซีไซเลน (3-aminopropyltriethoxysilane (APES)) และ 3-เมทาครีลอกซี
โพรพิลไตรเมทอกซีไซเลน (3-methacryloxypropyltrimethoxysilane (MPTS)) หลังจากปรับปรุง

พื้นผิวของไฮดรอกซีอะปาไทต์ด้วยสารคู่ควบไซเลนและนำมาตรวจสอบด้วยเครื่อง FTIR และเครื่องเอกซ์เรย์ฟลูออเรสเซนต์แบบกระจายพลังงาน (EDXRF) พบว่ามีสารคู่ควบไซเลนถูกดูดซับอยู่บนผิวของไฮดรอกซีอะปาไทต์ นอกจากนั้นยังพบว่ากลุ่มของไฮดรอกซีอะปาไทต์ที่ผ่านการปรับปรุงพื้นผิวแล้วมีขนาดลดลง ผลการศึกษาทางสัณฐานวิทยาหลังนำไฮดรอกซีอะปาไทต์ที่ผ่านการปรับปรุงพื้นผิวแล้วมาผสมกับพอลิแลกติกแอซิด พบว่าพื้นผิวของไฮดรอกซีอะปาไทต์สามารถเข้ากันได้ดีขึ้นกับเนื้อของพอลิแลกติกแอซิด รวมทั้งมีการกระจายตัวของไฮดรอกซีอะปาไทต์ในเนื้อของพอลิแลกติกแอซิดที่ดีขึ้น ด้วยเหตุนี้สมบัติทางกลและอุณหภูมิในการสลายตัวของคอมโพสิทจึงมีค่าสูงขึ้น นอกจากนี้เมื่อทดสอบด้วยเครื่องโครมาโทรกราฟีแบบเจลเลือกผ่าน (GPC) ยังพบว่าการปรับปรุงพื้นผิวของไฮดรอกซีอะปาไทต์ด้วยสารคู่ควบไซเลนสามารถลดการสลายตัวของโมเลกุลพอลิแลกติกแอซิดระหว่างเตรียมคอมโพสิทได้ด้วย

การศึกษาการสลายตัวของพอลิแลกติกแอซิดคอมโพสิทในสภาพแวดล้อมจำลอง โดยการแช่คอมโพสิทในสารละลายบัฟเฟอร์ของฟอสเฟต พบว่าคอมโพสิทที่ผสมด้วยไฮดรอกซีอะปาไทต์ที่ผ่านการปรับปรุงพื้นผิวมีการเปลี่ยนแปลงของความเป็นกรด-ด่างของสารละลายบัฟเฟอร์ของฟอสเฟตในระหว่างการแช่ ขนาดและสัณฐานวิทยาของชิ้นทดสอบ รวมทั้งโมเลกุลของพอลิแลกติกแอซิดน้อยกว่าคอมโพสิทที่ผสมด้วยไฮดรอกซีอะปาไทต์ที่ไม่ผ่านการปรับปรุงพื้นผิว โดยเป็นผลมาจากการยึดเหนี่ยวระหว่างไฮดรอกซีอะปาไทต์และเนื้อพอลิแลกติกแอซิดที่ดีขึ้นทำให้สารละลายบัฟเฟอร์ของฟอสเฟตมีโอกาสที่จะซึมเข้าไปในเนื้อของคอมโพสิทน้อยได้ลดลง ส่งผลให้สายโซ่ของพอลิแลกติกแอซิดเกิดการสลายตัวลดลง โดยสามารถทดสอบได้ด้วยเครื่อง GPC นอกจากการทดสอบการสลายตัวแล้วการศึกษาความไวทางชีวภาพ (Bioactivity) ของคอมโพสิทในสารละลายเทียมของร่างกายมนุษย์ (simulated body fluid (SBF)) ยังแสดงให้เห็นว่าการใช้ไฮดรอกซีอะปาไทต์จากกระดูกวัวสามารถเหนี่ยวนำให้เกิดการตกตะกอนของแคลเซียมฟอตเฟตบนคอมโพสิทได้และมีจำนวนมากขึ้นตามระยะเวลาในการแช่ อีกทั้งเมื่อทดสอบความเป็นพิษของสารละลายที่สกัดจากคอมโพสิทกับเซลล์กระดูกของมนุษย์ ผลที่ได้ชี้ให้เห็นว่าสารสกัดจากคอมโพสิทที่ได้ไม่มีความเป็นพิษต่อเซลล์กระดูกของมนุษย์ ณ สภาวะการทดลองที่กำหนด

สาขาวิชา วิศวกรรมพอลิเมอร์   ลายมือชื่อนักศึกษา _____

ปีการศึกษา 2552   ลายมือชื่ออาจารย์ที่ปรึกษา_____

                             ลายมือชื่ออาจารย์ที่ปรึกษาร่วม_____

                             ลายมือชื่ออาจารย์ที่ปรึกษาร่วม_____

SURIYAN RAKMAE : THE STUDY OF USING NATURAL

HYDROXYAPATITE AS A FILLER FOR POLY(LACTIC ACID)

COMPOSITES. THESIS ADVISOR : ASST. PROF. NITINAT

SUPPAKARN, Ph.D., 139 PP.

POLY(LACTIC ACID)/ HYDROXYAPATITE/ COMPOSITE/ SILANE
COUPLING AGENT/ BOVINE BONE

In this thesis, hydroxyapatite (HA) powder was produced from bovine bones in order to use as a filler for poly(lactic acid) (PLA) composites. Scanning electron microscope (SEM), X-ray diffractometer (XRD) and Fourier transform infrared spectrometer (FTIR) were used to characterize the obtained powder. SEM micrographs, XRD pattern, and FTIR spectrum of calcined bovine bone powder revealed that the obtained powder was in a form of crystalline carbonated HA, and highly agglomerated. So, the calcined bovine bone powder was called u-HA in this study. u-HA/PLA composites at various contents of HA where prepared by either melt-mixing or solution-mixing techniques. The u-HA/PLA composites prepared by melt-mixing exhibited the more homogeneous distribution of u-HA in PLA matrix as compared with the composites prepared by solution-mixing technique. In comparison, tensile modulus, tensile strength, and impact strength of the melt-mixed composites were higher than those of the solution-mixed composites. Moreover, decomposition temperatures of the melt-mixed composites were higher than those of the solution-mixed composites. Nonetheless, average molecular weights of PLA in the solution mixed composites, as confirmed by GPC, were significantly higher than those in the

melt-mixed composites. The surface of HA powder was modified with either 3-aminopropyltriethoxysilane (APES) or 3-methacryloxypropyltrimethoxysilane (MPTS). FTIR and EDXRF results confirmed the appearance of APES and MPTS on the HA surfaces. SEM micrographs of silane-treated HA/PLA composites revealed that modification of HA with APES or MPTS eased distribution of HA powder in PLA matrix and enhanced interfacial adhesion between both phases. Based on the results, the mechanical properties of silane-treated HA/PLA composites were better than those of untreated HA/PLA composites. Moreover, TGA and GPC results showed that the incorporation of silane-treated HA into the PLA matrix significantly increased thermal stability of the composite and decreased the thermal degradation of PLA chains. Additionally, *in vitro* degradation behaviors of untreated HA/PLA and silane-treated HA/PLA composites were also analyzed. The results showed that the stronger interfacial bonding between silane-treated HA and PLA matrix significantly delayed the *in vitro* degradation rate of the PLA, after immersing in PBS. Moreover, the results of bioactive study showed that the incorporation of u-HA into the PLA matrix significantly induced the formation of calcium phosphate compounds on the composite surface as evaluated by means of SEM, EDX, FTIR and XRD. In addition, *in vitro* cytotoxicity tests indicated that the extracts from all HA/PLA composites had no toxicity to human osteoblast cell.

School of Polymer Engineering   Student's Signature_____

Academic Year 2009   Advisor's Signature_____

                                                         Co-advisor's Signature_____

                                                         Co-advisor's Signature_____

ACKNOWLEDGEMENTS

I am deeply indebted to my thesis advisor, Asst. Prof. Dr. Nitinat Suppakarn, who always gives me a kind suggestions and supports me throughout the period of the study. Furthermore, the grateful thanks and appreciation are given to the thesis co-advisor, Asst. Prof. Dr. Yupaporn Ruksakulpiwat and Asst. Prof. Dr. Wimonlak Sutapun for their valuable suggestions.

My thanks go to Asst. Prof. Dr. Utai Meekum, Assoc. Prof. Dr. Jatuporn Wittayakun, Asst. Prof. Dr. Visit Vao-soongnern, Asst. Prof. Dr. Sirirat Tubsungneon Rattanachan for their valuable suggestion and guidance given as committee member.

I would like to express my a appreciation to the faculty and staff members of the School of Polymer Engineering and the Center for Scientific and Technological Equipment of Suranaree University of Technology. Special thanks are extended to Mr. Chalermpan Keawkumay and all friends for their help, support and encouragement.

Last but not least, I would like to thank my parents, Mr. Sittisak and Mrs. Jutarut Rakmae, and my younger brother, Mr. Suriyong Rakmae, who give me a valuable life and protect my mind from an evil with their unconditional loves.

Suriyan Rakmae

TABLE OF CONTENTS

Page

TABLE OF CONTENTS (Continued)

TABLE OF CONTENTS (Continued)

TABLE OF CONTENTS (Continued)

TABLE OF CONTENTS (Continued)

TABLE OF CONTENTS (Continued)

LIST OF TABLES

LIST OF FIGURES

LIST OF FIGURES (Continued)

LIST OF FIGURES (Continued)

LIST OF FIGURES (Continued)

SYMBOLS AND ABBREVIATIONS

%	=	Percent
º	=	Degree
ºC	=	Degree Celsius
µm	=	Micrometer
APES	=	3-aminopropyltriethoxysilane
cm	=	Centimeter
EDX	=	Energy dispersive X-Ray spectroscopy
EDXRF	=	Energy dispersive X-Ray fluorescence spectroscopy
eV	=	Electron volt
FTIR	=	Fourier transform infrared spectrometer
g	=	Gram
GPa	=	Gigapascal
h	=	Hour
HA	=	Hydroxyapatite
J	=	Joule
keV	=	Kilo electron volt
kV	=	Kilo volt
m^2	=	Square meter
m^3	=	Cubic meter
mg	=	Milligram
min	=	Minute

SYMBOLS AND ABBREVIATIONS (Continued)

mm	=	Millimeter
mol	=	Mole
M	=	Molar
$\overline{M}_n$	=	Average molecular weight by number
$\overline{M}_w$	=	Average molecular weight by weight
MPa	=	Megapascal
MPTS	=	3-metacryloxypropyltrimetoxysilane
N	=	Normal
P	=	Pascal
PBS	=	Phosphate-buffered solution
PLA	=	Poly(lactic acid)
psi	=	Pound per square inch
rpm	=	Revolution per minute
SBF	=	Simulated body fluid
SEM	=	Scanning electron microscope
wt%	=	Percent by weight
vol.%	=	Percent by volume
XRD	=	X-ray diffractomerter

CHAPTER I

INTRODUCTION

1.1 Background

Hydroxyapatite [HA: $Ca_{10}(PO_4)_6(OH)_2$] is a form of calcium phosphate which is similar to a major inorganic component in hard tissues of human body. HA has been considered as a biomaterial due to its biocompatibility and osteoconductivity (Chandrasekhar, Shaw, and Mei, 2005; Hasegawa *et al.*, 2006). Therefore, HA has been synthesized and used in various medical applications such as fillers, spacers and bone graft substitutes in orthopedic, maxillofacial applications and bone replacement. HA can be synthetically prepared or derived from natural sources, *e.g.* coral, bovine bone, swine bone. (Chandrasekhar *et al.*, 2005; Shikinami and Okuno, 2001; Ruksudjarit, Pengpat, Rujijanagul, and Tunkasiri, 2008). However, the major drawbacks of using HA in a form of single component, *e.g.* dense HA, porous HA, are its brittleness and the difficulty of processing. These problems have been solved by using HA as a filler for polymer matrices.

The synthetic HA powders are frequently used in biomaterial studies as a reinforcing filler for polymer composites. However, the synthetic HA is quite expensive. Also, its chemical composition and properties extremely depend on the preparation condition. In recent years, several attempts have been done to produce HA from natural sources for biomedical applications since the natural HA is less expensive and more compatible to human hard tissues (Chandrasekhar *et al.*, 2005; Shikinami *et al.*, 2001; Ruksudjarit *et al.*, 2008). In Thailand, there are high volumes

of bovine bone as a livestock waste. Normally, the bone is used in fertilizer, animal foods, and making porcelain (*i.e.* bone china). Using the bovine bone as a raw material for producing HA not only increase added value of the bovine bone but also reduce volumes of the livestock waste. As another approach to utilize bovine bone, this research aims to prepare bovine bone based HA powder and further use the powder as a filler for a polymer composite.

HA/polymer composites have become an interesting topic for many research groups because of the flexibility in tailoring properties of the composites, *e.g.* by varying types of polymer matrix. For an example, HA reinforced HDPE composite has been developed and successfully used in orbital surgery as a hard tissue replacement material (Wang, Deb, and Bonfield, 2000). Nevertheless, some orthopaedic implants such as bone screw, bone plate, *etc*. need temporary materials that stay intact until the healing process in the body is complete. After that, the materials must be degraded by hydrolytic or enzymatic action and excreted from the body as waste products. Thus, HA/bioresorbable polymer composites become important representatives of those materials since they combine the osteoconductivity and the bone bonding ability of HA with the resorbability of the biodegradable polymer. In addition, HA/bioresorbable polymer composites are also easy to process into required shapes (Zhang *et al.*, 2005; Ooi, Hamdi, and Ramesh, 2007; Hasegawa *et al.*, 2006; Deng, Hao, and Wang, 2001).

Many types of bioresorbable polymers have been developed and used in medical applications such as poly(lactic acid) (PLA), poly(3-hydroxybutyrate) (PHB), poly(glycolic acid) (PGA), poly(lactide-co-glycolide) (PLGA), poly(anhydrides), collagen, chitosan and poly(hydroxyalkanoates). Among these polymers, poly(lactic

acid) is a good candidate because it is biodegradable and essentially yields nontoxic byproduct after degradation (Russias *et al.*, 2006). From various research works, it is well known that degradation of pure PLA implanted *in vivo* produces intermediate acidic products, such as lactic acid, via hydrolysis of the polyester bonds. Subsequently, these acidic products are processed through normal metabolic pathways and are eliminated from the body as carbon dioxide (Suganuma and Alexander, 1993; Agrawal and Athanasiou, 1997; Horst, Robert, Suzanne, and Antonios, 1995). Hence, the composite between PLA and HA is a good alternative to be used as a biomaterial since it is combining bone-bonding potentials, strength and stiffness of HA with flexibility and bioresorbability of PLA. During healing process in human body, the polymeric part is metabolized and excreted while the HA is retained in the body and being a supporter for the growth of osteoblast cell (Furukawa *et al.*, 2000).

However, PLA matrix has methyl units ($-CH_3$) as side groups, therefore, PLA surface is hydrophobic in nature. This is in contrast to HA surface, which exhibits hydrophilic character. Because of the polarity difference between PLA and HA surfaces, the agglomeration of HA is observed in a HA/PLA composite system. Also, the composite failures mainly occur at the interface of HA and polymer matrix. These lead to poor mechanical properties of HA/PLA composites (Ignjatovic, Suljovrujic, Simendic, Krakovsky, and Uskokovic, 2001; Chandrasekhar *et al*., 2005).

Mechanical properties of the composite are the important factors that relate to applications of the material. To use a HA/PLA composite as a biomaterial, its mechanical properties need to be adjusted to be close to those of the replaced tissue, *e.g.* natural cortical bone has modulus of elasticity of 3-30 GPa. (Kasuga, Ota, Nogami, and Abe, 2001). To achieve the requirements imposed on the mechanical

properties of the composite, a good distribution of HA in PLA matrix and good adhesion between HA and PLA must be taken place. So, a lacking of effective adhesion between the HA and the PLA matrix needed to be solved. Therefore, an improvement of the interfacial adhesion between HA and PLA matrix has become an important area of studies. To improve the interfacial adhesion between HA and PLA matrix, the hydroxyl group presenting on the HA surface can react with organic molecules such as silane coupling agents, zirconyl salt, poly acids, poly(ethylene glycol), isocyanate and dodecyl alcohol (Liu, Wijn, Groot, and Blitterswijk, 1998). Generally, treating HA surface with a silane coupling agent is an effective method to improve the interfacial adhesion between HA particles and polymer matrix (Arami *et al.*, 2008).

In vitro experiment is a primary method usually used to evaluate cytotoxicity and bioactivity performances of biomaterials. This method refers to the technique of performing a given experiment in a controlled environment outside of a living organism, for example in a test tube (Tsuji and Ikarashi, 2004). Furthermore, to study the simultaneous degradation of HA/PLA composites in human body, the experiment is designed by simulating the condition similar to human body. The degradation of the composites is studied by immersing the composites in a buffer solution having properties similar to human body fluid. Various buffered solutions, for example, phosphate-buffered solution (PBS), Hank's balance salt solution (HBSS), sodium citrate buffered solution can be used for an *in vitro* study. (Tsuji *et al*., 2004; Verheyen *et al.*, 1993). The degradation of PLA is a complex process involving numerous variables, such as the crystallinity and molecular weight of PLA, processing conditions, shape and size of specimens, *etc*. Additionally, the

incorporation of an HA phase into the PLA matrix is an interesting factor that would affect *in vitro* degradation of HA/PLA composites (Navarro, Ginebra, Planell, Barrias, and Barbosa, 2005).

In this study, natural HA powder was produced from bovine bone by thermal treatment. The HA powder was treated with either 3-aminopropyltriethoxysilane (APES) or 3-methacryloxypropyltrimethoxysilane (MPTS). Then, natural HA powders with different surface modification were used to reinforce PLA. Effects of surface modification and filler content on morphological and mechanical properties of HA/PLA composites were examined. In addition, the degradation behavior of HA/PLA composites in buffer solution, *in vitro* testing, were investigated.

1.2   Research objectives

The objectives of this study are as follows:

(i)   To investigate characteristics of HA powder prepared from bovine bone.

(ii) To investigate effect of mixing process, melt-mixing and solution-mixing, on thermal properties, mechanical properties, morphological properties of natural HA/PLA composites.

(iii) To investigate effects of natural HA content and natural HA surface modification on thermal properties, mechanical properties, morphological properties and degradation behavior of natural HA/PLA composites.

1.3   Scope and limitation of the study

In this study, natural HA powder was produced from bovine bone by thermal treatment. The obtained HA was separated into two groups, *i.e.* untreated HA and silane-treated HA. Surface modification of HA powder was done using either 3-aminopropyltriethoxysilane (APES) or 3-methacryloxypropyltrimethoxysilane (MPTS). The amount of silane used is 2.0% based on the weight of HA powder. Untreated HA and silane-treated HA were investigated by a Fourier transform infrared spectrometer (FTIR), an X-ray diffractometer (XRD), a scanning electron microscope (SEM) and a thermogravimetric analyzer (TGA).

HA/PLA composites at various contents of HA powder were compounded through either solution-mixing or melt-mixing technique using an internal mixer and then the composites specimens were prepared by compression molding. Effects of HA content and surface modification on mechanical, thermal and morphological properties of natural HA/PLA composites were determined. A universal testing machine and an impact testing machine were used to measure the mechanical properties of the HA/PLA composites. Tensile fracture surfaces of the HA/PLA composites were evaluated using a SEM.

In vitro degradation behavior of HA/PLA composites was determined. The composites were immersed in a phosphate buffer solution (PBS) and simulated body fluid (SBF) at 37ºC for various time periods. The weight change and the thickness change of the composite specimens after immersing in PBS were measured. Also, the changes in pH of PBS solution were recorded. Additionally, molecular weight of PLA in neat PLA and HA/PLA composite before and after hydrolytic degradation in PBS were evaluated by a gel permeable chromatography (GPC). The surface of the

composites after immersing in SBF were characterized using SEM, EDX, XRD and FTIR.

1.4   References

Agrawal, C. M., Athanasiou, K. A. and Heckman, J. D. (1997). Biodegradable PLA-PGA polymers for tissue engineering in orthopadics. **Mater. Sci. Forum.** 250: 115-129.

Arami, H., Mahajerani, M., Mazloumi, M., Khalifehzadeh, R., Lak, A., and Sadrnezhaad, S. K. (2009). Rapid formation of hydroxyapatite nanostrips via microwave irradiation. **J. Alloy Compd.** 469: 391-394.

Chandrasekhar, R. K., Montgomery, T. S., and Wei, M. (2005). Biodegradable HA-PLA 3-D porous scaffolds: Effect of nano-sized filler content on scaffold properties. **Acta Biomater.** 1: 653-662.

Deng, X., Hao, J., and Wang, C. (2001). Preparation and mechanical properties of nanocomposites of poly(D,L-lactide) with Ca-deficient hydroxyapatite nanocrystals. **Biomaterials.** 22: 2867-2873.

Furukawa, T., Matsusue, Y., Yasunaga, T., Shikinami, Y., Okuno, M., and Nakamura, T. (2000). Biodegradation behavior of ultra-high-strength hydroxyapatite/poly(L-lactide) composite rods for internal fixation of bone fractures. **Biomaterials.** 21: 889-898.

Hasegawa, S., Ishii, S., Tamura, J., Furukawa, T., Neo, M., Matsusue, Y., Shikinami, Y., Okuno, M., and Nakamura, T. (2006). A 5–7 year *in vivo* study of high-strength hydroxyapatite/poly(L-lactide) composite rods for the internal fixation of bone fractures. **Biomaterials.** 27: 1327-1332.

Horst, A. R., Robert, L. C., Suzanne, G. E., and Antonios, G. M. (1995). Degradation of polydispersed poly(L-lactic acid) to modulate lactic acid release **Biomaterials.** 16: 441-447.

Ignjatovic, N., Suljovrujic, E., Simendic, J. B., Krakovsky, I., and Uskokovic, D. (2001). A study of HAp/PLLA composite as a substitute for bone powder using FT-IR spectroscopy. **Biomaterials.** 22: 271-275.

Kasuga, T., Ota, Y., Nogami, M., and Abe, Y. (2001). Preparation and mechanical properties of polylactic acid omposites containing hydroxyapatite fibers **Biomaterials.** 22: 19-23.

Liu, Q., Wijn, J. R., Groot, K., and Blitterswijk, C. A. (1998). Surface modification of nano-apatite by grafting organic polymer. **Biomaterials.** 19: 1067-1072.

Navarro, M., Ginebra, M. P., Planell , J. A., Barrias, C. C., and Barbosa M. A. (2005). In vitro degradation behavior of a novel bioresorbable composite material based on PLA and a soluble CaP glass. **Acta. Biomater.** 1: 411-419.

Ooi, C. Y., Hamdi, M., and Ramesh, S. (2007). Properties of hydroxyapatite produced by annealing of bovine bone. **Ceram. Int.** 33: 1171-1177.

Ruksudjarit, A., Pengpat, K., Rujijanagul, G., and Tunkasiri, T. (2008). Synthesis and characterrization of nanocrystalline hydroxyapatite from natural bovine bone. **Curr. Appl. Phys.** 8: 270-272.

Russias, J., Saiz, E., Nalla, R. K., Gryn, K., Ritchie, R. O., and Tomsia, A. P. (2006). Fabrication an mechanical properties of HA/PLA composites:A study of *in vitro* degradation. **Mater. Sci. Eng.** 26: 1289-1295.

Shikinami, Y. and Okuno, M. (2001). Bioresorbable devices made of forged composites of hydroxyapatite (HA) particles and poly-L-lactide (PLLA): Part I. Basic characteristics. **Biomaterials.** 20: 859-877.

Suganuma, J. and Alexander, H. (1993). Biological response of intramedullary bone to poly-L-lactic acid. **J. Appl. Biomater.** 15: 13-27.

Tsuji, H. and Ikarashi, K. (2004). *In vitro* hydrolysis of poly(-lactide) crystalline residues as extended-chain crystallites. Part I: long-term hydrolysis in phosphate-buffered solution at 37°C. **Biomaterials.** 25: 5449-5455.

Verheyen, C. C. P. M., Klein, C. P. A. T., Blieckhogervorst, J. M. A., Wolke, J. G. C., Blitterswijn, C. A., and Groot, K. (1993). Evaluation of hydroxylapatite/poly (L-lactide)composites: physico-chemical properties. **J. Mater. Sci. Mater. Med.** 4: 58-65.

Wang, M., Deb, S., and Bonfield, W. (2000). Chemically coupled hydroxyapatite-polyethylene composites: processing and characterization. **Mater. Lett.** 44: 119-124.

Zhang, S. M., Liu, J., Zhou, W., Cheng, L., and Guo, X. D. (2005). Interfacial fabrication and property of hydroxyapatite/polylactide resorbable bone fixation composites. **Curr. Appl. Phys.** 5: 516-518.

CHAPTER II

LITERATURE REVIEW

2.1   Preparation of natural hydroxyapatite

In recent years, several researchers investigated possibilities of producing natural hydroxyapatite from bovine bone. Ooi *et al.* (2007) studied the properties of HA bioceramic produced by heat treatment of bovine bone. They have found that the nanocrystalline apatite was observed when the annealing temperature was above 700ºC and up to 1000ºC. However, annealing beyond 1000ºC resulted in partial decomposition of the HA phase to form a minor phase of β-tricalciumdiphosphate (β-TCP). As the annealing temperature increased to 1200ºC, the intensity of the XRD characteristic peaks of β-TCP gradually increased.

Yoganand, Selvarajan, Wu, and Xue (2009) prepared HA by heat treatment of bovine bone at 850ºC for 5-6 h. The XRD spectrum indicated that the obtained product was hexagonal-phase HA. Then, the HA was powdered. SEM micrograph showed that HA powders were in highly irregular shapes, *e.g.* edges, angular, rounded, circular, dentric, porous and fragmented morphologies. In addition, after heat treatment, a disease-causing agent was not observed. (Ozyegin, Oktar, Goller, Kayali, and Yazici, 2004).

Benmarouanea, Hansena, and Lodini (2004) studied effect of heat treatment on microstructure of bovine bone based HA. The neutron diffraction pattern indicated

that heating the bone at 625ºC for 3 days did not change the orientation of HA crystallites, which still directed along the axis of the bone.

Ruksudjarit *et al.* (2008) used vibro-milling technique to produce HA nanopowders with high purity from bovine bone. The dried bone was calcined at 800ºC for 3 h and ground by vibro-milling at various times. XRD patterns of all ground bone powders corresponded to that of pure HA phase. SEM micrographs of HA powders after vibro-milling time of 2 h showed nanoneedle-like shape of HA powders with diameter less than 100 nm.

Lorprayoon (1989) synthesized HA and TCP using bone ash as a starting material. The bone was calcined at 700ºC for 8 h. TEM micrographs showed that the obtained bone ash was nano-scale particles. Then, the bone ash was dissolved and precipitated at various pH. The precipitated bone was heated to 1230-1280ºC for 2-3 h. The results showed that TCP was obtained when the precipitation was at pH of 8.0-8.5 while the single phase of HA was precipitated at pH of 9.7-10, confirmed by XRD patterns.

Haberko *et al.* (2006) investigated characteristics of HA produced from pig bone at elevated temperatures. They have found that the pig bone started to decompose at the temperatures over 700 ºC. As a result, calcium oxide and carbonate groups were partially removed from the system. Simultaneously, crystallite growth became intensive, specific surface area of the powder decreased and compacts of such powder started to shrink.

2.2   Surface treatment of hydroxyapatite by silanization

To enhance the integrity of HA/PLA composite, the HA can be surface treated with a coupling agent, such as organofunctional silanes, which in general effectively improves adhesion between HA and polymer matrix.

Dupraz, Wijn, Meer, and Groot (1996) modified surface of HA powder with several methoxysilane coupling agents (Table 2.1), *i.e.* vinyltriethoxysilane (VS), N-methylaminopropyltrimethoxysilane (TRIAMO), 3-methacryloxypropyltrimethoxy silane (MPTS), 3-aninopropyltriethoxysilane (APES) and N-(2-aminoethyl)-3-amino-propyltriethoxysilane (DAS). Low concentration of silane solution was prepared to retain the coupling agent as monomer or dimer. X-ray photoelectron (XPS) spectra of all HA samples revealed the presence of a few monolayers of thin silane films on HA powder. This indicated that silane coupling agents were able to chemically bond on the HA surface since a thin coating of silane film remained after washing the powder with water for several time. The stability of the silane coating film in a wet environment was measured by extracting the coated powders with water at 37°C for 5 days. XPS results showed that VS, MPS and DAS coatings were able to withstand a mild water extraction. This was due to silane-silane crosslinking prevented silane molecules from water extraction. In contrast, AMMO and TRIAMO coatings were completely removed.

Table 2.1 Chemical formular of organofunctional silane coupling agents

Name	Chemical formular
VS	$CH_2 = CH\text{-}Si\text{-}(OCH_3)_3$
MPTS	$CH_2 = C(CH_3)COOCH_2\text{-}CH_2\text{-}CH_2\text{-}Si\text{-}(OCH_3)_3$
APES	$NH_2\text{-}CH_2\text{-}CH_2\text{-}CH_2\text{-} Si\text{-}(OCH_2CH_3)_3$
TRIAMO	$CH_2\text{-}NH\text{-}CH_2\text{-}CH_2\text{-}CH_2\text{-} Si\text{-}(OCH_3)_3$
DAS	$NH_2\text{-}CH_2\text{-}CH_2\text{-} NH\text{-}CH_2\text{-}CH_2\text{-}CH_2\text{-} Si\text{-}(OCH_3)_3$

Shinzato, Nakamura, Kokubo, and Kitamura (2001) studied effect of the 3-methacryloxypropyltrimethoxysilane content on bending strength of poly(methyl methacrylate) (PMMA)/bioactive glass bead (GCB) composites. The glass beads were treated with different amounts of silane coupling agent, *i.e.* 0 (untreated GCB), 0.1, 0.2, 0.5, and 1.0wt% of the glass beads (silane-treated GCB). The bending strength of the PMMA/GCB composites before and after soaking in water at 75°C for 5 days was measured. At initial condition PMMA/silane-treated GCB composites had significantly higher bending strengths than PMMA/untreated GCB composites, but there were no significant differences between various types of PMMA/silane-treated GCB composite. Moreover, after soaking in water and by treating GCB with 0.2wt% of silane, the obtained PMMA/silane-treated GCB composite had the highest bending strength. The result implied that the siloxane bonds could make the theoretical monolayer of the silane coupling agent at 0.2wt% since the monolayer silane was believed to bind strongly to glass beads with PMMA. When the amount of the silane coupling agent was less than 0.2wt%, the number of siloxane bonds decreased leading to the less interfacial interaction between the two phases. When the amount of the

silane coupling agent was greater than 0.2wt%, the layer of the coupling agent became thicker. The formation of weak hydrogen bonds in thick coupling agent layer was the cause of the weak bending strength of PMMA/silane-treated GCB composites.

Zhang *et al.* (2005) investigated interfacial adhesion between silane-treated HA and PLA matrix. The HA powders were treated with 3-aminopropyltri ethoxysilane, 3-(2,3-cyclopropoxy)-propyltrimethoxysilane, 3-methypropenionyloxy-propyltrimethoxysilane. Thereafter, various silane-treated HA/PLA composites at 20vol.% HA were produced. IR spectrum showed the existence of silane molecules on surface of the modified HA. Interfacial adhesion between the HA and the polymer matrix can be improved by silane coupling agent since PLA bond chemically to silane coupling agents on HA surfaces. Moreover, SEM micrographs of the silane-treated HA/PLA composites indicated that the silane-treated HA particles were homogeneously dispersed in PLA matrix. Therefore, bending strength of silane-treated HA/PLA composites were higher than that of untreated HA/PLA composite.

Wen *et al.* (2008) developed a method to prepare HA/silicone rubber (SR) composite. HA was modified by vinyltriethoxysilane, poly (methylvinylsiloxane) (PMVS) and 2,5-bis(tertbutylperoxy)-2,5-dimethylhexane (DBPMH). SEM micro-graphs of silane-treated HA clearly showed that the HA powders uniformly dispersed within SR matrix and closely connected with the matrices with obscure interfaces.

Daglilar and Erkan (2007) modified surface of HA derived from bovine bone (BHA), synthetic HA and β-TCP with 3-methacryloxypropyltrimethoxysilane. Then, different amounts of the silane-treated filler were added to PMMA matrix. Compressive and three point bending properties of the composites showed that the

amount of ceramic filler was more effective in enhancing their mechanical properties than the silanation treatment itself.

Wang and Bonfield (2001) studied effect of adhesion between HA particles and HDPE matrix on mechanical properties of composites. HA surface were treated with 3-trimethoxysiylpropylmethacrylate before blending with HDPE. EDX pattern of the silane-treated HA showed bands of the carboxyl and SiO functional groups. The result indicated that the silane coupling agent was grafted on HA surface. The improvement in tensile strength and fracture strain of treated HA/HDPE composite were observed. This was due to the homogeneously distribution of silane-treated HA in polyethylene. Moreover, SEM micrograph of HA/HDPE composites showed HDPE fibril network formation on a HA particle.

Daglilar, Erkan, Gunduz, Ozyegin, Salman, Agathopoulos, and Oktar (2007) studied water adsorption behavior of PMMA reinforced with silane-treated bovine bone based HA powder. The HA powder was treated with 0.2wt% of 3-methacryloxypropyltrimethoxysilane. The experimental results showed that the addition of untreated HA powder in the polymer matrix enhanced water absorption of the composites. In contrast, the water absorption of silane-teated HA/PMMA composite was decreased.

Furuzono, Sonoda, and Tanaka (2000) developed a method for HA/silicone composite preparation. HA microparticles were surface modified by 3-aminopropyltriethoxysilane before adding into 10 ml of pure water. Subsequently, acrylic acid-grafted silicone sheet was immersed in the solution. FTIR spectrum of silane-trated HA particles confirmed that the silane coupling agent was covalently

bonded to the HA particles due to the appearance of the SiO stretching vibration at 1043 cm^{-1}.

2.3   Preparation of HA/PLA composites

Various methods have been successfully used to produce HA/PLA composite biomaterials, such as melt-mixing of HA and PLA, polymerization of lactide monomer onto HA particles, forging and hot pressing to obtain three-dimensional blocks of the composite. Nowadays, the composite specimens with mechanical characteristics close to the natural bone tissue are obtained only by forging and hot pressing methods.

Ingjatovic, Suljovrujic, Simendic, Krakovsky, and Uskokovic (2004) prepared specimens of HA/poly(L-lactide) (PLLA) composites using two-step procedure. Firstly, HA powder was prepared by precipitation of calcium nitrate and ammonium phosphate in an alkaline medium. PLLA was dissolved in chloroform, then, HA powder was added and then obtained mixture was vacuum evaporated. In the second step, the obtained powders were compacted by hot pressing to get specimens. The researchers have found that the hot pressing procedure was possible to change the porosity of HA/PLLA composites. The porosity of HA/PLLA composites were decreased by prolonging the hot pressing time. Moreover, SEM micrographs of HA/PLLA composites showed HA particles were finely distributed in the polymer matrix. In addition, hot pressing causes a decrease in crystallinity of PLLA in the HA/PLLA composite biomaterial as proved by wide-angle X-ray scattering (WAXS) and DSC analysis. The WAXS results indicate a significant decrease in PLLA crystallinity during hot pressing. DSC analyses confirmed these changes in

crystallinity degree and also indicated changes in glass transition, cold crystallization, and melting temperature of the PLLA polymer. In the given time interval of hot pressing from 0 to 60 min, insignificant qualitative changes in the HA and the PLLA phase were recorded by IR spectroscopy.

Shikinami *et al.* (1999) prepared HA/PLLA composites by fogging method. The small HA/PLLA granules of different amounts of HA (*i.e.* 20, 30, 40, and 50wt% of HA particles within a PLLA matrix) were collected by adding ethanol dropwise to a PLLA-HA/dichloromethane solution. The granules were then extruded to make a thick billet. Thereafter, this billet was forged at 103ºC into a thin billet without fibrillation and cut on a lathe into required shapes. The mechanical testing results, *i.e.* bending, tensile, compression and impact properties, indicated that the forged HA/PLLA composites generally have much higher mechanical strength compared with the HA/PLLA composites produced from other techniques. The devices made of forged composites have a crystalline morphology of complex (multi axial) orientation. So, they showed extremely high strength uniformly in all directions.

2.4   Properties of HA/PLA composites

2.4.1   Thermal properties

Ignjatovic *et al.* (2004) investigated thermal behavior of hot pressed HA/PLLA composites. The HA/PLLA composites were hot pressed for different pressing times, *i.e.* 5, 15, 30, 45, and 60 min. DSC thermograms and wide-angle X-ray scattering (WAXS) patterns of the HA/PLLA composites prepared at various hot pressing time revealed the decrease in glass transition temperature (T_g), melting temperature (T_m) and percent of crystallinity of PLLA component with prolonging hot

pressing time. The observations were due to the rearrangement of PLLA chains on the HA surfaces during the composite preparation. In addition, GPC results confirmed that the polymer chains were broken due to thermo-mechanical factors. TGA results showed that thermal stability of the obtained composites decreased with increasing hot pressing time.

Deng, Sui, Zhao, Cheng, and Yang (2007) studied the preparation of HA/PLLA hybrid nanofibrous scaffolds. PLLA and HA/PLLA scaffolds were fabricated using electrospinning technique. From DSC results, the HA/PLLA scaffolds exhibited lower melting enthalpies (34.8 J/g) than the PLLA scaffolds (44.6 J/g). The decrease in melting enthalpy of the HA/PLLA scaffold indicated that hybrid scaffolds contained microcrystals between PLLA (Shikinami *et al.*, 2001).

Zheng, Zhou, Li, and Weng (2007) studied shape memory properties of poly(D,L-lactide) (PDLLA)/HA composites. They have found that HA content played a very important role in changing of T_g of the composites. DSC results revealed that the T_g of neat PDLLA and HA/PDLLA composites at weight ratios of HA of 25, 30, 45, 50% were 53.7, 55.6, 56.8, 57.2, 59.0°C, respectively. The T_g of the composite increased with increasing HA content may be due to the existing interfacial interaction of PDLLA and HA.

Gay, Arostegui, and Lemaitre (2008) determined the thermal characteristics of PLLA and HA/PLLA composites using DSC. Effect of HA content on crystallisation and melting temperatures of the composites were measured. In the second heating scan, glass transition, crystallisation and melting points of PLLA and HA/PLLA composite were observed. The experiment had two heating cycles. In the first step, the sample was heated from 25 to 200°C (increment rate of 15°C/min).

Then, it was quenched at a rate of -15°C/min to 25°C. The second step, the quenched sample was run from 25°C to 200°C. The DSC results indicated that the glass transition of the composites increased slightly with HA content but there was no significant changes in the crystallization and the melting temperatures of the composites as compared with those of the neat PLA.

2.4.2 Mechanical properties

Chandrasekhar *et al.* (2005) synthesized porous HA/PLA scaffolds using a salt leaching technique. The compressive properties of HA/PLA composites were investigated as a function of HA content. The compression strength and the modulus of elasticity of the composites increased with increasing HA content. Additionally, the increases in compressive strength and elastic modulus of HA/PLA scaffolds with increasing HA content have also been observed in dense HA/PDLLA composites (Lin, Fang, Tseng, and Lee, 2007). In contrast, the bending strength of HA/PLA composites decreased with increasing HA content (Shikinami *et al.*, 1999). Thus, mechanical properties, such as strength and elastic modulus of PLA can be controlled by the amount of added HA particles in the composites.

Deng *et al.* (2001) studied the preparation and mechanical properties of nanocomposites of PDLLA with Ca-deficient HA nanocrystals (d-HA). Tensile testing results indicated that adding d-HA into the PLA matrix could significantly increase in the tensile modulus of d-HA/PLA composite. The yield stress of the composite slightly varied with d-HA loading. This is typically found when there is effective adhesion between the polymer matrix and the filler.

Kasuga, Ota, Nogami, and Abe (2000) studied the preparation and mechanical properties of PLA composites containing HA fibers (HAF). Tangent

moduli of elasticity were estimated using stress/strain curves obtained from the bending tests. The bending strength of HAF/PLA composite was insignificantly changed with the HAF content. On the other hand, the modulus of elasticity of the composites was improved with increasing HAF content. It was reported that the contents of HAF of 75wt% should be added into the PLA matrix in order to prepare the composites with modulus of elasticity close to that of natural bone.

Nejati, Firouzdor, Eslaminejad, and Bagheri (2009) studied effect of HA particle size on mechanical properties of HA/PLA composite. The mechanical properties of HA/PLA composites containing nano-scale HA were compared with those of PLA composites containing micro-scale HA. The compressive strength and the compressive modulus of the microcomposite and the nanocomposite scaffolds were higher than those of the pure PLLA scaffolds. The compressive strength of 50wt% nano-scale HA/PLA composite was significantly higher than that of the micro-scale HA/PLA composite. It may be attributed to the larger surface area of the nano-scale HA and the more uniform distribution of the nano-scale HA particles in PLLA matrix as compared with those of micro-scale HA particles. However, the compressive modulus of the microcomposites and the nanocomposite scaffolds were not statistically different.

2.4.3 Morphological properties

Todo, Park, Arakawa, and Takenoshita (2006) studied the relationship between microstructure and fracture behavior of bioabsorbable HA/PLLA composites. Effects of particle size and particle shape of HA on fracture surface of HA/PLLA composites were determined by SEM. SEM micrographs of fracture surfaces of HA/PLLA composites showed that the HA with plate and micro-scale

shape exhibited relatively rough surfaces. This was due to the ductile deformation of the PLLA matrix during the debonding of the HA/matrix interfaces. On the contrary, the HA with spherical and nano-scale shape exhibited smooth surfaces that corresponded to brittle fracture behavior due to the nano-scale interaction between the PLLA fibrils and the HA particles.

Takayama, Todo, and Takano (2008) investigated effect of HA particle size on the mechanical properties and fracture energy of HA/PLLA composites. SEM of cryofracture surfaces of HA/PLLA composites showed the good dispersion of micro-scale HA particles in PLLA matrix. On the other hand, SEM micrograph of PLA composites containing nano-scale HA exhibited more agglomeration of HA particles with various size of agglomerated particles. This indicated that the nano-scale HA particles easily agglomerated compared with the micro-scale HA particles. The existence of these agglomerations resulted in the reduction of the bending strength and the fracture energy because these are easily fractured due to weak bonding between particles and such localized fracture becomes the initiation of fast global fracture of the composite material. This mechanism was supported by the brittle fracture behavior. The micrograph of nano-scale HA/PLLA showed very smooth and flat fracture surface, indicating very low dissipated energy. This was in contrast to the fracture surface of the micro-scale HA/PLLA which exhibited a rough surface with interfacial failure at the micro-scale HA and PLLA interface and localized plastic deformation in the surroundings of the debonded particles.

2.4.4 *In vitro* degradation

Russias *et al.* (2006) investigated effect of fine-commercial HA powder and coarse HA whisker on *in vitro* degradation behavior of HA/PLA

composites. The mechanical properties of the composites were evaluated both before and after storage in a Hanks' balanced salt solution (HBSS) at various periods of time. The results indicated that composites with ceramic contents ranging between 70 and 85wt% had similar mechanical properties to human cortical bone. However, the properties of these composites were deteriorated with immersion in HBSS due to the degradation of the polymer phase. Microstructure of the composite clearly confirmed that the polymer bridges have degraded or disappeared after immersion in HBSS, causing a significant degradation of the mechanical properties of the composites. The degradation was more pronounced in composites with higher ceramic content due to the dissolution of the trapped polymer chains between the ceramic particles. In comparison, both fine HA and coarse HA based composites showed similar degradation pattern in a simulated environment.

Verheyen *et al.* (1993) examined physico-chemical behavior of the neat PLLA, the composites containing 30wt% and 50wt% of HA and the one-side HA-coated PLLA immersed three different buffer solutions, *i.e.* citrate buffer, Gomori's buffer and phosphate-buffered solution, for 24 weeks. The results showed that the releases of calcium ions, phosphate ions and L-lactate from the specimens increased with increasing immersing time in all types of buffers. Among three buffer solutions, the specimens immersed in citrate buffer solution released the highest amounts of calcium and phosphate ions. This was because calcium citrate complexes probably prevented precipitation of calcium phosphate on specimen surfaces. The drop of pH of PBS solution was observed after the immersion of HA-coated PLLA specimens for 8 weeks. It was possible that hydrolysis of the polymer releases H^+ ions, causing a decrease in the pH which led to an increase in the solubility of calcium

phosphates. This study indicated that the *in vitro* solubility of calcium phosphates depended on the surrounding medium as well as on the materials themselves. The pH change of the buffer solution and weight loss of HA/PDLLA composite during the hydrolysis process has been also observed. The results indicated that the composite with a higher HA/PDLLA weight ratio had a higher degradation rate. The lower pH value also implied that the higher amounts of degraded PLA dissolved in the buffer solution. Moreover, the surface area of PLA exposed to the solution increased with increasing HA content in the HA/PDLLA composites. From a chemical reaction viewpoint, this led to a higher reaction rate of hydrolysis of PLA with increasing HA content (Lin *et al.*, 2006).

Tsuji *et al.* (2004) investigated the hydrolysis of PLLA crystalline residues in PBS using gel permeation chromatography (GPC). To prepare PLLA crystalline residue, the PLLA films were melted at 200°C for 5 min and then crystallized or annealed at 160°C for 600 min followed by quenching to 0°C. To remove the PLLA chains in the amorphous regions, PLLA films was immersed in 100 ml of 0.15 m PBS at pH 7.4 and 97°C for 40 h. Then, the hydrolysis PLLA crystalline residues (20 mg) was performed in 100 ml of 0.15 M PBS at pH 7.4 and 37°C for the periods of time up to 512 days. PBS was replaced once a month. The average hydrolysis rates estimated from the changes in number average molecular weight (M_n) and peak top molecular weight (M_t) for the hydrolysis period from 192 to 512 days revealing that linear decreases of M_n and M_t in this period were 5.31 and 5.01 g mol^{-1} day^{-1}, respectively. The low hydrolysis rates indicated that the PLLA crystalline residues can remain for a long period. The hydrolysis of the PLLA crystalline residues

proceeded from their surface composed of very short chains with a free end along the chain direction but the hydrolysis form their lateral surface could not be traced.

Dueka, Zavaglia, and Belangero (1999) investigated effect of degree of PLA crystallinity on degradation process of PLA pin. Mechanical, thermal and morphological properties of PLA pin were evaluated before and after immersion in buffer solution. DSC result showed an increase in degree of crystallinity of PLA with increasing immersion time for all specimens. The PLA pin with lower crystallinity had higher bending strength than that with higher crystallinity.

Yuan, Mak, and Yao (2002) studied degradation of PLLA fibers in PBS (pH 7.4) and in a dilute NaOH solution (pH 11.0) at 80ºC. They have found that the viscosity-average molecular weights of the PLLA fibres dropped sharply and decreased by over 90% after 6 days of degradation. The thermal behaviours of the fibres showed that after immersion in both medias, the melting temperature of PLLA decreased while their crystallinities increased. The fibres completely lost their mechanical strength after 5 days of degradation in PBS or in dilute NaOH solution at 80ºC. In addition, SEM showed microcracks on the fiber surfaces across the fibre axis after degradation. These morphological defects confirmed the decrease in viscosity-average molecular weight of PLLA chain.

Kang *et al.* (2007) synthesized porous PLLA/β-TCP composite. The PLLA/β-TCP composite were immersed in dynamic simulated body fluid (DSBF) and in static simulated body fluid (SSBF) at 37ºC for 24 weeks. SEM micrographs of all specimens indicated that a large number of apatite layer were formed on the scaffolds, especially in SSBF. The molecular weight of specimens under flow SBF was higher compared with those tested under static conditions. This might be that flow of SBF

retarded the autocatalysis of PLLA. The porosity and mass change was related to the apatite formation and SBF flow. The changes in mass and porosity contributed to the formation of large number of apatite on the surface and in the interior of the materials. The formation of apatite may compensate the loss of mass due to dissolution of β-TCP and the hydrolysis of PLLA. Moreover, the addition of β-TCP into PLLA affects the degradation rate of PLLA in the composite scaffolds. The degradation rate of scaffolds could be adjusted by the additional fraction of β-TCP. Results indicated the possibility to modulate the degradation rate of the composite scaffolds by varying the content of β-TCP added to the polymer.

Navarro, Ginebra, Planell, Barrias, and Barbosa (2005) studied chemical and morphological changes of PLA/soluble calcium phosphate glass (G5) composite during its degradation in simulated physiological conditions. They have found that the G5 incorporated in the polymeric matrix induced morphological changes, such as the formation of cracks in the composite, which accelerated the degradation of the material. Additionally, G5 reacted with the aqueous medium inducing the formation of a calcium phosphate precipitate, which could enhance the interaction between the material and the bone tissue.

Li, Feng, and Cui (2006) prepared nano-HA/collagen/PLLA composite reinforced by high-strength chitin fibers. To further strengthen the scaffold, linking between PLLA and chitin fibers were produced by oil-soluble dicyclohexyl carbodimide (DCC). To prepare the linked PLLA/chitin fibers, the chitin fibers, PLLA and DCC (1:4:2) were dissolved into dichloromethane at 0ºC for 2 h. The linked PLLA/chitin fibers was taken out and washed by dichloromethane and dried. Thereafter, the reinforced nano-HA/collagen/PLLA composites were incubated at

37ºC in PBS solution. They have found that the nano-HA/collagen/PLLA composite reinforced by linked PLLA/chitin fibers showed better mechanical properties than the composite without PLLA/chitin linking. These results denoted that the strong interfacial bonding strength of the scaffold with linking could decrease the *in vitro* degradation rate.

2.5   References

Arami, H., Mahajerani, M., Mazloumi, M., Khalifehzadeh, R., Lak, A., and Sadrnezhaad, S. K. (2009). Rapid formation of hydroxyapatite nanostrips via microwave irradiation. **J. Alloy. Compd.** 469: 391-394.

Benmarouane, A., Hansena, T., and Lodini, A. (2004). Heat treatment of bovine bone preceding spatially resolved texture investigation by neutron diffraction. **Physica B.** 350: 611-614.

Chandrasekhar, R. K., Montgomery, T. S., and Wei, M. (2005). Biodegradable HA PLA 3-D porous scaffolds: Effect of nano-sized filler content on scaffold properties. **Acta Biomater.** 1: 653-662.

Daglilar, S. and Erkan, M. E. (2007). A study on bioceramic reinforced bone cements. **Mater. Lett.** 61: 1456-1459.

Daglilar, S., Erkan, M. E., Gunduz, O., Ozyegin, L. S., Salman, S., Agathopoulos, S., and Oktar, F. N. (2007). Water resistance of bone-cements reinforced with bioceramics. **Mater. Lett.** 61: 2295-2298.

Deng, X., Hao, J., and Wang, C. (2001). Preparation and mechanical properties of nanocomposites of poly(D,L-lactide) with Ca-deficient hydroxyapatite nanocrystals. **Biomaterials.** 22: 2867-2873.

Deng, X. L., Sui, G., Zhao, M. L., Chen, G. Q., and Yang, X. P. (2007). Poly(L-lactic acid)/hydroxyapatite hybrid nanofibrous scaffolds prepared by electrospinning. **J. Biomater. Sci. Polym. Edn.** 18: 117-130.

Dueka, E. A. R., Zavaglia, C. A. C., and Belangero, W. D. (1999). In vitro study of poly(lactic acid) pin degradation. **Polymer.** 40: 6465-6473.

Dupraz, A. M. P., Wijn, J. R., Meer, S. A. T., and Groot, K. (1996). Characterization of silane-treated hydroxyapatite powders for use as filler in biodegradable composites. **J. Biomed. Mater. Res.** 30: 231-238.

Furukawa, T., Matsusue, Y., Yasunaga, T., Shikinami, Y., Okuno, M., and Nakamura, T. (2000). Biodegradation behavior of ultra-high-strength hydroxyapatite/ poly(L-lactide) composite rods for internal fixation of bone fractures. **Biomaterials.** 21: 889-898.

Furuzono, T., Sonoda, K., and Tanaka, J. (2001). A hydroxyapatite coating covalently linked onto a silicone implant material. **J. Biomed. Mater. Res.** 56: 9-16.

Gay, S., Arostegui, S., and Lemaitre, J. (2009). Preparation and characterization of dense nanohydroxyapatite/PLLA composites. **Mater. Sci. Eng. C.** 29: 172-177.

Haberko, K., Bucko, M. M., Miecznik, J. B., Haberko, M., Mozgawa, W., Panz, T., Pyda, A., and Zarebski, J. (2006). Natural hydroxyapatite-its behaviour during heat treatment. **J. Euro. Ceram. Soc.** 26: 537-542.

Hasegawa, S., Ishii, S., Tamura, J., Furukawa, T., Neo, M., Matsusue, Y., Shikinami, Y., Okuno, M., and Nakamura, T. (2006). A 5–7 year *in vivo* study of high-strength hydroxyapatite/poly(L-lactide) composite rods for the internal fixation of bone fractures. **Biomaterials.** 27: 1327-1332.

Ignjatovic, N., Suljovrujic, E., Simendic, J. B., Krakovsky, I., and Uskokovic, D. (2001). A study of HAp/PLLA composite as a substitute for bone powder using FT-IR spectroscopy. **Biomaterials.** 22: 271-275.

Ignjatovic, N., Suljovrujic, E., Simendic, J., Krakovsky, I., and Uskokovic, D. (2004). Evaluation of hot-pressed hydroxyapatite/poly-L-lactide composite biomaterial characteristics. **J. Biomed. Mater. Res.** 71B: 284-294.

Ignjatovic, N. and Uskokovic, D. (2004). Synthesis and application of hydroxyapatite/polylactide composite biomaterial. **App. Surf. Sci.** 238: 314-319.

Kang, Y., Xu, X., Yin, G., Chen, A., Liao, L., Yao, Y., Huang, Z., and Liao, X. (2007). A comparative study of the *in vitro* degradation of poly(L-lactic acid)/β-tricalcium phosphate scaffold in static and dynamic simulated body fluid**. Eur. Polym. J.** l43: 1768-1778.

Kasuga, T., Ota, Y., Nogami, M., and Abe, Y. (2001). Preparation and mechanical properties of polylactic acid composites containing hydroxyapatite fibers. **Biomaterials.** 22: 19-23.

Lin, P. L., Fang, H. W., Tseng, T., and Lee, W. H. (2007). Effects of hydroxyapatite dosage on mechanical and biological behaviors of polylactic acid composite materials. **Mater. Lett.** 61: 3009-3013.

Liu, Q., Wijn, J. R., Groot, K., and Blitterswijk, C. A. (1998). Surface modification of nano-apatite by grafting organic polymer. **Biomaterials.** 19: 1067-1072.

Li, X., Feng, Q., and Cui, F. (2006). *In vitro* degradation of porous nano hydroxyapatite/collagen/PLLA scaffold reinforced by chitin fibres. **Mater. Sci. Eng. C.** 26: 716-720.

Lorprayoon, C. (1989). Synthesis of calcium hydroxyapatite and tricalcium phosphate from bone ash. **Ion. Polym. Order. Polym. Hi. Perf. Mater. Biomater.** 329-336.

Navarro, M., Ginebra, M. P., Planell, J. A., Barrias, C. C., and Barbosa, M. A. (2005). *In vitro* degradation behavior of a novel bioresorbable composite material based on PLA and a soluble CaP glass. **Acta Biomater.** 1: 411-419.

Nejati, E., Firouzdor, V., Eslaminejad, M. B., and Bagheri, F. (2009). Needle-like nano hydroxyapatite/poly(L-lactide acid) composite scaffold for bone tissue engineering application. **Mater. Sci. Eng. C.** 29: 942-949.

Ooi, C. Y., Hamdi, M., and Ramesh, S. (2007). Properties of hydroxyapatite produced by annealing of bovine bone. **Ceram. Int.** 33: 1171-1177.

Ruksudjarit, A., Pengpat, K., Rujijanagul, G., and Tunkasiri, T. (2008). Synthesis and characterrization of nanocrystalline hydroxyapatite from natural bovine bone. **Curr. Appl. Phys.** 8: 270-272.

Russias, J., Saiz, E., Nalla, R. K., Gryn, K., Ritchie, R. O., and Tomsia, A. P. (2006). Fabrication an mechanical properties of HA/PLA composites:A study of *in vitro* degradation. **Mater. Sci. Eng.** 26: 1289-1295.

Shikinami, Y. and Okuno, M. (2001). Bioresorbable devices made of forged composites of hydroxyapatite (HA) particles and poly-L-lactide (PLLA): Part I. Basic characteristics. **Biomaterials.** 20: 859-877.

Shikinami, Y. and Okuno, M. (2001). Bioresorbable devices made of forged composites of hydroxyapatite (HA) powders and poly L–lactide (PLLA). Part II: practical properties of miniscrews and miniplate. **Biomaterials.** 22: 3197-3211.

Shinzato, S., Nakamura, T., Kokubo, T., and Kitamura, Y. (2001). Bioactive bone cement: Effect of silane treatment on mechanical properties and osteoconductivity. **J. Biomed. Mater. Res.** 55: 277-284.

Tadakasu, M. and Toru, M., (1998). Crystallization behavior of poly(L-lactide). **Polymer.** 39: 5515-5521.

Takayama, T., Todo, M., and Takano, A. (2008). The effect of bimodal distribution on the mechanical properties of hydroxyapatite particle filled poly(L-lactide) composites. **J. Mech. Behav. Biomed. Mater.** 2: 105-112.

Todo, M., Park, S. D., Arakawa, K., and Takenoshita, Y. (2006). Relationship between microstructure and fracture behavior of bioabsorbable HA/PLLA composites. **Composites: Part A.** 37: 2221-2225.

Tsuji, H. and Ikarashi, K. (2004). *In vitro* hydrolysis of poly(L-lactide) crystalline residues as extended-chain crystallites. Part I: long-term hydrolysis in phosphate-buffered solution at 37°C. **Biomaterials.** 25: 5449-5455.

Verheyen, C. C. P. M., Klein, C. P. A. T., Blieckhogervorst, J. M. A., Wolke, J. G. C., Blitterswijn, C. A., and Groot, K. (1993). Evaluation of hydroxylapatite/poly (L-lactide)composites: physico-chemical properties. **J. Mater. Sci. Mater. Med.** 4: 58-65.

Wang, M., Deb, S., and Bonfield, W. (2000). Chemically coupled hydroxyapatite-polyethylene composites: processing and characterization. **Mater. Lett.** 44: 119-124.

Wang, M. and Bonfield, W. (2001). Chemically coupled hydroxyapatite-polyethylene composites:structure and properties. **Biomaterials.** 22: 1311-1320.

Wen, J., Li, Y., Zuo, Y., Zhou, G., Li, J., Jiang, L., and Xu, W. (2008). Preparation and characterization of nano-hydroxyapatite/silicone rubber composite. **Mater. Lett.** 62: 3307-3309.

Yuan, X., Mak, A. F. T., and Yao, K. (2002). Comparative observation of accelerated degradation of poly(l-lactic acid) fibres in phosphate buffered saline and a dilute alkaline solution. **Polym. Degrad. Stab.** 75: 45-53.

Yoganand, C. P., Selvarajan, V., Wu, J., and Xue, D. (2009). Processing of bovine hydroxyapatite (HA) powders and synthesis of calcium phosphate silicate glass ceramics using DC thermal plasma torch. **Vacuum.** 83: 319-325.

Zhang, S. M., Liu, J., Zhou, W., Cheng, L., and Guo, X. D. (2005). Interfacial fabrication and property of hydroxyapatite/polylactide resorbable bone fixation composites. **Curr. Appl. Phys.** 5: 516-518.

Zheng, X., Zhou, S., Li, X., and Weng, J. (2008). Shape memory properties of poly(D,L-lactide)/hydroxyapatite composites. **Biomaterials.** 27: 4288-4295.

CHAPTER III

A COMPARATIVE OBSERVATION ON PHYSICAL PROPERTIES OF BOVINE BONE BASED HA/PLA COMPOSITES FROM MELT-MIXING AND SOLUTION-MIXING TECHNIQUES

3.1   Abstract

Bovine bone based hydroxyapatite (u-HA) powder was produced by grinding heated bovine bone. SEM micrograph showed that the obtained powder, after calcination at 1100ºC, composed of agglomerated HA particles. u-HA/PLA composites at various contents of HA were prepared by either melt-mixing or solution-mixing techniques. The u-HA/PLA composites prepared by melt-mixing exhibited the more homogeneous distribution of u-HA in PLA matrix as compared with the composites prepared by solution-mixing technique. In comparison, tensile modulus, tensile strength and impact strength of the melt-mixed composites were higher than those of the solution-mixed composites. Moreover, decomposition temperatures of the melt-mixed composites were higher than those of the solution-mixed composites. Nonetheless, average molecular weights of PLA in the solution-mixed composites, as confirmed by GPC, were significantly higher than those in the melt-mixed composites.

3.2 Introduction

Hydroxyapatite (HA: $Ca_{10}(PO_4)_6(OH)_2$) has been investigated as a biomaterial and used in various medical applications because of its excellent biocompatibility, osteoconductivity and bone-bonding ability (Kothapalli, Shaw, and Wei, 2005; Shikinami *et al*., 2001; Ruksudjarit *et al*., 2008). HA can be obtained not only from chemical synthesis but also from natural sources, *e.g.* coral, bovine bone. In recent years, natural HA is attracting much attention from points of natural and less expensive material. HA can be used either in a single component form, or as a filler for polymer composites (Ruksudjarit *et al*., 2008; Coutand, Cyr, Deydier, Guilet, and Clastres, 2008; Fathi, Hanifi, and Mortazavi, 2008; Ooi *et al*., 2007; Deng *et al*., 2001). Many kinds of bioresorbable polymers have been developed and used in medical applications. Among those polymers, poly(lactic acid) (PLA) is a good candidate due to its biodegradability and yielding nontoxic byproducts after hydrolysis reaction (Kothapalli *et al*., 2005; Shikinami *et al*., 2001; Russias *et al*., 2006; Tsuji *et al*., 2004). Hence, a composite between HA and PLA is a good alternative for using as a biomaterial since it combines strength and stiffness of HA with flexibility and resorbability of PLA and, then, solves the drawbacks of both materials. Additionally, HA/PLA composite is easy to process into required shapes and is expected to be a promising composite as an implant in non-load bearing parts (Deng *et al.*, 2001; Russias *et al.*, 2006; Zhang *et al*., 2005).

However, one of the major problems for manufacturing of the HA/PLA composite is the agglomeration of the HA powder in the PLA matrix. In general, fine HA particles tend to combine together, through electrostatic or van der Waals forces to form agglomerated particles. This agglomeration of HA tends to decrease

mechanical properties of the composite. So, the selected technique for preparing the HA/PLA composites must have the ability to breake down agglomerated HA and disperse them into the PLA matrix (Mathieu, Bourban, and Manson, 2006). By an effective mixing process, homogeneous distribution of HA powder in PLA matrix and enhancement of mechanical properties of the composite are obtained. Nowadays, many techniques have been used to prepare HA/PLA composite, such as solution mixing (Lin *et al.*, 2007), forging (Shikinami *et al.*, 2001) and hot pressing method (Jamshidi, Hyon, and Ikada, 1988).

Melt-mixing and solution-mixing are frequently used techniques for preparing HA/PLA composites. Upon preparing the composite, melt-mixing technique generates higher shear force and higher temperature than solution-mixing technique. The high shear force and the high mixing temperature would promote the distribution of HA in PLA matrix. Nevertheless, melt-mixing technique would cause adverse effect to the PLA matrix since PLA is a thermally sensitive polymer leading to the deterioration of its molecular weight (Ignjatovic *et al.*, 2004). In contrast, solution-mixing technique causes lower shear force and lower temperature than melt-mixing technique. The low shear force and the low mixing temperature would protect PLA from thermal degradation. Conversely, the low shear force and the low mixing temperature might affect the distribution of HA in PLA matrix.

In this present study, bovine bone based HA was prepared and, then, incorporated into PLA by either solution-mixing or melt-mixing techniques. Effects of preparation technique and filler content on morphological, mechanical and thermal properties of HA/PLA composites were determined. Furthermore, degradation of PLA chains in the composites prepared by those two techniques was also investigated.

3.3   Experimental

3.3.1   Materials

PLA (4042D) was purchased from NatureWorks LLC Co, Ltd. Bovine bones were supplied by Limeiseng Co., Nakhon Ratchasima. Chloroform (AR grade) was purchased from Labscan Co, Ltd.

3.3.2   Preparation of u-HA powder

Bovine bones were burned in open air and were ground into powder using a ball milling machine. Then, the powder was calcined at 1100ºC for 3 h and the obtained powder was called u-HA.

3.3.3   Characterization of u-HA powder

The calcined bovine bone powder was analyzed by X-ray diffractometer (XRD) (OXFORD/D5005) with a Cu-Kα as a radiation source. A step size of 0.02º and a scan speed of 0.4º/min were used while the voltage was held at 35 kV.

Functional groups of u-HA powders were identified by a Fourier transform infrared spectrometer (FTIR) (BIO-RAD/FTS175C, KBr pellet technique). The spectrum was recorded in the 4000-400 cm^{-1} region with 2 cm^{-1} resolution.

In addition, a scanning electron microscope (SEM) (JOEL/JSM-6400) operating at 15 kV was used to reveal microstructure of the HA powder.

3.3.4   Preparation of u-HA/PLA composites

u-HA/PLA composites were prepared through either solution-mixing or melt mixing techniques. The weight ratios of HA/PLA are shown in Table 3.1.

For solution-mixing technique, 20 g of PLA was dissolved in 100 ml of chloroform at room temperature for 3 h. Then, u-HA was added to PLA solution

and the mixture was ball milled for 4 h. The mixture was poured onto clean Petri dishes and dried at room temperature for 48 h and at 70°C in a vacuum-oven for 24 h. Then, each composite resin was ground into small pieces (about 0.3 cm in length).

For melt-mixing technique, HA/PLA composites were prepared using an internal mixer (HAAKE/RHEOMIX). PLA and u-HA were mixed at 170ºC with a rotor speed of 70 rpm for 10 min. Each HA/PLA composite was left at room temperature for 24 h and ground into small pieces (about 0.3 cm in length).

Various molding dies according to ASTM D638-03 and D256 standards were used to prepare composite specimens for mechanical testing. The HA/PLA composite was heated in the dies from room temperature to 180°C and maintained at that temperature for 15 min. Subsequently, it was hot-pressed at 180ºC by a compression molding machine (GOTECH/GT-7014-A30) for 10 min under a pressure of 2000 psi and cooled to room temperature.

Table 3.1 Composition of HA/PLA composites

Designation	Filler content (wt%)	Preparation technique
PLA-S	-	solution-mixing
PLA-M	-	melt-mixing
1S	10	solution-mixing
2S	20	solution-mixing
3S	30	solution-mixing
4S	40	solution-mixing
1M	10	melt-mixing
2M	20	melt-mixing
3M	30	melt-mixing
4M	40	melt-mixing

3.3.5 Determination of morphological properties of u-HA/PLA composites

A scanning electron microscope (SEM) (JEOL/JSM-6400) operating at 15 kV was used to visualize fractures surfaces of the HA/PLA composites. All samples were coated with a thin layer of gold before examining.

3.3.6 Determination of thermal properties of u-HA/PLA composites

Thermal decomposition temperature and weight loss of u-HA/PLA composite were determined by a thermogravimetric analyzer (TGA) (TA INSTRUMENT/SDT2960). The sample was heated from room temperature to 600ºC under a nitrogen atmosphere at a heating rate of 10ºC/min.

3.3.7 Determination of PLA molecular weight

Molecular weights of the as-received PLA and the PLA in the HA/PLA composites were evaluated using a gel permeable chromatography (GPC). The GPC instrument was equipped with universal styrene-divinylbenzene copolymer columns (PLgel Mixed-C, 300×7.5 mm, 5µm), differential refractometer detector (AGILENT/RI-G1362A), online degasser (AGILENT/G1322A), autosampler (AGILENT/G1329A), thermostatted column compartment (AGILENT/G1316A) and quaternary pump (AGILENT/G1311A). Chloroform was used as an eluent. The eluent flow rate was kept constant at 0.5 ml/min. Temperature of the column and the detector was maintained at 40ºC and 35ºC respectively. Polystyrene standards (Shodek standard) with a molecular weights of $3.90×10^6$, $6.29×10^5$, $6.59×10^4$, $9.68×10^3$ and $1.30×10^3$ g/mol were used to generate a calibration curve. Compression-molded specimens of PLA and HA/PLA composites were dissolved and diluted using chloroform (2 mg/ml), and filtered before injection.

3.3.8 Determination of mechanical properties of u-HA/PLA composites

Tensile properties of HA/PLA composites were investigated according to ASTM D638-03 using a universal testing machine (INSTRON/5569).

Izod impact strength of unnotched HA/PLA specimens were determined using an impact testing machine (ATLAS/BPI) according to ASTM D256.

3.4   Results and discussion

3.4.1   Characterization of u-HA powder

XRD patterns of calcined bovine bone powder and pure HA are shown in Figure 3.1. All the peaks of the calcined bone powder matched with those of pure HA confirming that the bovine bone powder mainly composed of HA. In addition, the XRD pattern also indicated that the calcined bovine bone powder was in crystalline form. So, the bovine bone powder was called u-HA in this present study.
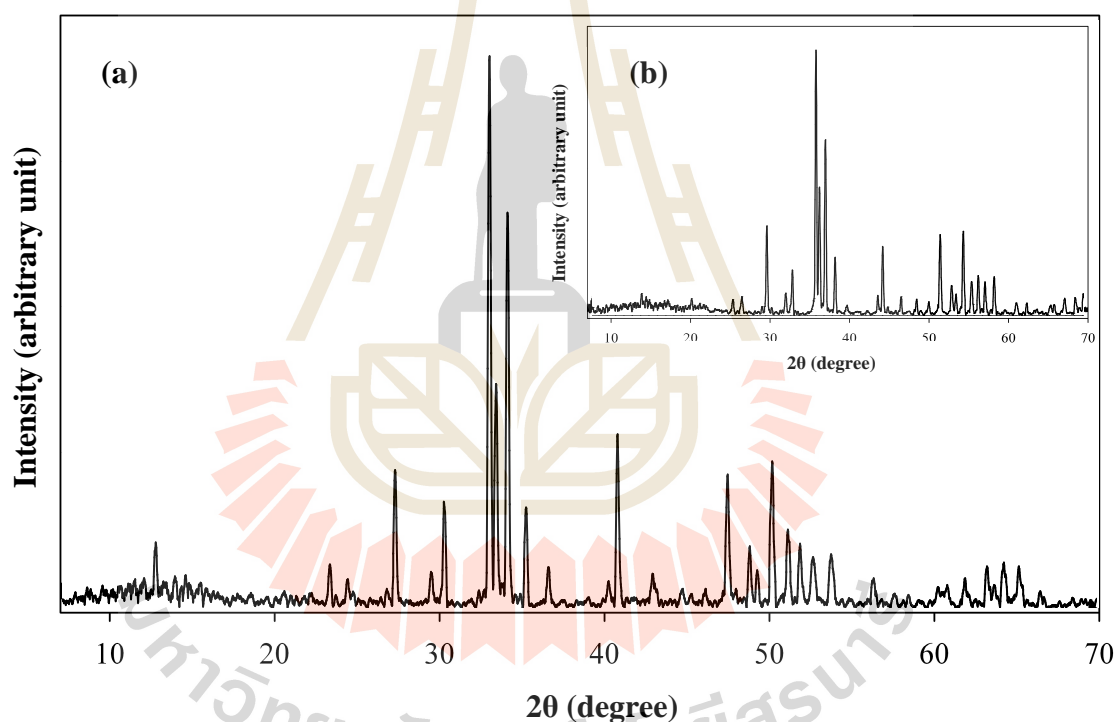
Figure 3.1 XRD pattern of (a) calcined bovine bone powder and (b) pure HA.

FTIR spectrum of u-HA is shown in Figure 3.2. The peaks at 1085, 1036, 963, 600 and 575 cm^{-1} were assigned to different vibration modes of PO_4^{3-} group in HA powder. The stretching and the bending vibration of structural OH

groups in the apatite lattice were observed at 3571 cm^{-1} and 632 cm^{-1}, respectively. Additionally, vibrational peaks corresponding to CO_3^{2-} groups were also observed at 1457, 1411 and 878 cm^{-1} (Fathi *et al.*, 2008; Ooi *et al.*, 2007). Therefore, these vibration peaks indicated that the calcined bovine bone powder was carbonated HA. The appearance of carbonate functional groups on surface of the obtained powder could be explained as follows: (1) During heating process, adsorbed carbon from atmosphere substituted the PO_4^{3-} groups of the HA or (2) The incompletely pyrolyzed carbon dissolved into the hydroxyapatite crystal (Shinzato *et al.*, 2001; Furuzono *et al.*, 2001; Wen *et al.*, 2008).
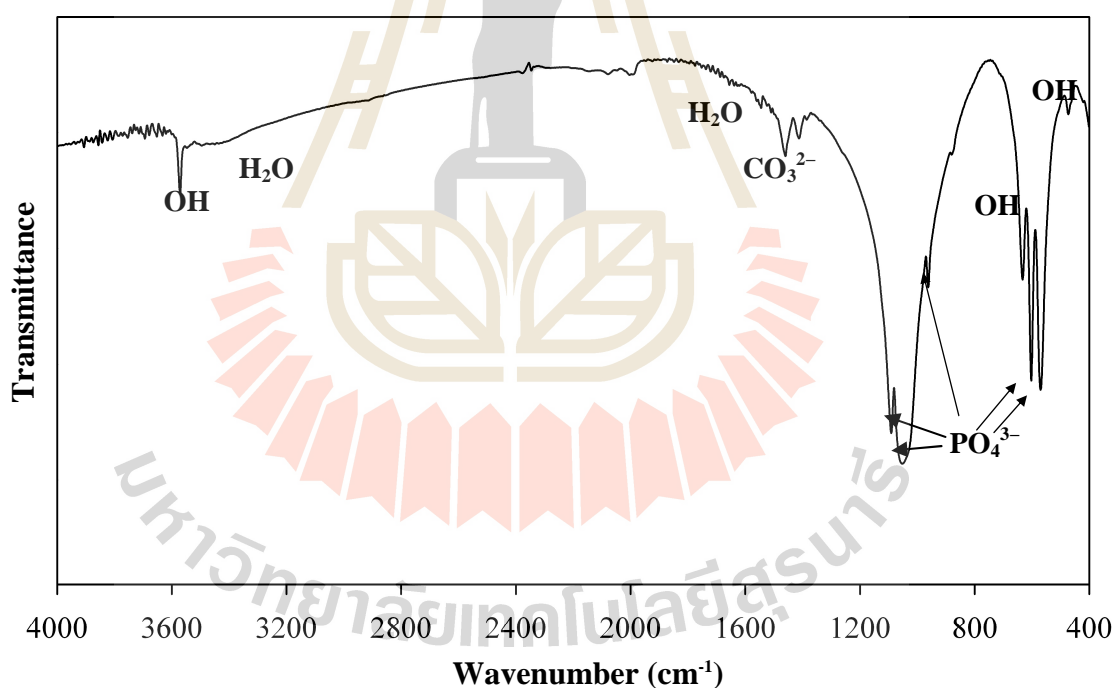
Figure 3.2 FTIR spectrum of bovine bone based HA after calcined at 1100ºC.

SEM micrographs of u-HA are shown in Figure 3.3 (a-b). The micrograph in Fig. 3.3 (a) shows the agglomeration of u-HA powder. The micrograph

at higher magnification (Fig. 3.3 (b)) revealed that the agglomerated u-HA composed of particles with irregular shape.

(a)   **(b)**
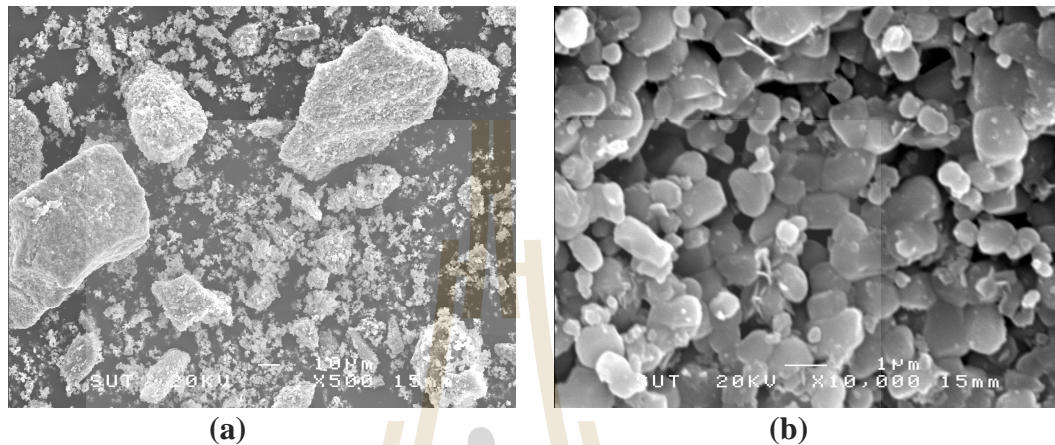
Figure 3.3 SEM micrographs of HA powders: (a) u-HA at low magnification (X500),

(b) u-HA at high magnification (X 10^4).

3.4.2   Morphological properties of u-HA/PLA composites

Figure 3.4 shows SEM micrographs of tensile fracture surfaces of the u-HA/PLA composites containing 20wt% of u-HA prepared by solution-mixing and melt-mixing techniques. In Figure 3.4 (a), agglomeration of u-HA in the composite prepared by solution-mixing technique was clearly observed. Also, a gap was noticeable at the interface between u-HA and PLA matrix. This indicated that there was no adhesion between u-HA surface and PLA matrix. On the other hand, u-HA in the composite prepared by melt-mixing technique exhibited more homogenous distribution and less agglomeration in the PLA matrix, as shown in Figure 3.4 (b). However, some u-HA agglomeration and the gap between two phases was also observed.

From the morphological micrographs, it was clearly shown that the melt-mixing technique led to a homogeneous distribution of u-HA particles in the PLA matrix whereas solution-mixing technique gave more agglomerated HA particles, isolating PLA rich zones and less intimate blending of the two components. According to the less homogeneous distribution of u-HA in the solution-mixed composites, the filamentous structure of PLA, after tensile testing, was observed (Figure 3.4 (a)), indicating the higher ductility of the composites as mentioned in the mechanical properties section (elongation at break).

(a)   **(b)**
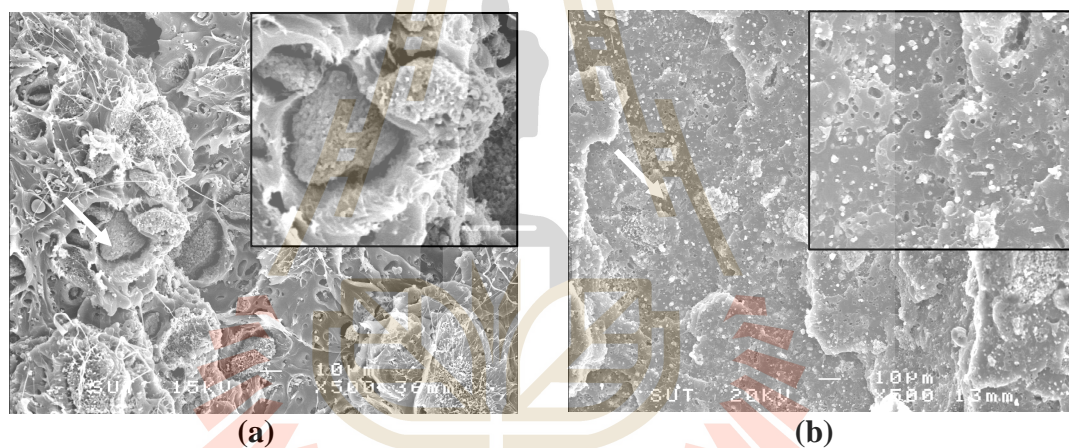
Figure 3.4 SEM micrographs of fracture surfaces of u-HA/PLA composites at 20wt% of u-HA: (a) solution-mixed composite and (b) melt-mixed composite.

3.4.3 Thermal properties of u-HA/PLA composites

Figure 3.5 (a-b) shows TGA and DTG thermograms of as-received PLA, processed PLA and u-HA/PLA composite prepared by either solution-mixing technique or melt-mixing technique. In addition, the onset of degradation temperature and the peak of degradation temperature of each sample are summarized in Table 3.2. According to the onset and the peak of degradation temperatures, as-received PLA had higher thermal stability than the processed PLA. These results implied that the chain scissions of PLA occurred during preparation.

In comparison at an equal content of u-HA, the melt-mixed composites had higher thermal stability than the solution-mixed composites. In the composites prepared by melt-mixing technique, the volatile products were probably blocked by the good distribution of u-HA in PLA matrix (Figure 3.4 (b)). In contrast, the composites prepared by solution-mixing technique exhibited more agglomeration of u-HA ((Figure 3.4 (a)), therefore, the composites would loss their volatilization blocking ability.

Moreover, the thermal stability of the composites prepared by both techniques decreased with increasing u-HA content. This may be because of the poor distribution of u-HA in PLA. At higher content of u-HA, u-HA tended to agglomerate in PLA matrix much more than it did at lower content of u-HA since there was polarity difference between HA surfaces and PLA matrix.

Table 3.2 The onset and the peak of degradation temperature of as-received PLA and
the composites at various processing conditions.

Designation	Preparation technique	Degradation temperature (°C)	
		Onset	Peak
as-received PLA	-	297	380
PLA-S	solution-mixing	293	372
PLA-M	melt-mixing	293	372
2S	solution-mixing	272	335
2M	melt-mixing	285	348
4S	solution-mixing	254	316
4M	melt-mixing	265	325
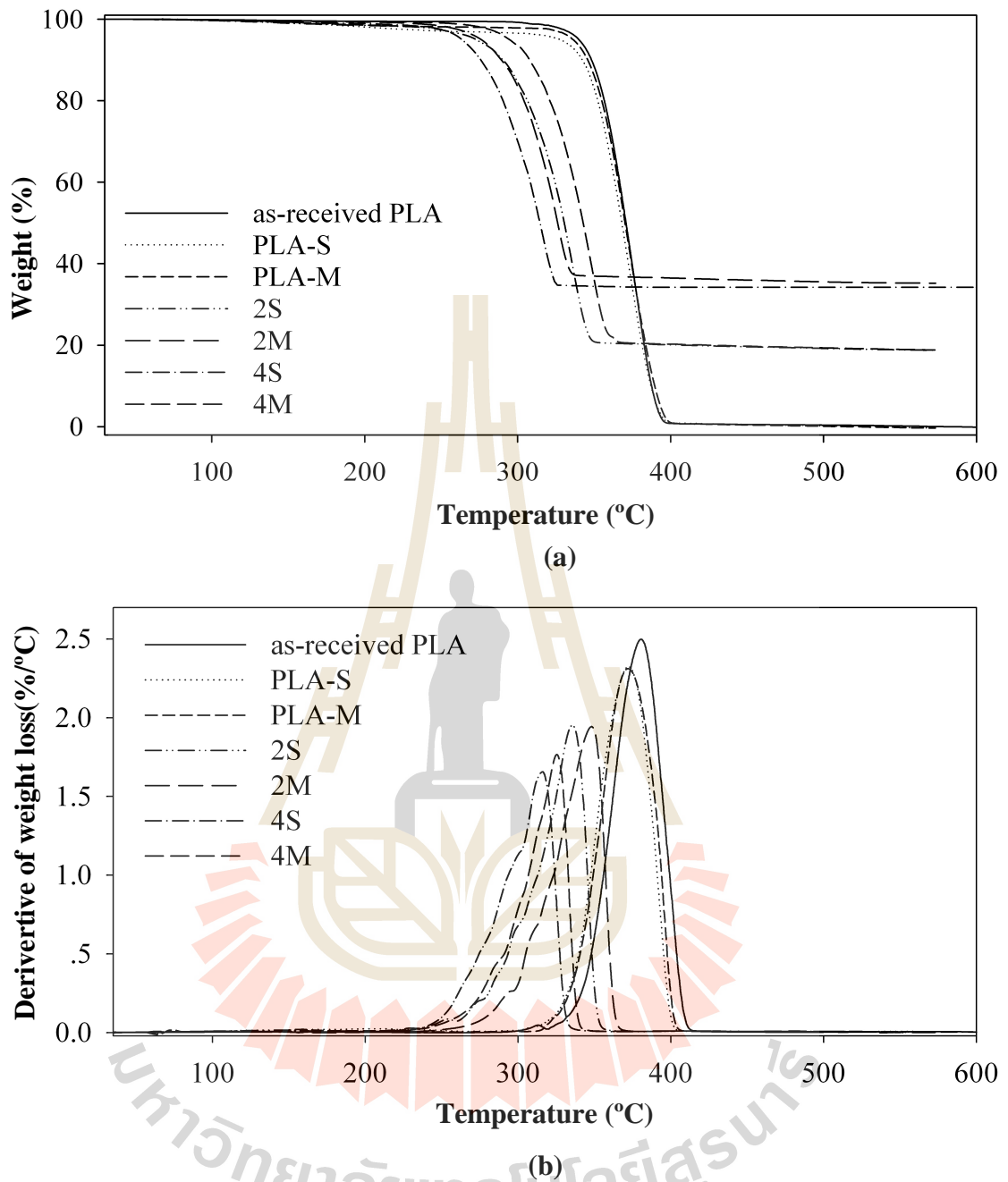
Figure 3.5 (a) TGA and (b) DTGA thermograms of as-received PLA, PLA and

u-HA/PLA composite prepared by solution-mixing technique (PLA-S,

2S, 4S), PLA and u-HA/PLA composites prepared by

melt-mixing technique (PLA-M, 2M, 4M).

Several researchers have studied thermal properties of polymer composites. They found in their system that the thermal decomposition temperature of the polymer composites increased as compared with that of the neat polymer. According to their works, an increase in thermal stability of a polymer composite could be explained in two aspects: either decomposition products are blocked by a high thermally stable filler (Fukushima, Tabuani, and Camino, 2009) or the filler in the composite acts as a barrier preventing heat transfer (Ignjatovic *et al.*, 2004). This was in contrast to the present results. All processed samples exhibited lower thermal stability than as-received PLA. This was probably due to the limit in the distribution and dispersion of u-HA in PLA matrix.

3.4.4 Average molecular weight of PLA in u-HA/PLA composites

It was known that PLA chains can be easily broken at a particular temperature range resulting in lower molecular weight PLA, oligomers, monomers and gas-products (Ignjatovic *et al.*, 2004). Therefore, during the preparation of HA/PLA composite, the PLA chains could possibly be degraded by the high processing temperature. Molecular weight of PLA in as-received PLA and in HA/PLA composites prepared by different preparation technique were further investigated by GPC techniques. Table 3.3 illustrates molecular weights and molecular weight distribution of PLA in as-received PLA, processed PLA and u-HA/PLA composites which were affected by preparation techniques and u-HA content.

Based on the GPC results, $\overline{M}_n$ and $\overline{M}_w$ of PLA after solution-mixing (PLA-S) and PLA after melt-mixing (PLA-M) were lower than those of as-received PLA. Also, its MWD was increased. The decrease in molecular weight and the

increase in MWD of the processed PLA after passing through both mixing techniques revealed the occurrence of PLA chain scission. As compared between two techniques, $\overline{M}_w$ and $\overline{M}_n$ of PLA-S were higher than those of PLA-M while MWD of PLA-S was narrower than that of PLA-M. It was due to the thermal oxidative degradation of PLA chain during melt-mixing process. These results were similar to the research work investigated by Signori, Coltelli, and Bronco (2009). They have found that the increase in MWD of PLA after thermal degradation. This was a course of a random rearrangement of PLA chains upon chain scission and chain recombination. Additionally, Perego, Cella, and Bastioli (1996) reported a decrease in PLA molecular weight during high temperature processing. They have found that after injection molding of PLA at 195°C, molecular weight of PLA was decreased by 14-40%.

In comparison, the PLA chains in melt-mixed composites had lower $\overline{M}_w$ and $\overline{M}_n$ than those in solution-mixed composites. Additionally, MWD of PLA in the composites prepared by melt-mixing technique were higher than those of the composites prepared by solution-mixing technique. At an equal content of u-HA, the more distribution of u-HA in the melt-mixed composites (Figure 3.4 (b)) increased the chance of OH groups on u-HA surface to interact with PLA chains and, further, the breaking of bonds in the PLA chains would occur. The interaction between OH on u-HA surface and PLA chains led to the more decrease in the molecular weight of PLA. This result was similar to the research work done by Ignjatovic *et al.* (2004). They have investigated the effect of the hot pressing on the structure and characteristics of HA/PLLA composite and found that the OH groups at the end of PLA chain can destroy the PLA basic chain under the influence of thermal energy.

In addition, the molecular weight of PLA of the composites prepared by both techniques decreased with increasing u-HA content while their MWD increased. These results indicated that PLA chain scission upon composite preparation increased with increasing of u-HA content. As increasing u-HA content in the composites, the PLA matrix was more exposed to OH-containing surface of u-HA by which PLA molecules underwent more chain scission.

However, there are various factors affecting the decrease in molecular weight of PLA during melt-mixing preparation which have been reported by other research works (Wang, Joseph, and Bonfield, 1998; Mathieu *et al*., 2006). The mechanisms leading to breakdown of PLA chains are proposed as follows; firstly, hydrolysis of ester bond on PLA backbone. An increase in hydrolysis degradation of PLA chains is potentially due to the presence of water absorbed on filler surface, therefore, the filler should also be thoroughly dried to eliminate water traces. Secondly, zipper-like depolymerization will be occurred when trace amount of catalyst still present in the system. Thirdly, oxidative random chain scission will be occurred if melt-mixing processing were done under air atmosphere. The last two mechanisms are intermolecular transesterification to monomer or oligomers and intramolecular transesterification to form monomers or oligomers. According to the results in this section, it should be noted that oxidative random chain scission of PLA was the reasonable mechanisms for the lowering in $\overline{M}_n$ and $\overline{M}_w$ and the increasing in MWD of PLA chains in the u-HA/PLA composites. Also, this mechanism was accelerated in the presence of OH-containing surface of HA.

Table 3.3 Molecular weight of PLA in as-received PLA and the composites at various processing conditions.

Designation	Preparation technique	Average molecular weight		MWD
		$\overline{M}_w$	$\overline{M}_n$	
as-received PLA	-	2.83×10^5	1.31×10^5	2.16
PLA-S	solution-mixing	2.54×10^5	1.02×10^5	2.49
PLA-M	melt-mixing	1.94×10^5	0.76×10^5	2.55
1S	solution-mixing	2.34×10^5	0.97×10^5	2.41
2S	solution-mixing	2.21×10^5	0.87×10^5	2.54
3S	solution-mixing	2.11×10^5	0.75×10^5	2.81
4S	solution-mixing	2.02×10^5	0.69×10^5	2.93
1M	melt-mixing	0.67×10^5	0.11×10^5	6.09
2M	melt-mixing	0.61×10^5	0.10×10^5	6.10
3M	melt-mixing	0.56×10^5	0.09×10^5	6.22
4M	melt-mixing	0.53×10^5	0.08×10^5	6.63

3.4.5 Mechanical properties of u-HA/PLA composites

Tensile modulus, elongation at break, tensile strength and impact strength of u-HA/PLA composites are illustrated in Figure 3.6-3.9, respectively. Tensile moduli of u-HA/PLA composites were higher than those of the as-received PLA as observed in Figure 3.6. In comparison, at the same filler content, the composites prepared by melt-mixing technique has higher tensile moduli than the composites prepared by solution-mixing technique. The higher stiffness of the melt-mixed composites was because of the good distribution and dispersion of u-HA in PLA matrix (Figure 3.4 (b)). In addition, the tensile moduli of the composites

prepared by both techniques increased with increasing u-HA content since the rigid

u-HA filler has more chance to restrict the molecular motion and the deformation of
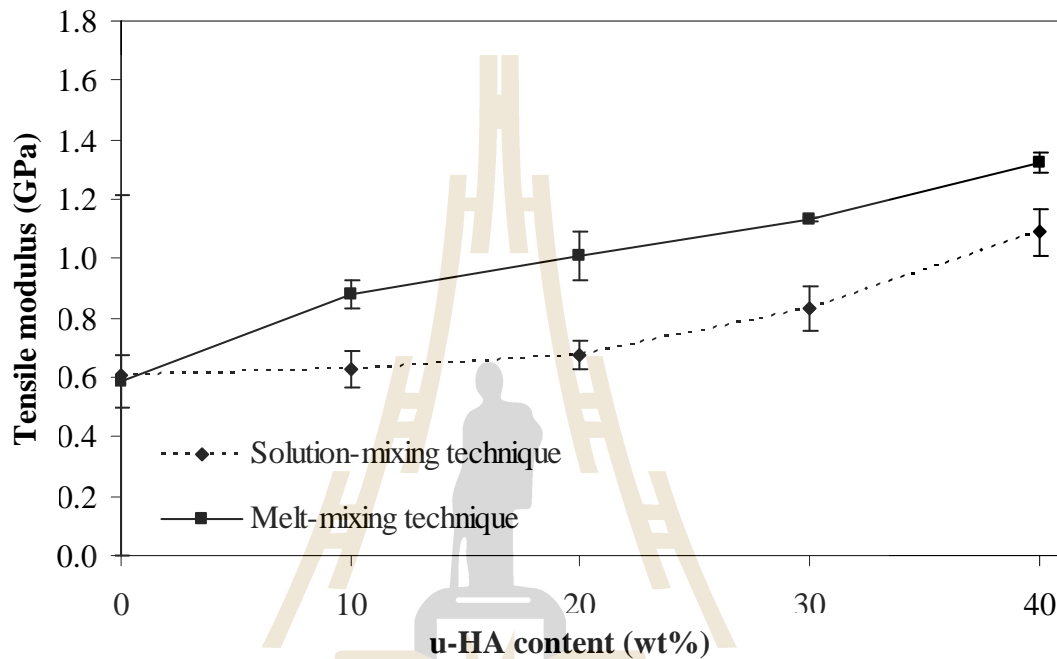
the PLA chains.

Figure 3.6 Tensile modulus of HA/PLA composites at various u-HA contents.

Elongation at break of all HA/PLA composites was lower than that of

the as-received PLA, as shown in Figure 3.7. The incorporated HA decreased the

mobility of PLA chains and led to the decreasing in ductility of the composites. In

comparison, the solution-mixed composite had slightly higher elongation at break

than the melt-mixed composite of the corresponding HA content. According to the

SEM micrographs, the less homogeneous distribution of u-HA in the solution-mixed

composites created the filamentous structure of PLA indicating the higher ductility of
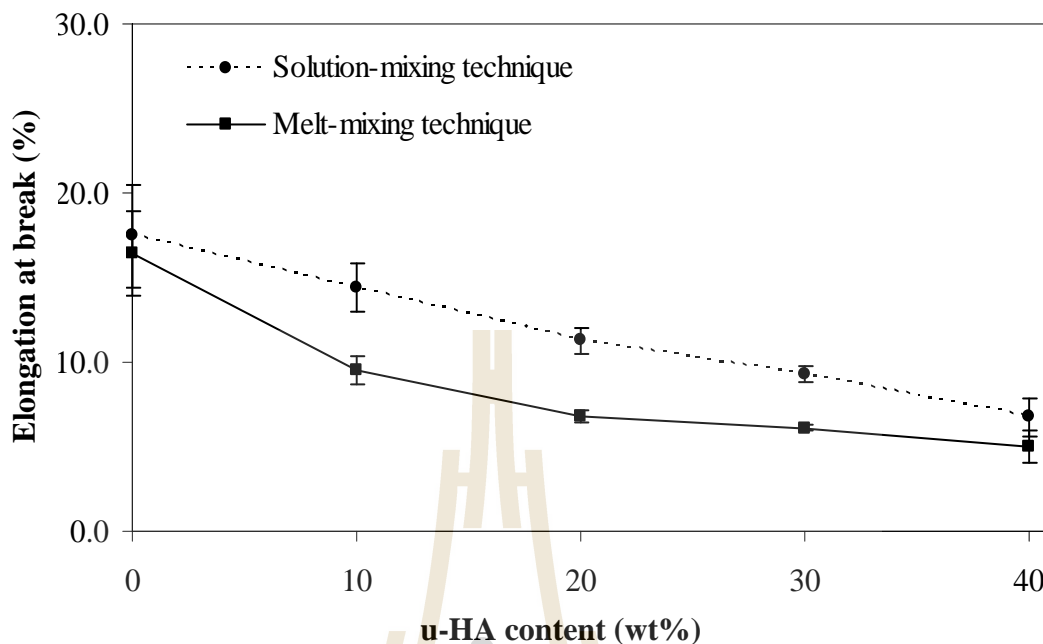
the composites.

Figure 3.7 Elongation at break of HA/PLA composites at various u-HA contents.

As shown in Figure 3.8, the lowering in tensile strength of the composites than those of PLA-S and PLA-M was observed. This was because u-HA as foreign inclusion disrupted the interaction between PLA molecules. Moreover, tensile strength of the composites prepared by both techniques was decreased with increasing u-HA content. This indicated the weak interaction between the two phases.

In addition, the tensile strength of the composites prepared by melt-mixing technique was higher than that of the composites prepared by solution-mixing technique. The u-HA agglomeration and the poor adhesion between agglomerated u-HA and PLA matrix illustrated in Figure 3.4 (a) could be the main reason that was responsible for the obvious reduction in the tensile strength of the solution-mixed composites. On the other hand, the more homogeneous distribution and the less agglomeration of u-HA in PLA matrix of melt-mixed composites create smaller size of voids by which tensile strength was increased.
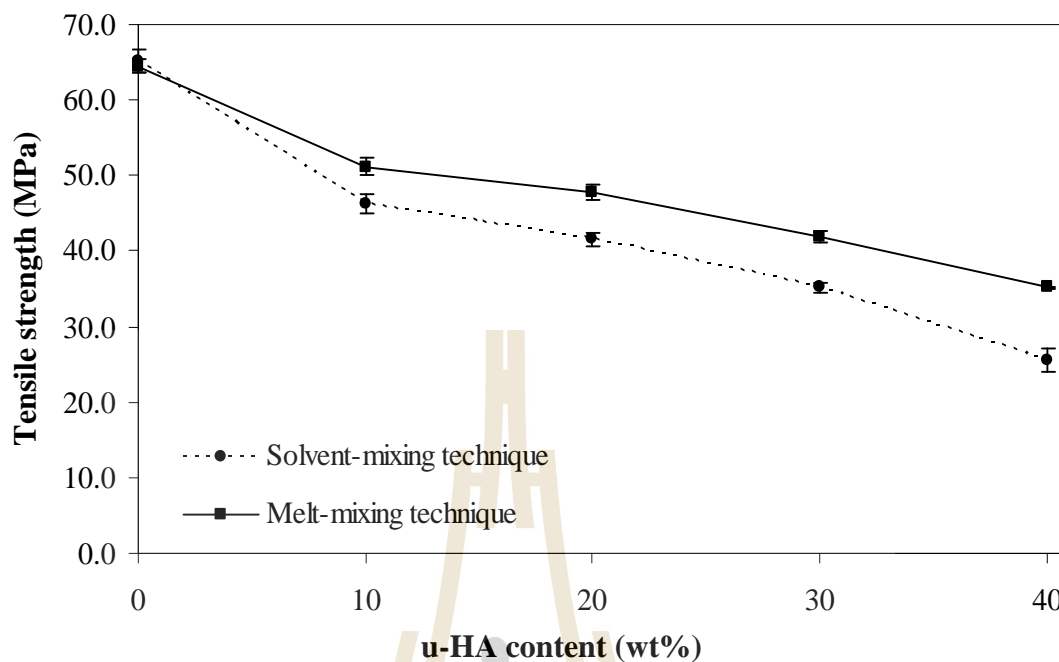
Figure 3.8 Tensile strength of HA/PLA composites at various u-HA contents.

Based on tensile modulus and tensile strength results, it should be noted that the difference between two techniques was much more emphasized with increasing u-HA content. This could be explained as follows ; at low content of u-HA, the u-HA could easily distribute into PLA matrix by both preparation techniques. On the other hand, at high content of u-HA, the melt mixing technique with high shear force and high temperature could distribute u-HA into PLA matrix better than the solution-mixing technique. This led to the more effective enhancement of tensile modulus and tensile strength of the u-HA/PLA composites.

In addition, impact strength of all u-HA/PLA composites was lower than that of the as-received PLA as shown in Figure 3.9. This was because u-HA disturbed matrix continuity and limited the ability of polymer chains to absorb impact energy. The large agglomerates and a large gap around agglomerated u-HA are the

site of stress concentration, which can act as a microcrack initiator. However, the composites prepared by melt-mixing technique showed less reduction in impact strength than the composites prepared by solution-mixing technique. This result was because the melt-mixed process dispersed u-HA into PLA matrix better than the solution-mixed process. Therefore, the melt-mixed composites with smaller size of agglomerated u-HA could dissipate impact energy better than the solution-mixed composites.
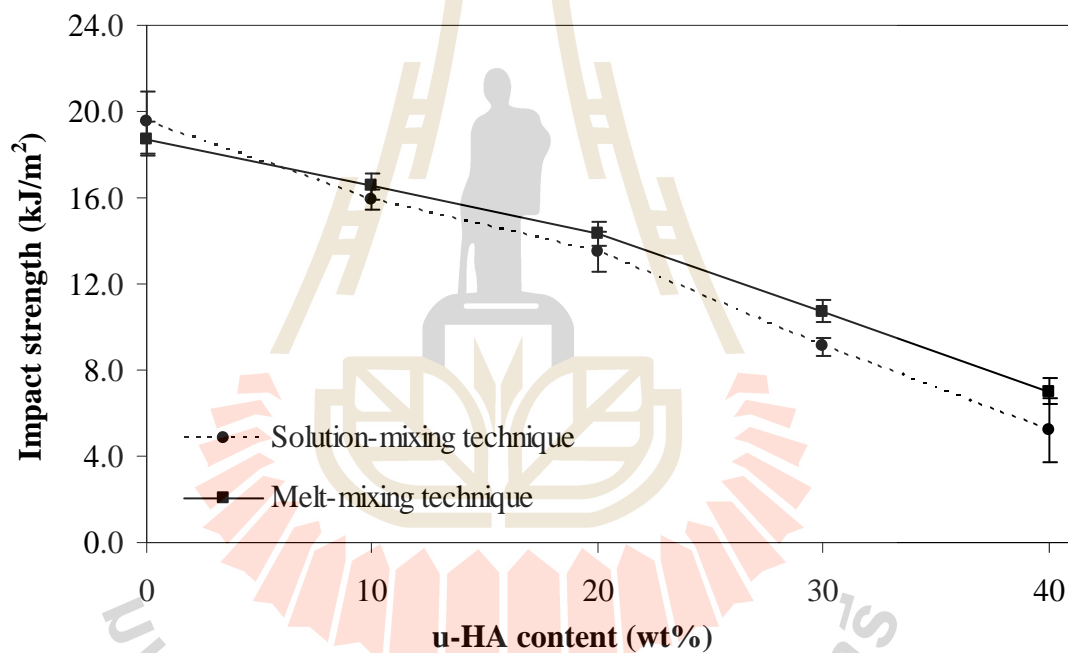
Figure 3.9 Impact strength of HA/PLA composites at various u-HA contents.

In comparison, the results showed that the composites prepared by melt-mixing technique had higher tensile modulus, tensile strength and impact strength (Figure 3.6, 3.8 and 3.9, respectively) than those of the composite prepared by solution-mixing technique. This was because of better distribution, better dispersion and smaller size of u-HA in PLA matrix as the results of high temperature

and high shear force during the melt-mixing process. The high rotor speeds generated the force and thus pressure exerted on the PLA melt and leading to a more homogeneous composite. Also, a high mixing temperature led to an improved dispersion of the u-HA in the PLA matrix, due to a lower viscosity of the melted PLA (Ignjatovic *et al.*, 1999). The degradation of PLA chains at high mixing temperature were observed. Nonetheless, the degradation of PLA chains was in an acceptable level as seen from the mechanical properties of the melt-mixed composites.

Moreover, the major drawback found in the composite prepared by solution-mixing technique is the use of an organic solvent. Mathieu *et al.* (2006) reported the presence of residual chloroform in PLA composites, determined by nuclear magnetic resonance (^{1}H NMR). It was well known that organic solvents are potentially toxic for living organisms. Therefore, the remaining chloroform in the composites, that expected to be used in biomedical applications, may cause adverse effects to biocompatibility of the materials.

According to the results, it should be noted that the homogeneously distributed HA in PLA matrix had more influence on the mechanical properties of the composites than the degradation of PLA chains upon preparation. In order to obtain u-HA/PLA composites with good mechanical properties and avoid the use of an organic solvent, melt-mixing technique was selected.

3.5 Conclusions

In this study, HA powder was prepared from natural source, *i.e.* bovine bone, and used as a filler for preparing PLA composites. Processing technique and u-HA content were the factors that influenced mechanical properties of u-HA/PLA composites. To form HA/PLA composites, u-HA was incorporated into PLA matrix by either melt-mixing or solution mixing techniques. With increasing u-HA content, tensile strength and impact strength of the composites were decreased while the tensile moduli of the composites were increased. In comparison between two preparation techniques, the melt-mixed composites have higher tensile strength, tensile modulus and impact strength than those prepared by solution-mixing technique. However, the PLA chains in the composites prepared by melt-mixing technique degraded much more than those in the composites prepared by solution-mixing technique as confirmed by GPC results.

3.6 References

Coutand, M., Cyr, M., Deydier, E., Guilet, R., and Clastres, P. (2008). Characteristics of industrial and laboratory meat and bone meal ashes and their potential applications. **J. Hazard. Mater.** 150: 522-532.

Deng, X., Hao, J., and Wang, C. (2001). Preparation and mechanical properties of nanocomposites f poly(D, L-lactide) with Ca-deficient hydroxyapatite nanocrystals**. Biomaterials.** 22: 2867-2873.

Fathi, M. H., Hanifi, A., and Mortazavi, V. (2008). Preparation and bioactivity evaluation of bone- like hydroxyapatite nanopowder. **J. Mater. Proc. Technol.** 202: 536-542.

Fukushima, K., Tabuani, D., and Camino, G. (2009). Nanocomposites of PLA and PCL based on montmorillonite and sepiolite. **Mater. Sci. Eng. : C.** 29: 1433-1441.

Furuzono, T., Sonoda, K., and Tanaka, J. (2001). A hydroxyapatite coating covalently linked onto a silicone implant material. **J. Biomed. Mater. Res.** 56: 9-16.

Ignjatovic, N., Tomic, S., Dakic, M., Miljkovic, M., Plavsic, M., and Uskokovic, D. (1999). Synthesis and properties of hydroxyapatite/poly-L-lactide composite biomaterials. **Biomaterials.** 20: 809-16.

Ignjatovic, N., Suljovrujic, E., Simendic, J. B., Krakovsky, I., and Uskokovic, D. (2004). Evaluation of hot-pressed hydroxyapatite/poly-L-lactide composite biomaterial characteristics. **J. Biomed. Mater. Res**. 71B: 284-294.

Jamshidi, K., Hyon, S. H., and Ikada, Y. (1988). Thermal characterization of polylactides. **Polymer.** 29: 2229-2234.

Kothapalli, C. R., Shaw, M. T., and Wei, M. (2005). Biodegradable HA-PLA 3-D porous scaffolds: Effect of nano-sized filler content on scaffold properties. **Acta Biomater.** 1: 653-662.

Lin, P. L., Fang, H. W., Tseng, T., and Lee, W. H. (2007). Effects of hydroxyapatite dosage on mechanical and biological behaviors of polylactic acid composite materials. **Mater. Lett.** 61: 3009-3013.

Mathieu, L. M., Bourban, P. E., and Manson, J. A. E. (2006). Processing of homogeneous ceramic/polymer blends for bioresorbable composites. **Comp. Sci. Technol.** 66: 1606-1614.

Ooi, C. Y., Hamdi, M., and Ramesh, S. (2007). Properties of hydroxyapatite produced by annealing of bovine bone. **Ceram. Int**. 33: 1171-1177.

Perego, G., Cella, G. D., and Bastioli, C. (1996). Effect of molecular weight and crystallinity on poly(lactic acid) mechanical properties. **J. Appl. Polym. Sci.** 59: 37-43.

Ruksudjarit, A., Pengpat, K., Rujijanagul, G., and Tunkasiri, T. (2008). Synthesis and characterization of nanocrystalline hydroxyapatite from natural bovine bone, **Curr. Appl. Phys.** 8: 270-272.

Russias, J., Saiz, E., Nalla, R. K., Gryn, K., Ritchie, R. O., and Tomsia, A. P. (2006). Fabrication and mechanical properties of HA/PLA composites: A study of *in vitro* degradation. **Mater. Sci. Eng. : C.** 26: 1289-1295.

Shikinami, Y. and Okuno, M. (2001). Bioresorbable devices made of forged composites of hydroxyapatite (HA) powders and poly L-lactide (PLLA). Part II: practical properties of miniscrews and miniplate. **Biomaterials.** 22: 3197-3211.

Shinzato, S., Nakamura, T., Kokubo, T., and Kitamura, Y. (2001). Bioactive bone cement: Effect of silane treatment on mechanical properties and osteoconductivity. **J. Biomed. Mater. Res.** 55: 277-284.

Signori, F., Coltelli, M. B., and Bronco, S. (2009). Thermal degradation of poly(lactic acid) (PLA) and poly(butylenesadipate-co-terephthalate) (PBAT) and their blends upon melt processing. **Polym. Degrad. Stab.** 94: 74-82.

Tsuji, H. and Ikarashi, K. (2004). *In vitro* hydrolysis of poly(L-lactide) crystalline residues as extended-chain crystallites. Part I: long-term hydrolysis in phosphate-buffered solution at 37ºC. **Biomaterials.** 25: 5449-5455.

Wachsen, O., Platkowski, K., and Reichert, K. H. (1997). Thermal degradation of poly-L-lactide-studies on kinetics, modelling and melt stabilisation. **Polym. Degrad. Stab.** 57: 87-94.

Wang, M., Joseph, R., and Bonfield, W. (1998). Hydroxyapatite-polyethylene composites for bone substitution: effects of ceramic particle size and morphology. **Biomaterials.** 19: 2357-66.

Wen, J., Li, Y., Zuo, Y., Zhou, G., Li, J., Jiang, L., and Xu, W. (2008). Preparation and characterization of nano-hydroxyapatite/silicone rubber composite. **Mater. Lett.** 26: 3307-3309.

Zhang, S. M., Liu, J., Zhou, W., Cheng, L., and Guo, X. D. (2005). Interfacial fabrication and property of hydroxyapatite/polylactide resorbable bone fixation composites. **Curr. Appl. Phys.** 5: 516-518.

CHAPTER IV

EFFECT OF SURFACE MODIFIED BOVINE BONE

BASED HYDROXYAPATITE ON PHYSICAL

PROPERTIES AND *in vitro* CYTOTOXICITY

OF HA/PLA COMPOSITES

4.1   Abstract

In this work, hydroxyapatite (HA) was produced from bovine bone in order to use as a filler for poly(lactic acid) (PLA) composites. The surface of HA powder was modified with either 3-aminopropyltriethoxysilane (APES) or 3-methacryloxypropyl trimethoxysilane (MPTS). FTIR and EDXRF results confirmed the appearance of APES and MPTS on the HA surfaces. SEM micrographs of silane-treated HA/PLA composites revealed that modification of HA with APES or MPTS eased distribution of HA powder in PLA matrix and enhanced interfacial adhesion between both phases. Based on the results, the mechanical properties of silane-treated HA/PLA composites were better than those of untreated HA/PLA composites. In addition, *in vitro* cytotoxicity tests indicated that the extracts from all HA/PLA composites had no toxicity to human osteoblast cell.

4.2 Introduction

Hydroxyapatite [HA: $Ca_{10}(PO_4)_6(OH)_2$] is a form of calcium phosphate which is similar to a major mineral phase in hard tissues of human body. HA has been found to be an application as a biomaterial because of its excellent biocompatibility and bone-bonding ability. It has been used in various medical applications such as bone replacement (Kothapalli *et al.*, 2005; Shikinami *et al.*, 2001; Hasegawa *et al.*, 2006; Fathi *et al.*, 2008). HA can be synthetically prepared or derived from natural sources, *e.g.* coral, bovine bone, swine bone. In recent years, several attempts have been done to produce HA from natural sources for biomedical applications since the natural HA is less expensive and more compatible to human hard tissues (Benmarouane *et al.*, 2004, Ruksudjarit *et al.*, 2008; Yoganand *et al.*, 2009). In Thailand, bovine bone as a livestock waste is normally used in fertilizer, animal foods, and in making porcelain (*i.e.* bone china). Using the bovine bone as a raw material for producing HA is not only to reduce volumes of the livestock waste but also to increase added value of the bovine bone. However, HA is brittle and difficult to process into required shapes. One attempt to solve this problem is mixing HA with a flexible polymer, especially with a bioresorbable polymer.

Many kinds of bioresorbable polymers, *e.g.* poly(lactic acid) (PLA), poly(3-hydroxybutyrate) (PHB), have been developed and used in medical applications. Among those polymers, PLA is a good candidate as a biomaterial due to its biocompatibility, biodegradability and yielding nontoxic byproducts after hydrolysis reaction (Deng *et al.*, 2001; Ignjatovic *et al.*, 2001). Hence, a composite between PLA and HA is a good alternative for using as a biomaterial since it combines strength and

stiffness of HA with flexibility and resorbability of PLA and, then, solving the drawbacks of both materials (Russias *et al.*, 2006; Tsuji *et al.*, 2004).

However, the major drawbacks found in HA/PLA composites are the agglomeration of HA and the failure at the interface between HA and the polymer matrix. These are due to the polarity difference between PLA matrices and HA surfaces. PLA matrix has methyl groups (-CH$_3$) as side group of a polymer chain and, thus, PLA surface shows hydrophobicity. This is in contrast to HA surface which exhibits hydrophilic property (Shikinami *et al*., 2001; Liu *et al.*, 1998; Zhang *et al.*, 2005). Based on mechanical properties of HA/PLA composites, an improvement of the interfacial adhesion between HA particles and PLA matrix has become an important area of studies. The HA surface can be modified with a coupling agent, such as organofunctional silanes, by which the interfacial adhesion between filler and polymer matrix is effectively improved (Russias *et al.*, 2006; Dupraz *et al.*, 1996).

In this present study, bovine bone based HA was prepared and was treated with 3-aminopropyltriethoxysilane (APES) or 3-methacryloxypropyltrimethoxysilane (MPTS), and then incorporated into PLA. The characteristics of untreated HA and silane-treated HA were investigated. In addition, effects of filler characteristic and filler content on morphological and mechanical properties of HA/PLA composites were determined. Furthermore, *in vitro* cytotoxicity of the HA/PLA composites was also investigated.

4.3   Experimental

4.3.1   Materials

PLA (4042D) was purchased from NatureWorks LLC Co. Ltd. Bovine bones were supplied by Limeiseng Co., Nakhon Ratchasima, Thailand. 3-aminopropyltriethoxysilane (APES) and 3-methacryloxypropyltrimethoxysilane (MPTS) were purchased from Optimal Tech Co.,Ltd. and Aldrich, respectively. Chemical structures of these silane coupling agents are shown in Figure 4.1.

(a)   **(b)**
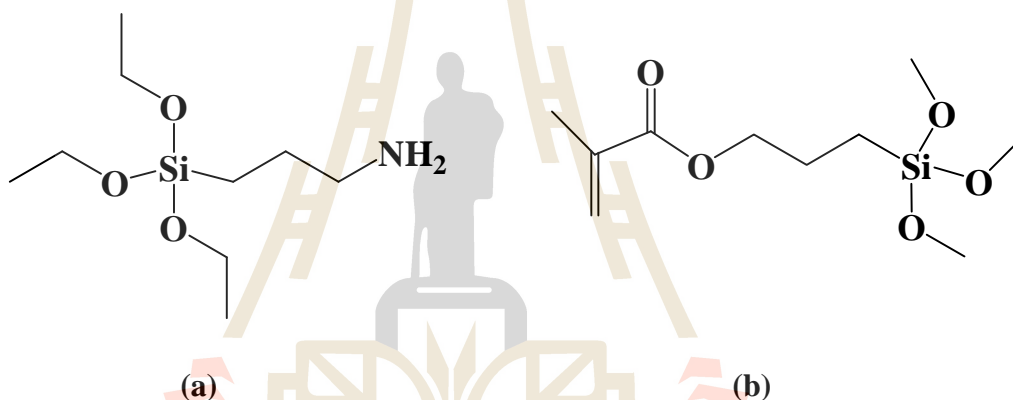
Figure 4.1 Chemical structures of (a) 3-aminopropyltriethoxysilane and (b) 3-methacryloxypropyltrimethoxysilane.

4.3.2   Preparation of HA powder

Bovine bones were burned in open air and ground into powder using a ball milling machine. Then, the powder was heat treated at 1100ºC for 3 h; the obtained powder was called untreated HA (u-HA). After that, the powder was modified by either APES or MPTS. The content of silane used for modification was 2.0wt% based on weight of HA powder. To prepare silane solution, the APES was dissolved in distilled water whereas MPTS was dissolved in 30vol.% of alcoholic solution. The pH of each silane solution was adjusted to 3.5 using acetic acid. HA powder was soaked in each silane solution and left under agitation at room temperature. After 3 h of agitation, the pH of each solution was increased to 7.0 with 0.1 N NaOH solution to encourage condensation and formation of siloxanols on HA surface (Ooi *et al.*, 2007). Then, both silane-treated powders were washed and dried at 60ºC overnight in an oven. The APES treated HA and MPTS treated HA were designated as a-HA and m-HA, respectively.

4.3.3   Preparation of HA/PLA composites

HA/PLA composites were prepared through melt-mixing technique using an internal mixer (HAAKE/RHEOMIX). PLA and HA were mixed at 170ºC with a rotor speed of 70 rpm for 10 min. The weight ratios of HA/PLA in each composite are shown in Table 4.1. Each HA/PLA composite was left at room temperature for 24 h before grinding into small pieces. To prepare composite specimens for mechanical tests, the ground HA/PLA composite was heated in dumbbell-shaped and rectangular-shaped molds from room temperature to 180ºC and maintained at that temperature for 10 min. Subsequently, it was hot-pressed vertically for 5 min at 180ºC under a pressure of 1.4×10^{7} Pa and cooled to room temperature.

Table 4.1 Composition of HA/PLA composites.

Composite designations	Filler	Silane coupling	Filler content (wt%)
1A	u-HA	-	10
2A	u-HA	-	20
3A	u-HA	-	30
4A	u-HA	-	40
1B	a-HA	APES	10
2B	a-HA	APES	20
3B	a-HA	APES	30
4B	a-HA	APES	40
1C	m-HA	MPTS	10
2C	m-HA	MPTS	20
3C	m-HA	MPTS	30
4C	m-HA	MPTS	40

4.3.4   Characterization of HA powder

Functional groups of u-HA, m-HA and a-HA powders were identified by a Fourier transform infrared spectrometer (FTIR) (BIO-RAD/FTS175C, diffuse reflectance technique) in the 4000-400 cm^{-1} region with 2 cm^{-1} resolution.

Elemental compositions of the u-HA, m-HA and a-HA powders were analyzed by an energy dispersive X-Ray fluorescence spectroscopy (EDXRF) (OXFORD/ED2000). EDXRF measurements were carried out with a rhodium lamp (energy range 10^4 eV). The X-ray tube was operated at 5.0 kV, the pulse rate was kept

at 20 kcps and the measurement resolution was kept at 170 eV. Each peak of the recorded spectrum is a characteristic of a particular element.

In addition, a scanning electron microscopy (SEM) (JOEL/JSM-6400) operating at 15-20 kV was used to reveal microstructures of u-HA, m-HA and a-HA powders. Median particle sizes of u-HA, m-HA and a-HA powders were measured by a diffraction particle analyzer (MASTERSIZER S/MSS).

4.3.5 Characterization of HA/PLA composites

A scanning electron microscopy (SEM) (JOEL/JSM-6400) operating at 20 kV was used to visualize tensile fracture surfaces of the HA/PLA composites. All samples were coated with a thin layer of gold before examination. Tensile properties of HA/PLA composites were investigated according to ASTM D638-03 using a universal testing machine (INSTRON/5569). Moreover, izod impact strength of unnotched HA/PLA specimen was determined according to ASTM D256 using an impact testing machine (ATLAS/BPI).

4.3.6 Cytotoxicity of HA/PLA composites

Cytotoxicity of HA/PLA composites was determined based on a procedure modified from ISO 10993-5:1999(E) (test on extracts) using assessment of cell damage by morphological means. Human osteoblasts were used as cultured cells. Dulbecco's modified eagle medium (DMEM), complete medium supplemented with 10% horse serum, was used as a culture medium and an extraction vehicle. The culture medium was prepared under sterile condition to prevent microbial inflection. The pH of medium was maintained in a range of 7.2-7.4. HA/PLA composite specimens for the cell tests, *i.e.* 4A, 4B and 4C, were sterilized by ethylene oxide gas. Under an aseptic environment, the sterilized HA/PLA composite specimens were then

extracted by DMEM with an extraction ratio of 3.18 cm^2/ml using roller mixers at $37\pm2°C$ for 24 ± 2 h. The media without test specimen (the blank cultured media), subjected to the same extraction condition, was used as a reagent control. Thermanox (Nunc) coverslip and polyurethane film containing 0.1% zinc diethyldithiocarbamate (ZDEC) were used as a negative control material and a positive control material, respectively. The extracts were then filtered by 0.22 micron membrane filter prior to test. For cytotoxic determination, h-OBs of 45,000 cells/ml with either the control or a specimen extract were incubated in a 95 ± 5% humidified atmosphere with 5 ± 0.1% CO_2 at $37\pm2°C$ for 24 h. After the cell culture experiments, the cells were stained with neutral red for the cell viability assay. The morphologies of cells were determined using a trinocular phase contrast microscope.
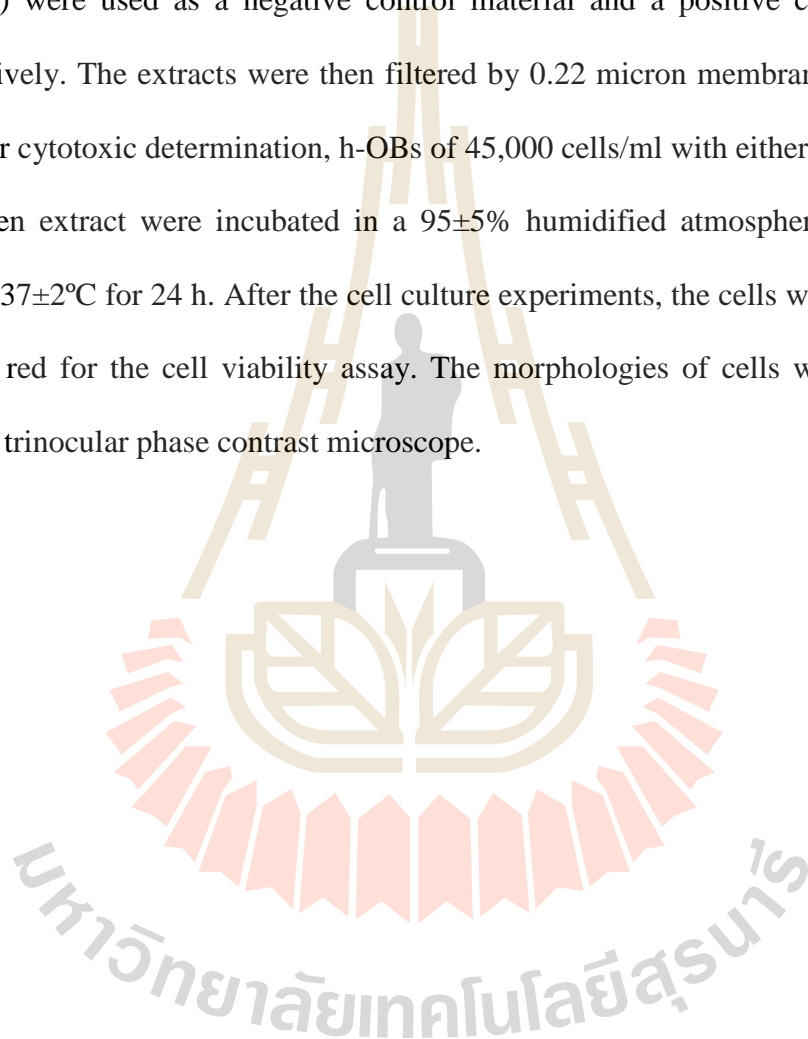
4.4 Results and discussion

4.4.1 Characterization of HA powder

FTIR spectrum of u-HA is shown in Figure 4.2 (a). The peaks at 1085, 1036, 963, 600 and 575 cm^{-1} were assigned to different vibration modes of PO_4^{3-} group in HA powder. The stretching and the bending vibration of structural OH groups in the apatite lattice were observed at 3571 cm^{-1} and 632 cm^{-1}, respectively. Additionally, vibrational peaks corresponding to CO_3^{2-} groups were also observed at 1457, 1411 and 878 cm^{-1} (Fathi *et al.*, 2008; Ooi *et al.*, 2007). FTIR pattern indicated that the calcined bovine bone powder was carbonated HA. The appearance of carbonate functional groups on surface of the obtained powder could be explained as follows: 1) During heating process, adsorbed carbon from atmosphere substituted the PO_4^{3-} groups of the HA or 2) The incompletely pyrolyzed carbon dissolved into the hydroxyapatite crystal (Ooi *et al.*, 2007; Shinzato *et al.*, 2001; Furuzono *et al.*, 2001; Wen *et al.*, 2008). Figure 2 (b-c) shows FTIR spectra of the silane-treated HA powders. The additional peaks, compared with FTIR spectrum of u-HA, were observed. The peaks around 2950-2850 cm^{-1} were C–H stretching vibration of carbon chains of APES and MPTS deposited on HA surface. Also, the peak at 1080 cm^{-1} was attributed to the Si-O stretching vibration of both silane coupling agents. Additionally, FTIR spectrum of m-HA showed C=O stretching vibration of the deposited MPTS at 1712 cm^{-1} (Kothapalli *et al*., 2005; Liu *et al*., 1998; Wen *et al*., 2008; Bleach, Nazhat, Tanner, Kellomaki, and Tormala, 2002).
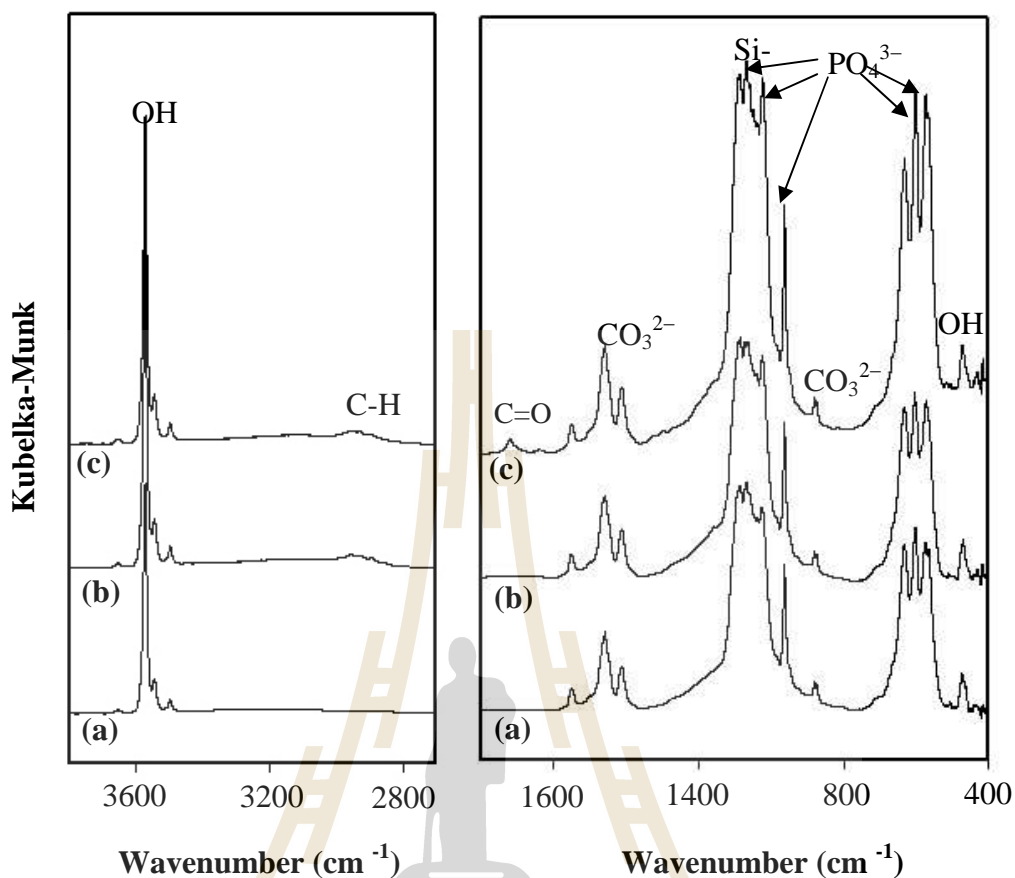
Figure 4.2 FTIR spectra of (a) u-HA, (b) a-HA and (c) m-HA.

Elemental compositions on the surfaces of u-HA, a-HA and m-HA are shown in Table 4.2 The major elements found on the u-HA surface were Ca and P, however, small amounts of Si were also observed. These Si atoms may come from impurity in raw material. In comparison between silane-treated HA and u-HA powders, the EDXRF results of a-HA and m-HA powders shows higher content of Si atoms on the powder surface. These results indicated the presence of silane molecules on the surface of the treated HA powders. This was a positive factor which could provide effective adhesion between PLA matrix and silane-treated HA powder. However, the percentage of the silane deposited on HA surface depended on silane

coupling type as shown in Table 4.2 According to another research group, parts of primary amino silane would be easier removed by rinsing with organic solvent or water than those of metacryloxy silane (Zhang *et al*., 2005).

Table 4.2 Elemental composition and median particle size of untreated HA and silane-treated HA.

Designation	Elemental composition (%)				Median particle size (µm) (D (*v*, 0.5))
	Ca	P	O	Si	
u-HA	25.5	11.5	62.2	0.06	14.30
a-HA	24.2	11.3	63.9	0.11	4.76
m-HA	23.6	11.0	64.5	0.13	4.53

In addition, SEM micrographs of u-HA, a-HA and m-HA are shown in Figure 4.3 (a-c). The micrographs in Figure 4.3 (a) shows the agglomeration of u-HA powder. On the other hand, the micrographs of silane-treated HA in Figure 4.3 (b) and (c) show the smaller sizes of agglomerated HA powders compared with those of u-HA. From the SEM observation, the agglomeration sizes of u-HA, a-HA and m-HA were consistent with their average particle size measured by the particle size analyzer (Table 4.2). These results indicated that silane surface treatment tended to reduce the agglomeration of HA powders. In preparation of HA/PLA composites, the less powder agglomeration would lead to better processability and, accordingly, enhance mechanical properties of the composites.

(a)

(b)

(c)
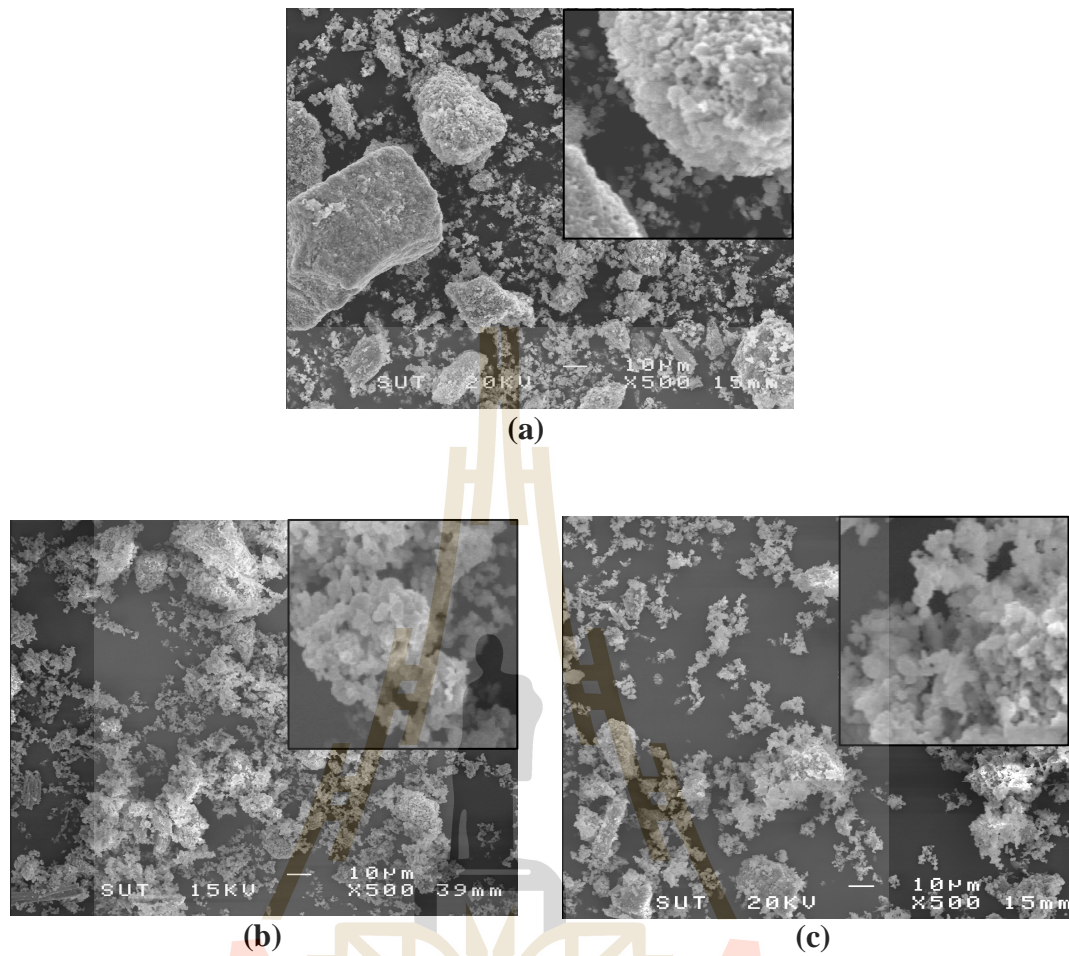
Figure 4.3 SEM micrographs of HA powders: (a) u-HA, (b) a-HA and (c) m-HA.

4.4.2 Characterization of HA/PLA composites

Tensile modulus, elongation at break, tensile strength and impact strength of HA/PLA composites at various HA contents are illustrated in Figure 4.4-4.7. As seen in the figures, the mechanical properties of silane-treated HA/PLA composites were better than those of untreated HA/PLA composites of the equal HA content.

Tensile moduli of HA/PLA composites were higher than that of the neat PLA as shown in Figure 4.4. Also, the tensile moduli of the composites increased

with increasing HA content. The stiffness enhancement of the HA/PLA composites was because the rigid HA filler restricts the molecular motion and the deformation of the PLA chains. At an equal content of filler, the tensile moduli of both a-HA/PLA and m-HA/PLA were slightly higher than that of u-HA/PLA composites.
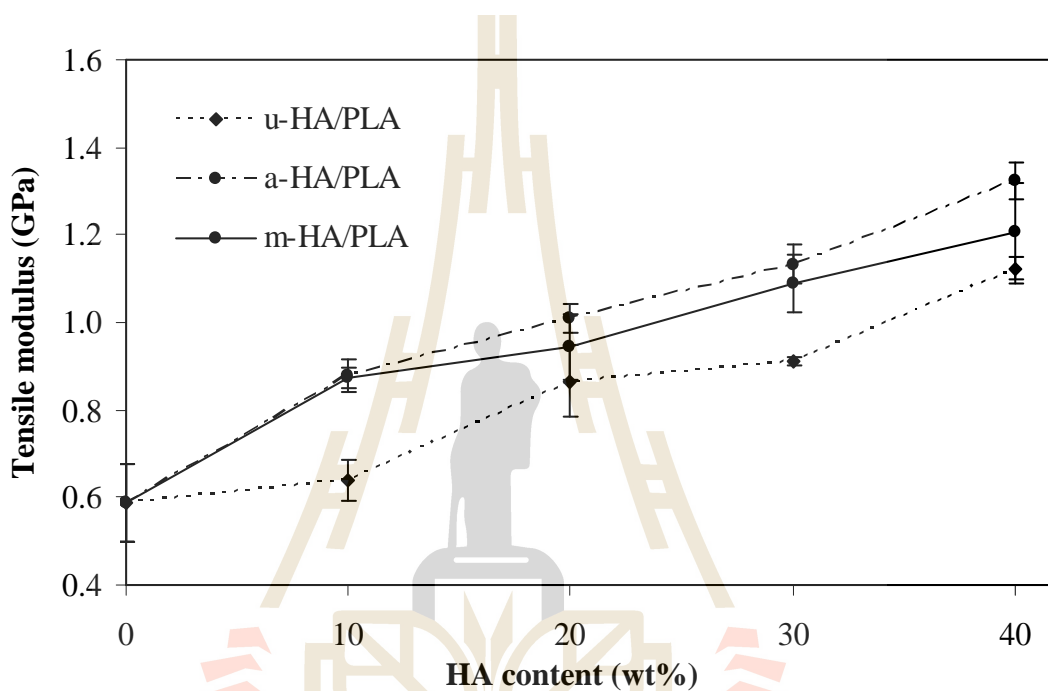
Figure 4.4 Tensile modulus of HA/PLA composites at various HA contents.

Elongation at break of all HA/PLA composites was lower than that of the neat PLA as shown in Figure 4.5. The incorporated HA was the cause of the lower elongation at break of the composites whether or not the HA was surface treated since HA decreased the mobility of PLA chains and led to the decreasing in ductility of the composites. Nevertheless, the PLA composites with silane-treated HA showed higher elongation at break than the corresponding PLA composites with u-HA. This was due to the good dispersion of silane-treated HA in PLA matrix.
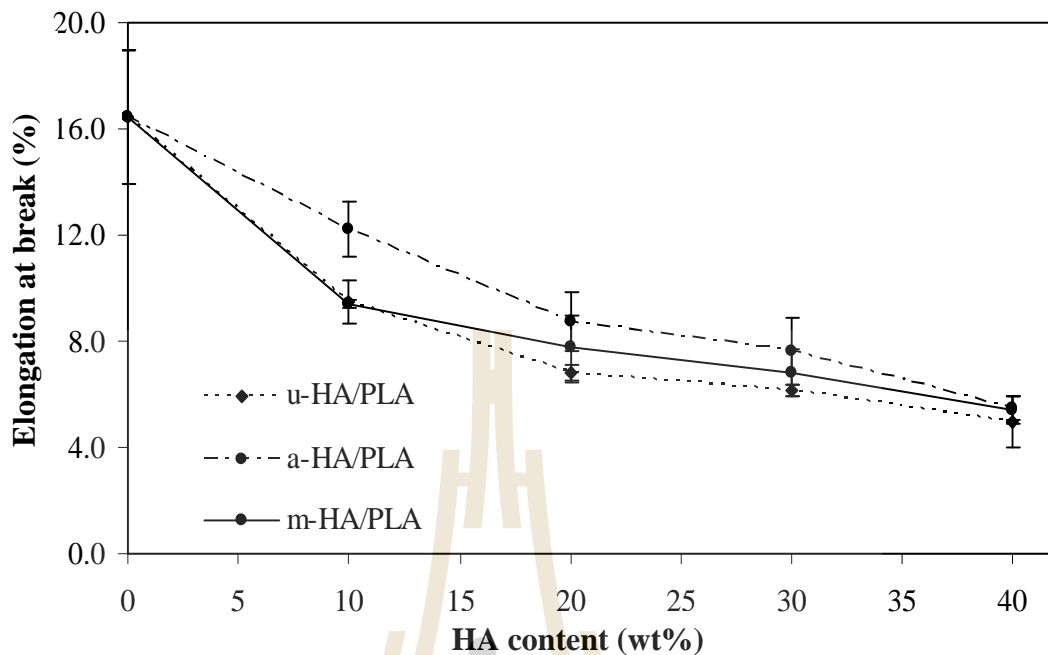
Figure 4.5 Elongation at break of HA/PLA composites at various HA contents.

Tensile strength of HA/PLA composites were slightly lower than that of the neat PLA as shown in Figure 4.6. The tensile strength of the composites continued to decrease with increasing HA content. The decrease in tensile strength of composites with increasing filler content was also observed by other research works (Bleach *et al.*, 2002; Hiljanen, Heino, and Seppala, 1998; Zhongkui *et al.*, 2005). The lowering of tensile strength of the composites was due to the debonding of HA from the polymer matrix by which voids were created (Kasuga *et al.*, 2001; Todo *et al.*, 2006; Takayama *et al.*, 2008). According to this idea, the HA agglomeration observed in tensile fracture surface of HA/PLA composite (Figure 4.8) could be the main reason that was responsible for the reduction in tensile strength of the HA/PLA composites. Nevertheless, the m-HA/PLA composite exhibited the highest tensile strength while the corresponding u-HA/PLA composite show the lowest tensile

strength. This could be attributed to the enhancement of the interaction between HA and PLA as a result of treating HA surface with a silane coupling agent.
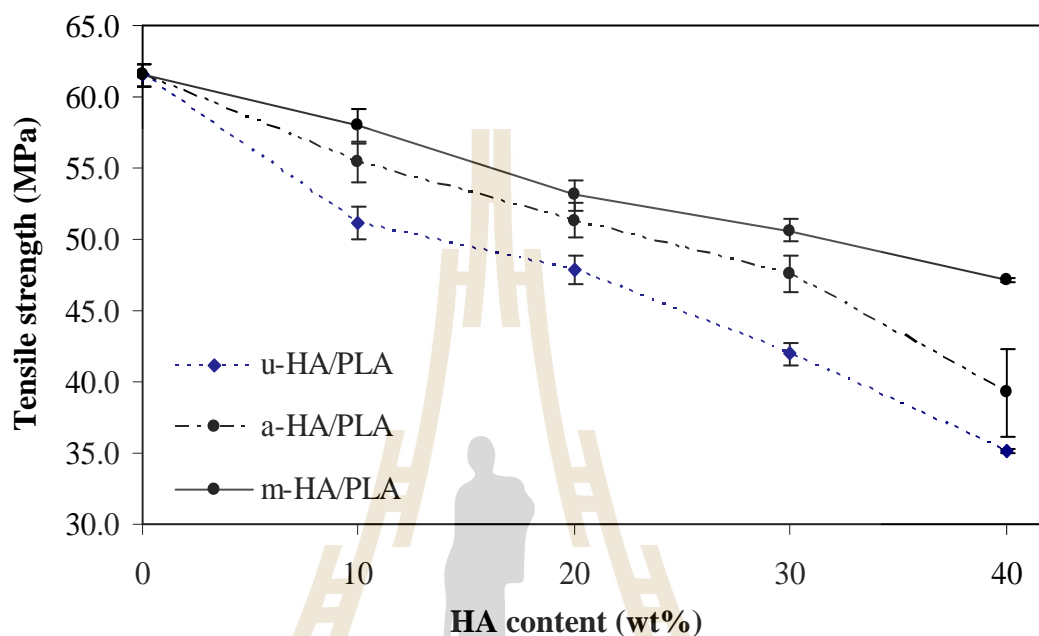
Figure 4.6 Tensile strength of HA/PLA composites at various HA contents.

In cases of m-HA and a-HA/PLA composites, the deposited silane coupling agent on HA surface acted as a bridge between two phases. The most probable reason of the bonding between silane-treated HA and PLA matrix is a degree of solubility of oligomeric siloxanols on HA surface to form interdiffusion and interpenetrating network (IPN) at interphase region (Edwin, 1991). In order to optimize the interfacial interaction, organofunction of the silane coupling agent should be selected to match chemical reactivity, solubility characteristics and structural characteristics of the polymer. Between two types of the silane coupling agent, MPTS exhibited hydrophobic property while APES showed hydrophilic property. Therefore, MPTS was probably more compatible with PLA matrix than

APES. So, m-HA/PLA composite exhibited higher tensile strength than those of u-HA/PLA and a-HA/PLA composites.

Impact strength of HA/PLA composites was attributed to a number of local deformation in the composites. The impact strength of all HA/PLA composites was lower than that of the neat PLA as shown in Figure 4.7. This was because HA disturbed matrix continuity and limited the ability of polymer chains to absorb impact energy. The large agglomerates observed in SEM micrograph of fracture surface of u-HA/PLA composite (Figure 4.8 (a)) were the site of stress concentration, which can act as a microcrack initiator. Moreover, a gap around agglomerated HA indicated the weak PLA-HA interaction. The gap interrupted stress transfer between PLA and HA and led to crack initiation during impact testing. However, the composites with silane-treated HA showed less reduction in impact strength than those with u-HA. Also, the PLA composite containing m-HA showed the highest impact strength. This result was probably due to the better dispersion of the silane-treated HA in PLA matrix.
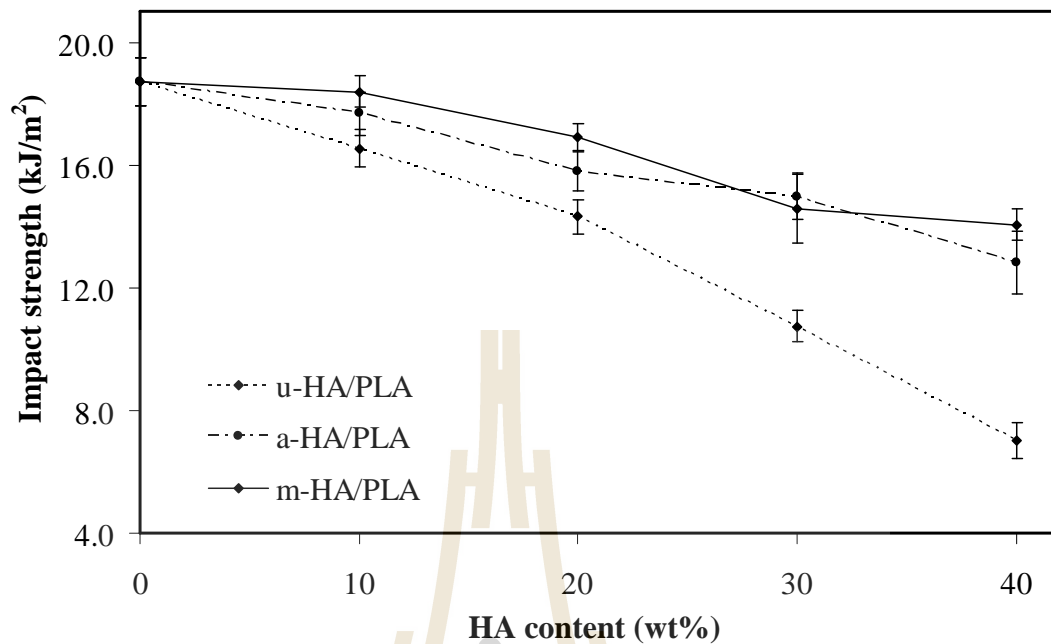
Figure 4.7 Impact strength of HA/PLA composites at various HA contents.

SEM micrographs of tensile fracture surfaces of the HA/PLA composites containing 20wt% of HA are illustrated in Figure 4.8 (a-c). They show that the agglomeration of HA in the PLA phase was found in all types of the PLA composites. Nevertheless, the microstructures of PLA composite containing silane-treated HA in Figure 4.8 (b-c), compared with that of the u-HA/PLA composite in Figure 4.8 (a), illustrated more homogenous dispersion of HA in the PLA matrix with smaller sizes of HA agglomeration. As incorporating HA into PLA, u-HA seemed to have stronger particle-particle interaction than the silane-treated HA. As a result, the u-HA tended to agglomerate during composite processing more than the silane-treated HA did.
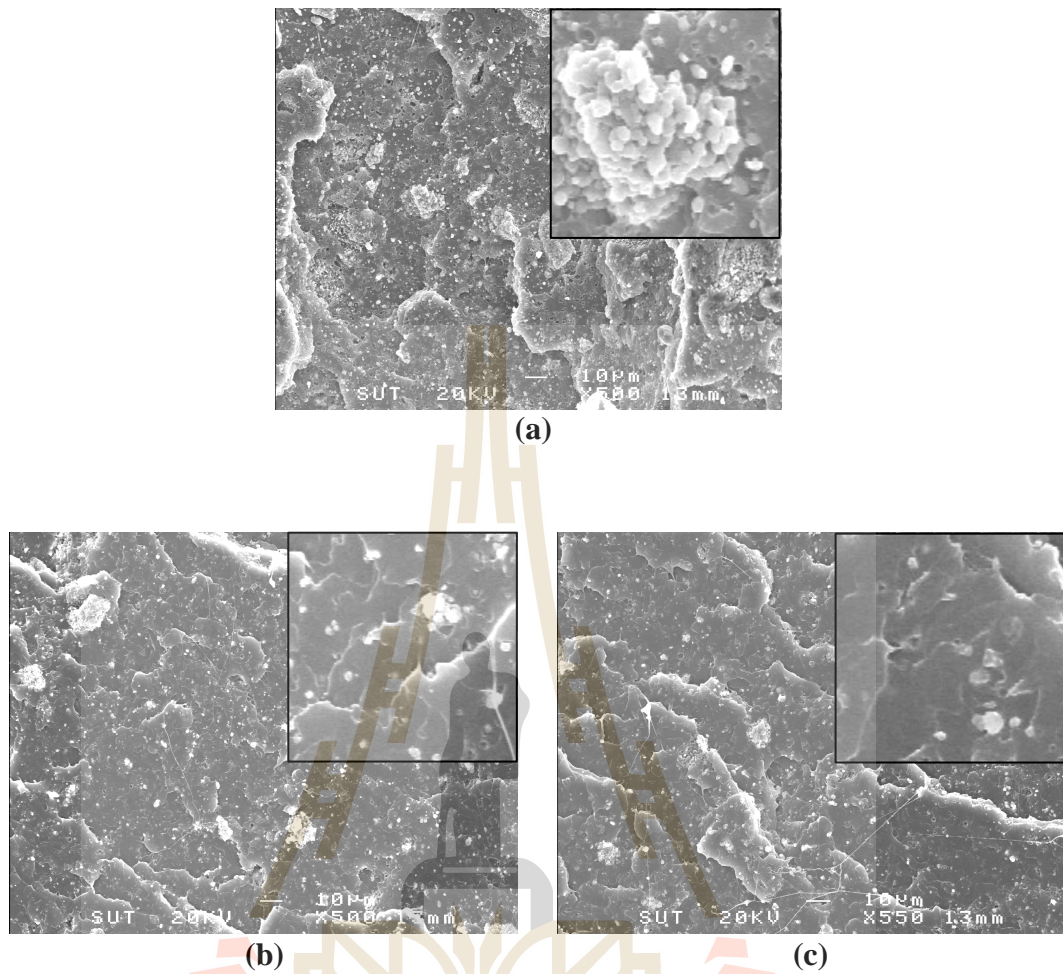
Figure 4.8 SEM micrographs of tensile fracture surfaces of PLA composites at 20wt% of (a) u-HA, (b) a-HA and (c) m-HA.

In addition, a gap at the interface between u-HA and PLA matrix was observed on the tensile fracture surface of u-HA/PLA composite in Figure 4.8 (a). This revealed local deformation of PLA around these particles. Nevertheless, the gaps between silane-treated HA and PLA interface became smaller as shown in Figure 4.8 (b-c). This suggested that treating HA surface with APES or MPTS can improve interfacial adhesion between PLA and HA. At higher magnifications, as shown in Figure 4.9, silane-treated HA uniformly dispersed within PLA matrixes and closely

adhered to the matrix interface. This result was consistent with the morphology of silane-treated HA shown in Figure 4.3 (c-d).

(a) **(b)**
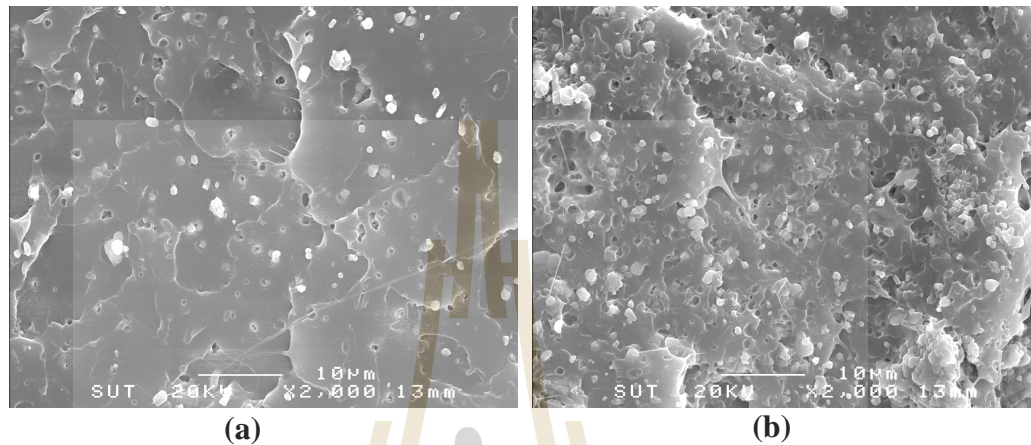
Figure 4.9 SEM micrographs of tensile fracture surfaces at high magnification of composite with m-HA at (a) 10wt% and (b) 40wt%.

4.4.3 *In vitro* cytotoxicity of HA/PLA composites

In order to use the HA/PLA composites in a biomedical application, cytotoxicity and biocompatibility of the composites must be investigated. A preliminary investigation on cytotoxicity of the extracts from HA/PLA composites was performed in this present work. After culturing, the h-OBs cell morphologies were observed. Figure 4.10 (a-g) shows morphologies of the h-OBs cells responded with the reagent control and the extracts from the negative control material, the positive control material, pure PLA and three types of HA/PLA composite specimens, respectively.
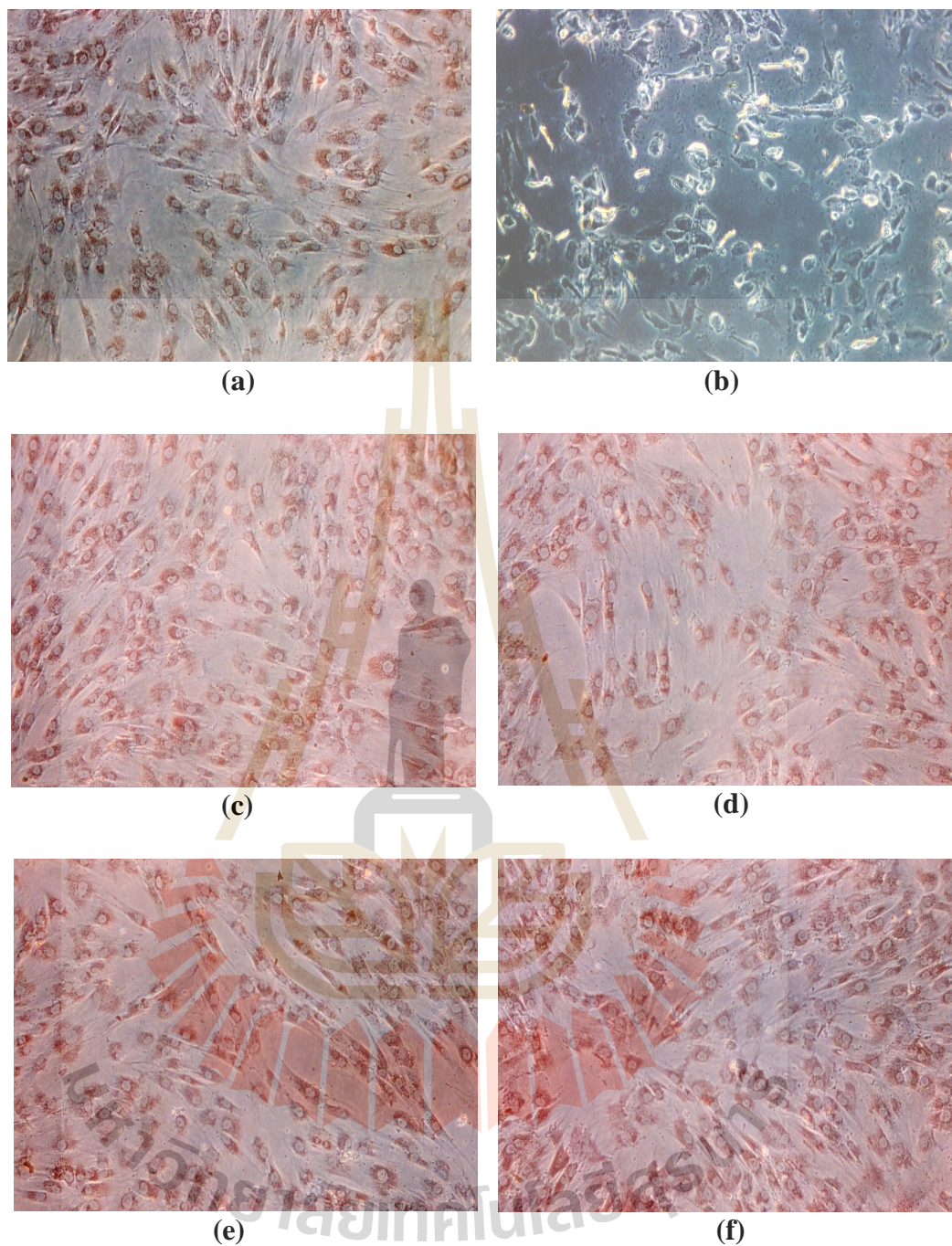
Figure 4.10 Micrographs of h-OBs cells morphology responded with (a) the negative control material extract, (b) positive control material extract, (c) pure PLA extract, (d) u-HA/PLA composite extract, (e) a-HA/PLA composite extract and (f) m-HA/PLA composite extract.

In the negative control material extract (Figure 4.10 (a)), cells morphologies after incubation for 24 h revealed positive staining indicating that these were none cytotoxic (cytotoxicity scale = 0). On the other hand, the h-OBs cells in the positive control material extract exhibited dead cells visible; negative staining was observed (cytotoxicity scale = 3). In addition, Figure 10 (c-f) illustrates morphology of h-OBs cells cultured in the extracts from pure PLA and all types of HA/PLA composites. From the figures, the morphologies of h-OBs cells in the different extracts were similar to those of the reagent control and the negative control material extract. These results demonstrated that u-HA/PLA composite, a-HA/PLA composite and m-HA/PLA composite did not release any substance in the level that was harmful to the h-OBs.

4.5   Conclusions

Preparing biomedical materials from bovine bone is an alternative approach to obtain a suitable bone replacement material with an inexpensive expense. In this study, carbonated HA was produced from thermal treated bovine bone and used as a filler for PLA composites. The results from mechanical test and *in vitro* cytotoxicity test suggested a potential of using bovine bone based HA/PLA composite as a biomaterial. Tensile strength, tensile modulus, elongation at break and impact strength of PLA composites can be improved by modifying u-HA surface with either APES or MPTS. The enhancement of mechanical properties of silane-treated HA/PLA composites was caused by the good dispersion of silane-treated HA in PLA matrix and the good interfacial interaction between the two phases. However, the mechanical

properties of silane-treated HA/PLA composites still need to be enhanced or adjusted in order to meet requirement for a specific medical application.

4.6   References

Benmarouane, A., Hansena, T., and Lodini, A. (2004). Heat treatment of bovine bone preceding spatially resolved texture investigation by neutron diffraction. **Physica B.** 350: 611-614.

Bleach, N. C., Nazhat, S. N., Tanner, K. E., Kellomaki, M., and Tormala, P. (2002). Effect of filler content on mechanical and dynamic mechanical properties of particulate biphasic calcium phosphate-polylactide composites. **Biomaterials.** 23: 1579-1585.

Deng, X., Hao, J., and Wang, C. (2001). Preparation and mechanical properties of nanocomposites of poly(D,L-lactide) with Ca-deficient hydroxyapatite nanocrystals. **Biomaterials.** 22: 2867-2873.

Dupraz, A. M. P., Wijn, J. R., Meer, S. A. T., and Groot, K. (1996). Characterization of silane-treated hydroxyapatite powders for use as filler in biodegradable composites. **J. Biomed. Mater. Res.** 30: 231-238.

Edwin P. P. (1991). **Silane coupling agents.** 2nd ed. New York: Plenum Press; 1991. p. 144-149.

Fathi, M. H., Hanifi, A., and Mortazavi, V. (2008). Preparation and bioactivity evaluation of bonelike hydroxyapatite nanopowder. **J. Mater. Proc. Technol.** 202: 536-542.

Furuzono, T., Sonoda, K., and Tanaka, J.(2001). A hydroxyapatite coating covalently linked onto a silicone implant material. **J. Biomed. Mater. Res.** 56: 9-16.

Hasegawa, S., Ishii, S., Tamura, J., Furukawa, T., Neo, M., Matsusue, Y., Shikinami, Y., Okuno, M., and Nakamura, T. (2006). A 5-7 year *in vivo* study of high-strength hydroxyapatite/poly(L-lactide)composite rods for the internal fixation of bone fractures. **Biomaterials.** 27: 1327-1332.

Hiljanen-Vainio, M., Heino, M., and Seppala, J. V. (1998). Reinforcement of biodegradable poly(ester-urethane) with fillers. **Polymer.** 39: 865-872.

Ignjatovic, N., Suljovrujic, E., Simendic, J. B., Krakovsky, I., and Uskokovic, D. (2001). A study of HAp/PLLA composite as a substitute for bone powder using FT-IR spectroscopy. **Biomaterials.** 22: 271-275.

Kasuga, T., Ota, Y., Nogami, M., and Abe, Y. (2001). Preparation and mechanical properties of Poly(lactic acid) composites containing hydroxyapatite fibers. **Biomaterials.** 22: 19-23.

Kothapalli, C. R., Shaw, M. T., and Wei, M. (2005). Biodegradable HA-PLA 3-D porous scaffolds: Effect of nano-sized filler content on scaffold properties. **Acta Biomater.** 1: 653-662.

Liu, Q., Wijn, J. R., Groot, K., and Blitterswijk, C. A. (1998). Surface modification of nano-apatite by grafting organic polymer. **Biomaterials.** 19: 1067-1072.

Ooi, C. Y., Hamdi, M., and Ramesh, S. (2007). Properties of hydroxyapatite produced by annealing of bovine bone. **Ceram. Int.** 33: 1171-1177.

Ruksudjarit, A., Pengpat, K., Rujijanagul, G., and Tunkasiri, T. (2008). Synthesis and characterization of nanocrystalline hydroxyapatite from natural bovine bone. **Curr. Appl. Phys.** 8: 270-272.

Russias, J., Saiz, E., Nalla, R. K., Gryn, K., Ritchie, R. O., and Tomsia, A. P. (2006). Fabrication an mechanical properties of HA/PLA composites:A study of *in vitro* degradation. **Mater. Sci. Eng. C.** 26: 1289-1295.

Shikinami, Y. and Okuno, M. (2001). Bioresorbable devices made of forged composites of hydroxyapatite (HA) powders and poly L-lactide (PLLA). Part II: practical properties of miniscrews and miniplate. **Biomaterials**. 22: 3197-3211.

Shinzato, S., Nakamura, T., Kokubo, T., and Kitamura, Y. (2001). Bioactive bone cement: Effect of silane treatment on mechanical properties and osteoconductivity. **J. Biomed. Mater. Res.** 55: 277-284.

Takayama, T., Todo, M., and Takano, A. (2008). The effect of bimodal distribution on the mechanical properties of hydroxyapatite particle filled poly(L-lactide) composites. **J. Mech. Behav. Biomed. Mater.** 2: 105-112.

Todo, M., Park, S. D., Arakawa, K., and Takenoshita, Y. (2006). Relationship between microstructure and fracture behavior of bioabsorbable HA/PLLA composites. **Composits: Part A.** 37: 2221-2225.

Tsuji, H. and Ikarashi, K. (2004). *In vitro* hydrolysis of poly(lactide) crystalline residues as extended-chain crystallites. Long-term hydrolysis in phosphate-buffered solution at 30ºC. **Biomaterials.** 25: 5449-5455.

Wen, J., Li, Y., Zuo, Y., Zhou, G., Li, J., Jiang, L., and Xu, W. (2008). Preparation and characterization of nano-hydroxyapatite/silicone rubber composite. **Mater. Lett.** 62: 3307-3309.

Yoganand, C. P., Selvarajan, V., Wu, J., and Xue, D. (2009). Processing of bovine hydroxyapatite (HA) powders and synthesis of calcium phosphate silicate glass ceramics using DC thermal plasma torch. **Vacuum.** 83: 319-325.

Zhang, S. M., Liu, J., Zhou, W., Cheng, L., and Guo, X. D. (2005). Interfacial fabrication and property of hydroxyapatite/polylactide resorbable bone fixation long-term composite. **Curr. Appl. Phys.** 5: 516-518.

Zhongkui, H., Peibiao, Z., Chaoliang, H., Xueyu, Q., Aixue, L., Li, C., Xuesi, C., and Xiabin, J. (2005). Nano-composite of poly(L-lactide) and surface grafted hydroxyapatite: Mechanical properties and biocompatibility. **Biomaterials.** 26: 6296-6304.
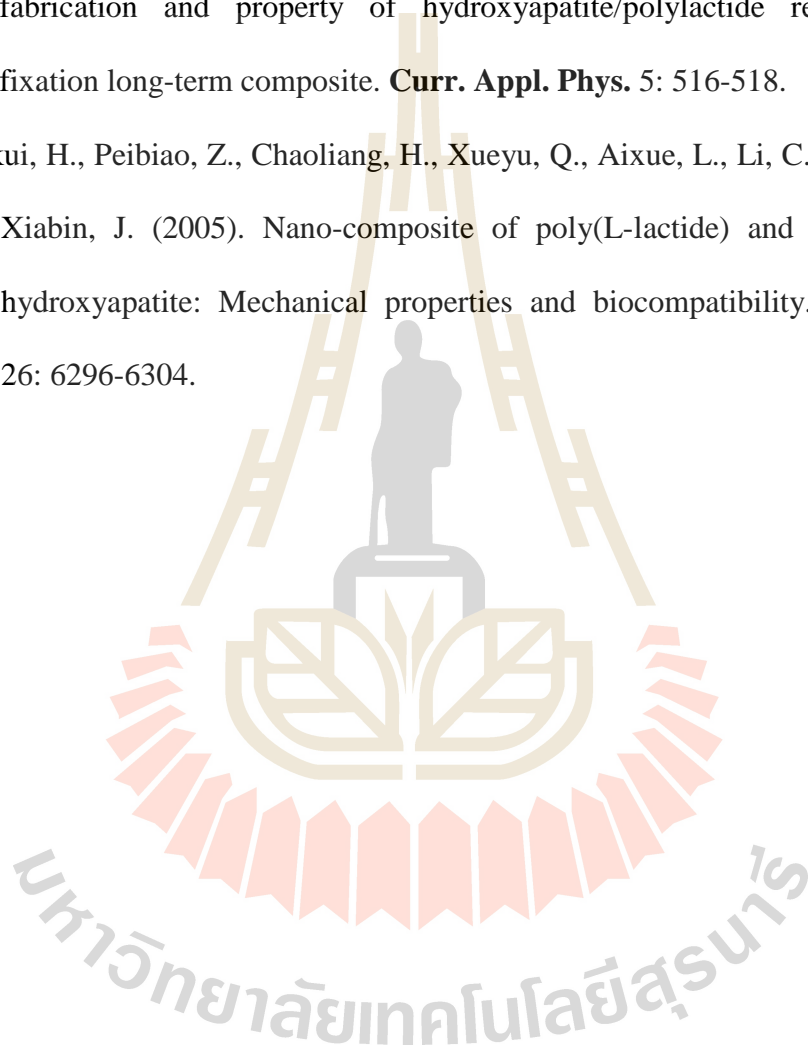
CHAPTER V

THERMAL PROPERTIES AND *in vitro* DEGRADATION

OF BOVINE BONE BASED HA/PLA COMPOSITES

5.1 Abstract

In this present study, effect of silane coupling on thermal properties of bovine bone based hydroxyapatite (u-HA)/PLA composites and on molecular weight of PLA upon processing of the composites were studied. TGA and GPC results showed that the incorporation of silane-treated HA into the PLA matrix significantly increased thermal stability of the composite and decreased the thermal degradation of PLA chains. In addition, the *in vitro* degradation of HA/PLA composites were analyzed. PLA and HA/PLA composites specimens were immersed in phosphate-buffered solution at 37ºC for the periods of time up to 8 weeks. The changes in specimen weight, pH of PBS solution and PLA molecular weight were investigated. In addition, the changes in morphologies of the specimens were also examined. The results showed that the stronger interfacial bonding between silane-treated HA and PLA matrix significantly delayed the *in vitro* degradation rate of the PLA. In addition, the results of bioactive study showed that the incorporation of u-HA into the PLA matrix significantly induced the formation of calcium phosphate compound on the composite surface, after 3 days of immersion in SBF, and generously covered the surface with a fairly thick layer after 7 days as evaluated by means of SEM, EDX, FTIR and XRD.

5.2   Introduction

Numerous of bioresorbable and biodegradable materials have been studied and applied for biomedical applications, including those based on bioresorbable polymer such as poly(lactic acid) (PLA), poly(3-hydroxybutyrate) (PHB) (Wanga, Yang, Wu, Cheng, Yu, Chen, and Chen, 2005), poly(ethylene glycol) (Wan, Chen, Yang, Bei, and Wang, 2003). The most widely used bioresorbable polymer is PLA, from points of its biocompatibility, biodegradability and yielding nontoxic byproducts after hydrolysis reaction (Kothapalli *et al.*, 2005; Shikinami *et al.*, 2001; Russias *et al.*, 2006; Tsuji *et al.*, 2004). However, mechanical properties of PLA should be improved in order to achieve optimum performance for specific applications, *e.g.* bone substitute material. Preparation of composite between bioactive fillers and PLA matrix is a commonly used method to improve the mechanical properties of PLA. Furthermore, the incorporation of these fillers resulted in an increase of the bioactivity of the composites.

Hydroxyapatite [HA: $Ca_{10}(PO_4)_6(OH)_2$] is good candidate as the filler for preparing PLA composites due to its osteoconductivity for bone growth and bone bonding ability (Benmarouane *et al.*, 2004; Ruksudjarit et *al.*, 2008; Yoganand *et al.*, 2009). In addition, HA can be synthetically prepared or derived from natural sources, *e.g.* coral (Sivakumar, Kumart, Shantha, and Rao, 1996), bovine bone (Shikinami *et al.*, 2001; Ruksudjarit *et al.*, 2008), swine bone (Haberko *et al.*, 2006). The natural HA is less expensive material than synthetic HA, so, choosing natural HA is an alternative choice for preparing PLA composite. Natural HA/PLA composite is an interesting composite expecting to be used as a biomedical application.

Devices prepared from HA/PLA composites can be processed via various methods, such as forging (Shikinami *et al.*, 2001) and hot pressing method (Cam, Hyon, and Ikada, 1995). However, HA/PLA composite processing still has some problems, such as thermal stability, dispersion of HA and compatibility of HA-PLA. These problems need to be concerned in the search for property enhancement of the composite specimens. Various research works have used silane coupling agent to enhance the homogeneous dispersion and compatibility of HA in PLA matrix (Daglilar *et al.*, 2007; Wang *et al.*, 2001). In those research works, they found that the incorporating of silane-treated HA led to the higher mechanical properties of the composites.

HA/PLA composite is usually proposed as an implant material, so, the *in vitro* degradation behavior study has become an interesting area of the study. By the *in vitro* study, it would be possible to predict the degradation behavior of the composites during period of implant time. Moreover, the degradation behavior *in vitro* can be used as a preliminary result for searching the HA/PLA composites with a suitable degradation properties for an implant material.

It is known that there are numerous factors affecting the polymer degradation mechanisms such as chemical structure, crystallinity and molecular weight of PLA, *etc.* Besides, the addition of HA phase into the PLA matrix increases the complexity of the degradation pattern of the material due to various parameter, *e.g.* shape and size of HA particles, composite processing condition, (Russias *et al.*, 2006; Cam *et al.*, 1995; Stefani, Coudane, and Vert, 2006; Navarro *et al.*, 2005; Li *et al.*, 2006). Some studies have reported dramatic changes in PLA degradation with the incorporation of some calcium phosphate compounds (Navarro *et al.*, 2005).

The scopes of the present study were to explore influence of silane coupling agent on thermal properties of HA/PLA composites during processing and on molecular weight of PLA upon processing of HA/PLA composites. In addition, the *in vitro* degradation of HA/PLA composites in phosphate-buffered solution at 37ºC for the periods of time up to 8 weeks was studied. Furthermore, the detailed degradation of the composites in a simulated body fluid (SBF) were also investigated.

5.3 Experimental

5.3.1 Materials

PLA (4042D) was purchased from NatureWorks LLC Co. Ltd.. Bovine bones were supplied by Limeiseng Co., Nakhon Ratchasima, Thailand. 3-aminopropyltriethoxysilane (APES) and 3-methacryloxypropyltrimethoxysilane (MPTS) were purchased from Optimal Tech Co., Ltd. and Aldrich, respectively. Dibasic sodium phosphate ($NaHPO_4 \cdot 2H_2O$), monobasic sodium phosphate ($NaH_2PO_4 \cdot 2H_2O$), Potassium chloride (KCl) and dibasic potassium phosphate ($KHPO_4 \cdot 2H_2O$) were purchased from Carlo Erba Reagent Spa. Sodium chloride (NaCl) was purchased from VWR International buba/sprl. Sodium hydrogen carbonated ($NaHCO_3$), Sodium sulfate (Na_2SO_4) and tris(hydroxymethyl) methylamine ($NH_2C(CH_2OH)_3$) were purchased from Fisher Scientific UK, Ltd. Magnesium dichloride ($MgCl_2 \cdot 6H_2O$) was purchased from Ajex chemicals. Calcium chloride ($CaCl_2$) was purchased from APS Ajex finechem.

5.3.2 Preparation of bovine bone based HA powders

Bovine bones were burned in open air and were ground into powder using a ball milling machine. Then, the powder was heat treated at 1100ºC for 3 h and the obtained powder was called u-HA. Next, the powder was modified by either APES (a-HA) or MPTS (m-HA) in acidic solution at pH of 3.5 for 3 h, subsequently, each solution was neutralized with 0.1 N NaOH solution. The content of silane based on weight of HA powder was 2.0wt%. After that, the silane-treated HA powders were washed and dried overnight in an oven at 80ºC. APES treated HA and MPTS treated HA were called a-HA and m-HA, respectively.

5.3.3 Preparation of phosphate-buffered solution and simulated human body fluid

Gomori buffers, the most commonly used phosphate buffers, consist of a mixture of monobasic dihydrogen phosphate and dibasic monohydrogen phosphate. By varying the amount of each salt, a pH range of buffers can be prepared that buffer well between pH 5.8 and pH 8.0. To prepare 0.15 M phosphate buffered solution (PBS) with pH of 7.4, 23.4 g of $NaH_2PO_4 \cdot 2H_2O$ and 26.7 g of $NaHPO_4 \cdot 2H_2O$ were separately dissolved in 1 litre of distilled water. Then, 810 ml of $NaH_2PO_4 \cdot 2H_2O$ solution was mixed together with 190 ml of $NaHPO_4 \cdot 2H_2O$ solution.

Simulated body fluid (SBF) in which inorganic ion concentrations are similar to those of human extracellular fluid were prepared. This fluid was used to immerse the composite specimens in order to observe *in vitro* the formation of HA on HA/PLA composites. To prepare simultaneous human body fluid, 750 ml of distilled water was poured into a 1000 ml beaker and each chemical listed in Table 5.1 was added one by one in the 1st-8th order. The added chemical must be completely

dissolved before adding the other. Subsequently, $NH_2C(CH_2OH)_3$, the 9th reagent, should be added little by little with less than about 1g, in order to avoid inhomogeneous increase in pH of the solution.

Table 5.1 Reagents for preparation of SBF (pH 7.40, 1 L).

Order	Reagent	Amount
1	NaCl	8.036 g
2	$NaHCO_3$	0.352 g
3	KCl	0.225 g
4	$K_2HPO_4 \cdot 3H_2O$	0.230 g
5	$MgCl_2 \cdot 6H_2O$	0.311 g
6	1.0 M HCl	40 ml
7	$CaCl_2$	0.293 g
8	Na_2SO_4	0.072 g
9	$NH_2C(CH_2OH)_3$	6.063 g
10	1.0 M HCl	Appropriate amount for adjusting pH

5.3.4 Preparation of HA/PLA composites

HA/PLA composites were prepared using an internal mixer (HAAKE/RHEOMIX). PLA and u-HA were mixed at 170ºC with 70 rpm for 10 min. The weight ratios of HA/PLA in each composite are shown in Table 5.2. Each HA/PLA composite was left at room temperature for 24 h before grinding into small pieces. Subsequently, it was hot-pressed by a compression molding machine (CARBOLITE) for 10 min at 180ºC under a pressure of 2000 psi and cooled to room temperature.

Table 5.2 Composition of HA/PLA composite.

Designation	Filler	Silane coupling agent	Filler content (wt%)
1A	u-HA	-	10
2A	u-HA	-	20
3A	u-HA	-	30
4A	u-HA	-	40
1B	a-HA	APES	10
2B	a-HA	APES	20
3B	a-HA	APES	30
4B	a-HA	APES	40
1C	m-HA	MPTS	10
2C	m-HA	MPTS	20
3C	m-HA	MPTS	30
4C	m-HA	MPTS	40

5.3.5 Determination of thermal properties of HA and HA/PLA composites

Thermal degradation temperature and weight loss of untreated HA powder, silane-treated HA powders and HA/PLA composites were determined by a thermogravitric analyzer (TGA) (TA INSTRUMENT/SDT2960). The sample was heated from room temperature to 600ºC at a heating rate of 10ºC/min under a nitrogen atmosphere.

5.3.6 Determination of molecular weight of neat PLA and HA/PLA composites

Molecular weight of PLA in neat PLA and in HA/PLA composite were evaluated by a gel permeable chromatography (GPC) using chloroform as an eluent. The chromatographer consisted of a styrene-divinylbenzene copolymer column (PLgel Mixed-C, 300×7.5 mm, 5μm), differential refractometer detector (AGILENT/RI-G1362A), online degasser (AGILENT/G1322A), autosampler (AGILENT/G1329A), thermostatted column compartment (AGILENT/G1316A) and quaternary pump (AGILENT/G1311A). The eluent flow rate was kept constant at 0.5 ml/min. Temperature of the column and the detector were maintained at 40ºC and 35ºC, respectively. Polystyrene standards (SHODEK STANDARD) with molecular weights of 3.90×10^6, 6.29×10^5, 6.59×10^4, 9.58×10^3 and 1.30×10^3 g/mol were used to generate a calibration curve. PLA and HA/PLA composites were dissolved and diluted using chloroform (2 mg/ml) and filtered before $\overline{M}_w$ determination.

5.3.7 Determination of *in vitro* degradation of PLA and HA/PLA composites

In vitro hydrolytic degradation of HA/PLA composites were determined by soaking PLA and HA/PLA composites in a phosphate-buffered solution (PBS) (0.15 M, pH 7.4). Three specimens ($4 \times 12 \times 63$ mm^3) of each sample were placed in a 100 ml test tube filled with 35 ml PBS solution. The immersed specimens were incubated at 37ºC for 0, 1, 2, 3, 4, 6 and 8 weeks. The buffer solution in all test tubes was weekly replaced by fresh PBS solution. This was done in order to maintain a constant volume of PBS solution and to imitate, to some extent, the *in vivo* flow model of continuously refreshing extracellular fluids.

At the end of each period, pH of PBS solution in each test tube was measured by pH meter (JENWAY/3020). The specimens were removed from PBS and wiped with a filter paper to remove surface water. The wet weight (W_w) and thickness of the samples (T_t) were measured. Then, these specimens were rinsed by distilled water for 3 times and vacuum dried at a temperature of 45ºC to a constant weight (W_d). Water absorption of the HA/PLA composites from PBS solution was determined. The percentage increase in weight, thickness change and percentage decrease in weight of the specimen during the specimen immersion in PBS solution was calculated by the following equations:

$$\text{Increase in weight, \%} = \left[\frac{(W_w - W_o)}{W_o}\right] \times 100 \qquad (5.1)$$

$$\text{Thickness change, \%} = \left[\frac{(T_t - T_o)}{T_o}\right] \times 100 \qquad (5.2)$$

$$\text{Weight loss, \%} = \left[\frac{(W_o - W_d)}{W_o}\right] \times 100 \qquad (5.3)$$

Where W_o is an initial weight of the specimen; W_w is the wet weight of the specimen after removing from PBS; W_d is the weight of the specimen after removing from PBS and drying at 45ºC; T_o is an initial thickness of the specimen; T_t is the immediately measured thickness of the specimen after removed from PBS, respectively.

Additionally, the change in PLA molecular weight and morphological properties of the PLA composites after PBS immersion were investigated using a gel permeation chromatograph (GPC) and a scanning electron microscope (SEM), respectively. To investigate surface of the HA/PLA composites, specimens were coated with a thin layer of gold before examination using the SEM (JOEL/JSM-6400) operating at 10 kV.

5.3.8 Determination of bioactive properties of PLA and HA/PLA composites

Bioactive properties of HA/PLA composites were determined by immersing PLA and HA/PLA composites in a simultaneous body fluid (SBF) (pH 7.4). A specimen ($4\times12\times10$ mm^3) of each sample was placed in a 100 ml test tube filled with 35 ml SBF solution. The specimens were incubated at 37ºC for 0, 1, 2 weeks. At the end of each period, the specimens were removed from PBS and, then, the morphological properties of PLA and HA/PLA composites were investigated using a SEM (JOEL/JSM-6400) operating at 10-15 kV. To investigate surfaces of the PLA and the HA/PLA composites, samples were coated with a thin layer of gold before examination.

The precipitates formed on the surface of the composite, after 1 week of immersion, were scratched and analyzed by X-ray diffractometer (XRD) (OXFORD/D5005) with a Cu-Kα as a radiation source. A step size of 0.02º and a scan speed of 0.4º/min were used while the voltage was held at 35 kV.

Functional groups of the scratched precipitates were identified by a Fourier transform infrared spectrometer (FTIR) (BIO-RAD/FTS175C, KBr pellet

technique). The spectrum was recorded in the 4000-400 cm^{-1} region with 2 cm^{-1} resolution.

In addition, elemental compositions of the precipitates were analyzed by an energy dispersive x-ray spectrometer (EDX) (OXFORD INSTRUMENT/LINK ISIS6209). Each peak of the recorded spectrum is a characteristic of a particular element.

5.4 Results and Discussion

5.4.1 Thermal properties of HA and HA/PLA composites

Figure 5.1 shows TGA thermograms of u-HA, m-HA and a-HA. All of them were thermally stable during the given temperature range since their weight losses were less than 1wt% during the temperature range of 35-600ºC. The m-HA and a-HA showed higher decomposition temperatures and less weight losses than u-HA indicating the appearance of deposited silane coupling agent on HA surface increased thermal atability of HA powder.
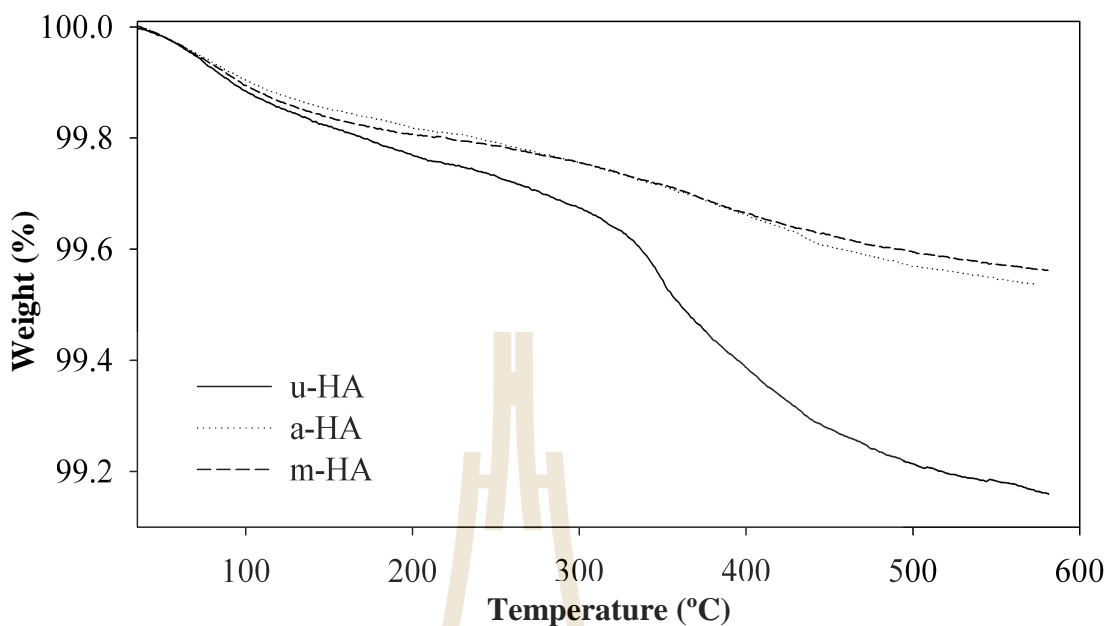
Figure 5.1 TGA thermograms of u-HA, a-HA and m-HA.

Figure 5.2 shows TGA thermograms of neat PLA, u-HA/PLA, a-HA/PLA and m-HA/PLA composites at various contents of the HA. The neat PLA had higher thermal stability than u-HA/PLA composites as shown in Figure 5.2 (a). In addition, the composites containing u-HA exhibited significantly lower thermal stability with increasing filler content as compared between 20wt% and 40wt% of u-HA. In contrast, thermal stability of the composites containing silane-treated HA was slightly increased with increasing filler content, as shown in Figure 5.2 (b-c).

As reported by several research groups, an increase in thermal stability of a polymer composite can be explained in two aspects: either polymer decomposition products are blocked by a good distribution, good adhesion and good dispersion of better thermal stability of filler (Fukushima *et al.*, 2009) or the good distribution and good dispersion of filler in the composite acts as a barrier preventing heat transfer (Ignjatovic *et al.*, 2004). In addition, the results from chapter 3

suggested that u-HA/PLA composites occurred thermal oxidative upon processing and the OH groups on HA surface accelerated the reaction. By treating HA surface with a silane coupling agent, OH groups on the HA surface were less exposed to PLA matrix. Thermal oxidation of PLA in silane-treated HA/PLA composite was then slow down as confirmed by the initial $\overline{M}_w$ of 4A, 4B and 4C in table 5.4. According to other reports the increase in thermal stability of the silane-treated HA/PLA composites with increasing HA content was due to the better distribution and adhesion between silane-treated HA and PLA matrix as well as the less exposion of OH groups on HA surface to the PLA matrix.
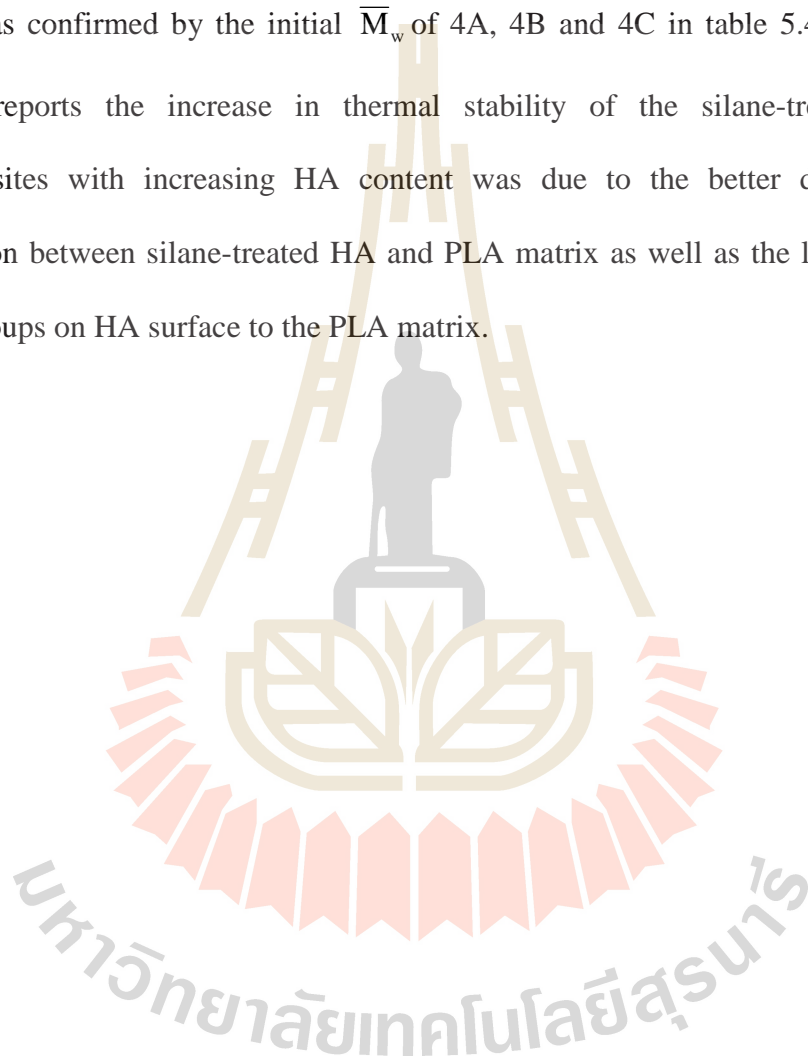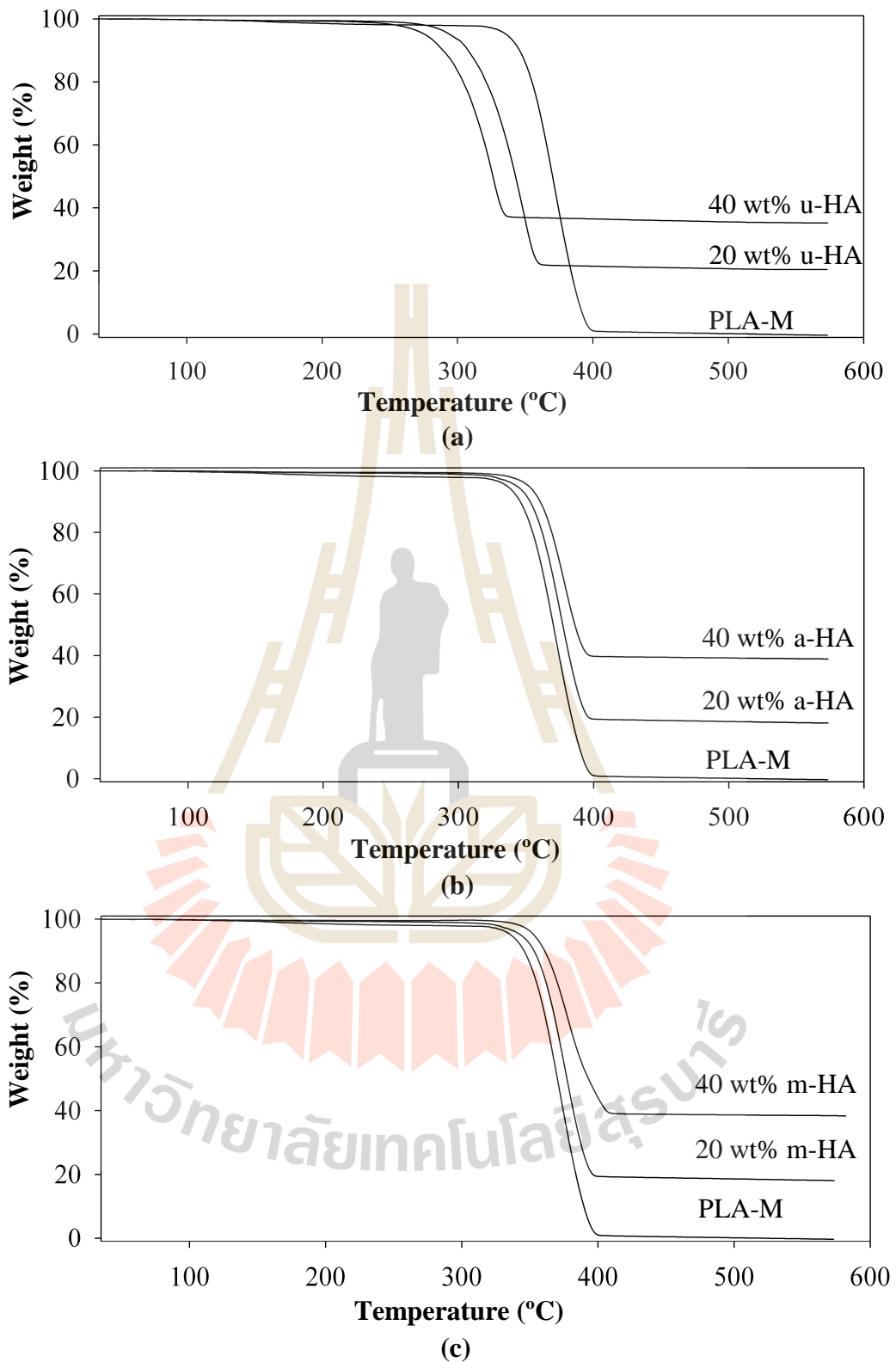
Figure 5.2 TGA thermograms of (a) b-HA/PLA, (b) a-HA/PLA and (c) m-HA/PLA

composites with HA contents of 20wt% and 40wt%.

5.4.2 Change in molecular weight and molecular weight distribution of PLA after processing

It is known that PLA chains can be easily broken at a particular temperature range. Subsequently, molecular weight of PLA is decreased; monomers and gas-products are formed (Ignjatovic *et al.*, 2004). Therefore, during the preparation of HA/PLA composite, the PLA chains could possibly be degraded by high processing temperature. This was further investigated by GPC technique. Effects of HA surface treatment and HA content on molecular weight of PLA are illustrated in Table 5.3. Based on GPC results, it was clearly shown that the degradation of PLA chains in the composites containing m-HA and a-HA was slow down.

The planar conformation of PLA basic structure is defined as $H–[–O–CH(CH_3)–CO–]_n–OH$. One can predict where the breaking of bonds in the basic chain will occur. Gupta and Deshmukh (1982) reported that the thermal degradation of PLA chain is a one-step process with the first-order reaction kinetics. The OH groups at the end of PLA chain can destroy the basic chain under the influence of thermal energy. In each of these reactions, the OH group regenerates and the process continues. In addition, the OH groups on untreated HA surface can also directly destroyed the PLA basic chain (Ignjatovic *et al.*, 2004). According to their works, the appearance of OH groups in the composite system has an important influence on the PLA molecular weight. However, it is known that some silane coupling agents can be bonded with OH group on HA surface. Treating HA surface with a silane coupling agent, as done in this study, before incorporating into PLA matrix decreased amounts of OH groups on HA surface. Therefore, PLA chains in the composites were less attacked and their molecular weight were less degraded.

Table 5.3 Effect of HA surface treatment and HA content on molecular weight of PLA in neat PLA and the composites.

Designation	Average molecular weight		MWD
	$\overline{M}_w$	$\overline{M}_n$	
as-received PLA	2.83×10^5	1.31×10^5	2.16
PLA-M	1.94×10^5	0.76×10^5	2.55
1A	0.67×10^5	0.11×10^5	6.09
2A	0.61×10^5	0.10×10^5	6.10
3A	0.56×10^5	0.09×10^5	6.22
4A	0.53×10^5	0.08×10^5	6.63
1B	1.62×10^5	0.33×10^5	4.90
2B	1.33×10^5	0.18×10^5	7.38
3B	1.29×10^5	0.15×10^5	8.60
4B	1.24×10^5	0.13×10^5	9.53
1C	1.52×10^5	0.29×10^5	5.24
2C	1.47×10^5	0.23×10^5	6.39
3C	1.37×10^5	0.19×10^5	7.21
4C	1.24×10^5	0.15×10^5	8.27

5.4.3 *In vitro* degradation of PLA and HA/PLA composites

5.4.3.1 Change in pH of PBS solution

Neat PLA and HA/PLA composite specimens were put into vials and immersed in PBS solution. Then, pH values of the PBS solution at various immersion time were measured as illustrated in Figure 5.3. For the neat PLA specimens at the immersion time up to 4 weeks, the pH of the PBS solution remained constant at about 7.4 and followed by a slight decrease.

In comparison between HA/PLA composites, the pH values of the PBS solution after immersing u-HA/PLA composites were lower than those of the PBS solution after immersing silane-treated HA/PLA composites (*i.e.* 2B, 4B, 2C and 4C). Additionally, the pH of the PBS solution after immersing u-HA/PLA composites decreased faster with increasing u-HA content.
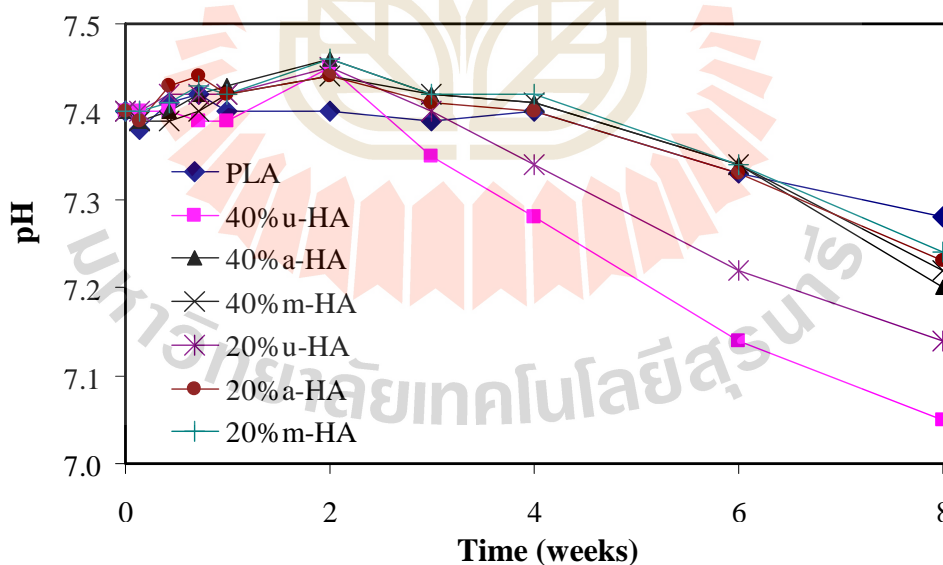

Figure 5.3 Changes in pH of PBS solution after immersion of neat PLA, u- HA/PLA, a-HA/PLA and m-HA/PLA composites.

Generally, the decrease in the pH value of the PBS is due to the formation of the degraded acidic molecules and their release from the composite. However, in the present study, a part of the acidity of the degradation products could be neutralized by alkaline calcium phosphate in the composite. This observation was similar to other research works, Li *et al*. (2004) found that the basic ions released from the wollastonite powder neutralized the acidic degradation products of the polyhydroxybutyrate-polyhydroxyvalerate (PHBV) and compensated the pH decrease. Moreover, the compensated acidification of the PBS, due to acidic products of the biodegradable polyester degradation, by exchanging of protons in PBS for alkali in the Bioglass® particles were also reported (Stamboulis, Hench, and Boccaccini, 2002; Boccaccini and Maquet, 2003). Therefore, the pH value of the PBS solution slightly increased after the first two weeks of the immersion of HA/PLA composites. The rapid decrease in pH after 4 weeks of immersion is possibly caused by the more hydrolysis of PLA where H^+-ions come into the solution, exceeding the buffering capacity of PBS. As the degraded acidic molecules accumulated and released from the composite, the pH values of PBS obviously decreased. In addition, the poor adhesion between u-HA and PLA and the poor distribution of u-HA in the matrix could release more acidic molecules from the composite into the PBS. In this case, the pH values of the PBS after immersing u-HA/PLA composites were lower than those of the PBS after immersing silane-treated HA/PLA composite.

5.4.3.2 Effect of *in vitro* dedradation on the size of composites

Figure 5.4 shows percentage of width and thickness changes of neat PLA, u-HA/PLA, a-HA/PLA and m-HA/PLA composites during *in vitro* degradation. As shown in Figure 5.4 (a), in the first four weeks of *in vitro* degradation a slight increase in thickness of the neat PLA specimens was observed as compared with those of the HA/PLA composite specimens. The increased in size at initial time of immersion should be attributed to the relaxation of stress of the u-HA/PLA, a-HA/PLA and m-HA/PLA composites generated in the fabrication when the specimens were incubated in the PBS at 37ºC (Yang *et al.*, 2008).

After four weeks of immersion, the increases in thickness of the a-HA/PLA and the m-HA/PLA composites were less than that of u-HA/PLA composites. These phenomena were probably attributed to the hydrophilicity of the deposited silane coupling agent on the HA surface leading to the less swelling of the silane-treated HA composite. According to SEM micrographs of u-HA/PLA composites, it should be noted that u-HA is a hydrophilic material resulting in the gap occurrence at interface between u-HA and PLA matrix. These gaps would lead to the faster diffusion of PBS into inner site of the composite, then, the thickness swelling of u-HA/PLA composites was greater than those of silane-treated HA/PLA composites. As shown in Figure 5.4 (b), similar phenomena were found in width changes of all specimens during *in vitro* degradation.
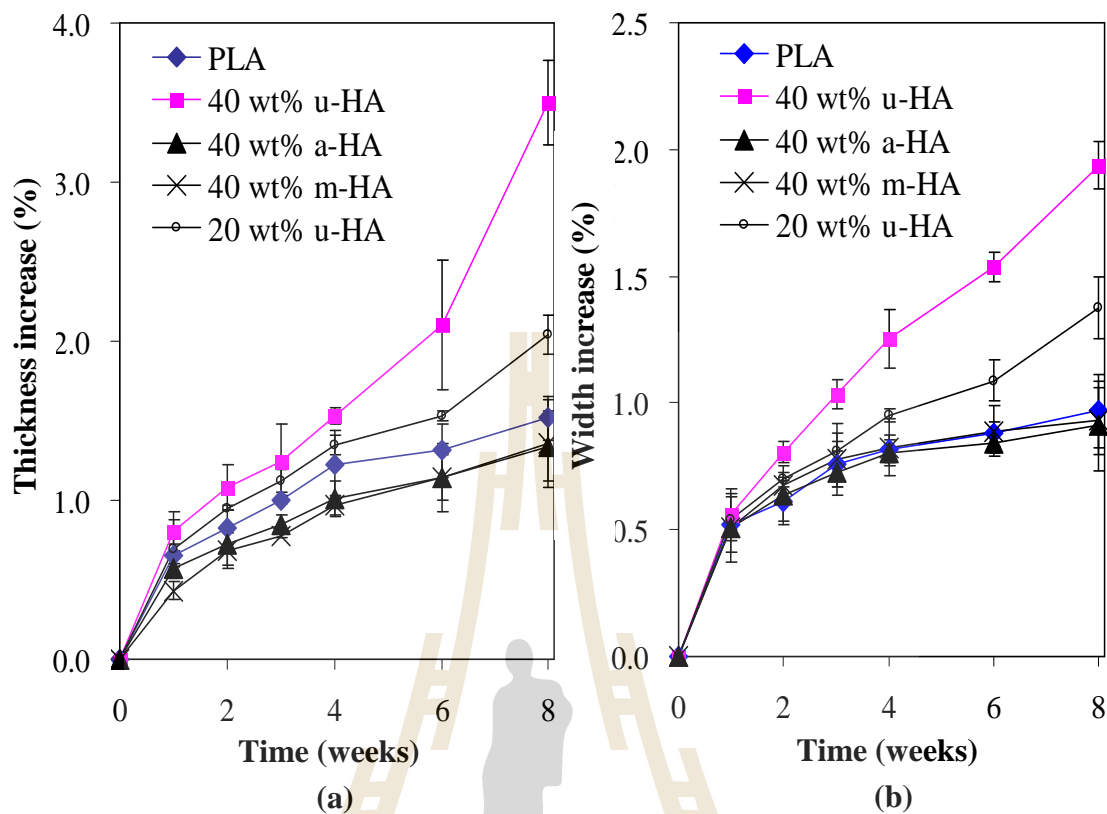
Figure 5.4 Dimensional changes of the neat PLA and the composite specimens upon

immersion in PBS solution: (a) thickness change and (b) width change.

5.4.3.3 Effect of *in vitro* dedradation on the weight of composites

It was shown in Figure 5.5 that all specimens after *in vitro* experiment tended to increase their weight with increasing the immersion time. As seen, the weight of neat PLA increased slower than that of the composite. For the composites, at the equal content of filler, the u-HA/PLA composites showed higher increase in weight than that of silane-treated HA/PLA composite. The rapid increase in weight of u-HA/PLA composite indicated that water can easily diffuse through the matrix. This result was probably due to the porosity or gap in the composite matrix created by lacking of adhesion between u-HA and PLA matrix. Additionally, by increasing filler contents, the gradual increase in weight of the composites were also observed especially for the u-HA/PLA composites.

Subsequently, all specimens were dried at 45ºC to constant weight before measuring the weight loss. The weight of the neat PLA, u-HA/PLA, a-HA/PLA and m-HA/PLA composites was measured at different immersion periods. As shown in Figure 5.6, the neat PLA showed a slight weight loss, less than 0.4%, during the experimental periods.

Figure 5.5 Water absorption of the neat PLA and the composite specimens upon

immersion in PBS: (a) effect of filler types, (b) effect of untreated HA

content, (c) effect of MPTS-treated HA content and

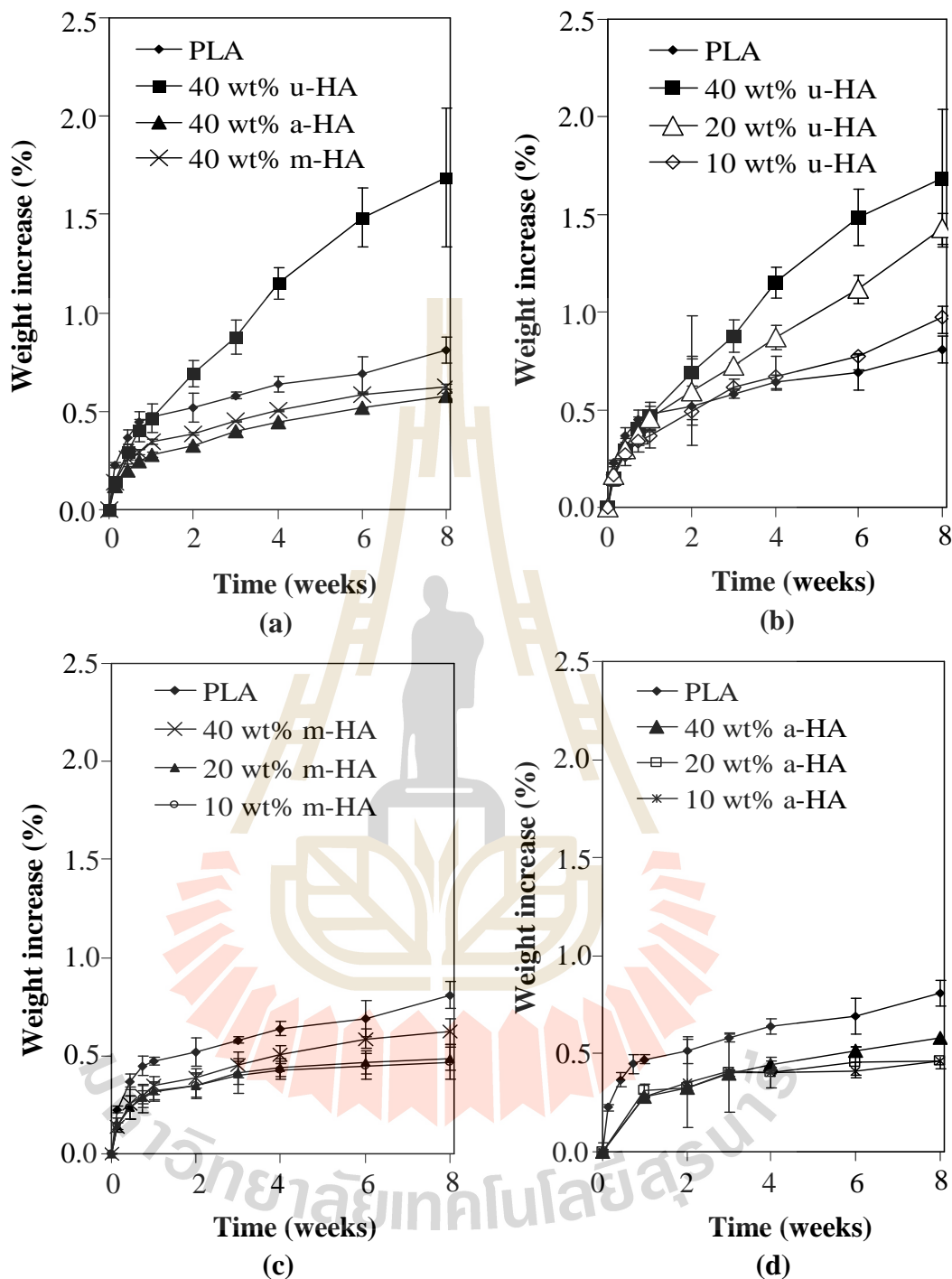(d) effect of APES-treated HA content.

Figure 5.6 Weight changes of the neat PLA and the composites specimens upon

immersion in PBS: (a) effect of filler type, (b) effect of untreated HA

content, (c) effect of MPTS-treated HA content and
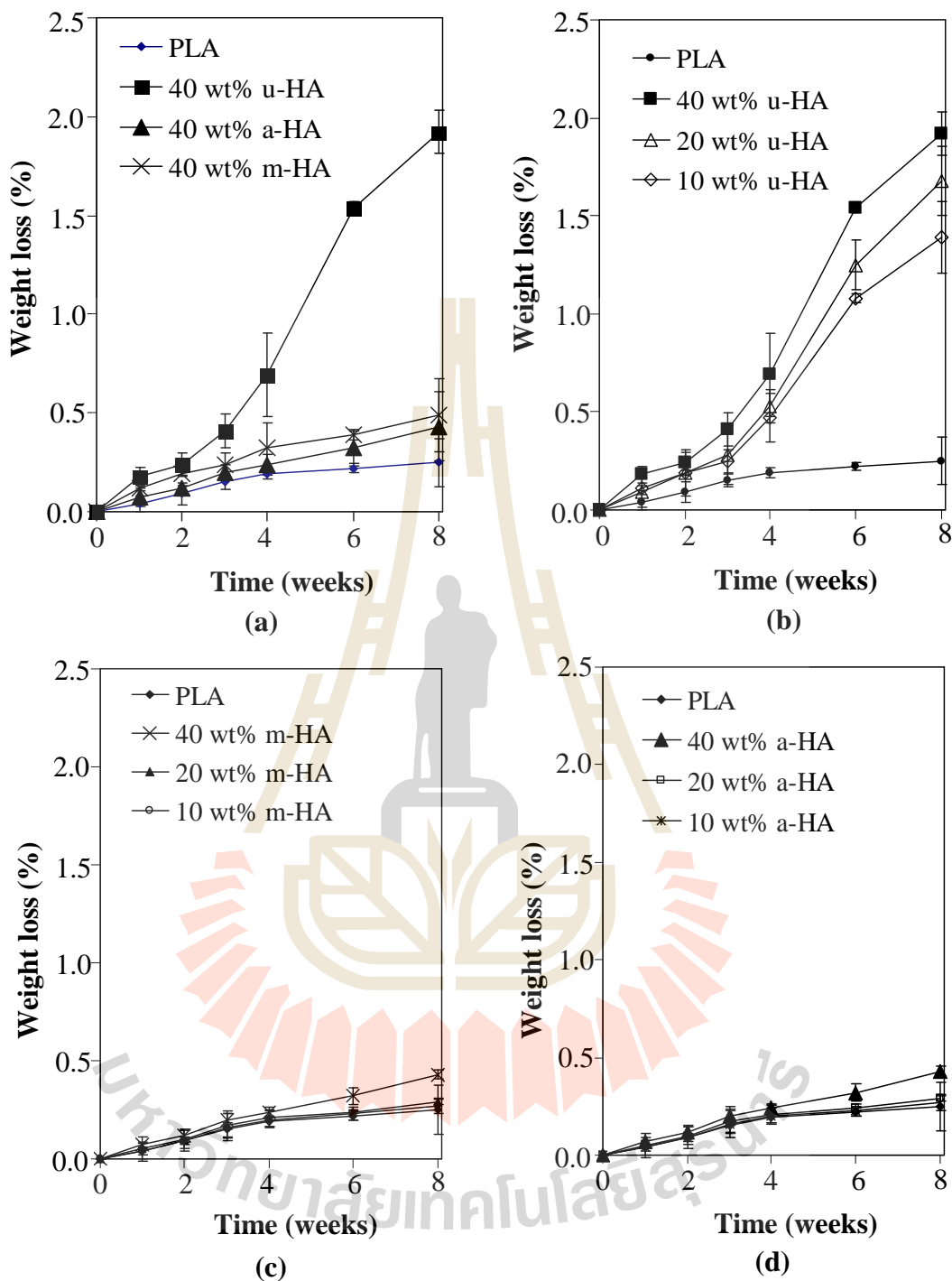
(d) effect of APES-treared HA content.

However, the weight loss profiles of the composites were different from that of neat PLA. For the u-HA/PLA, a-HA/PLA and m-HA/PLA composite specimens, after incubating in PBS, exhibited increases in weight loss as functions of HA content and types of surface modified HA as shown in Figure 5.6 (a-d). The weight loss of u-HA/PLA composite specimens was the highest, as compared with those of the silane-treated HA/PLA composite specimens. This was due to the higher chance of PBS penetration via the u-HA and PLA interface and leakage of the degradation products throughout surface cracks, created by low surface adhesion, and the solubility of the HA particles themselves (Navarro *et al.*, 2005). Moreover, the weight loss of all composite specimens increased with increasing HA content. It seemed that treating HA surface with silane coupling agent diminished those causes of weight loss of the composites mentioned previously.

5.4.3.4 Changing in molecular weight of PLA molecules

The decrease in molecular weight of PLA chains with immersion time are shown in Table 5.4 and Table 5.5. As seen, the molecular weight of PLA in all specimens gradually decreased with increasing immersion time. At 1, 4, and 8 weeks after immersion in PBS, the PLA molecular weights in the u-HA/PLA composite specimen were decreased about 38.65, 49.48 and 52.06% of their initial values, respectively, while those in the a-HA/PLA and m-HA/PLA specimens were 3.22, 7.25, 13.71, 6.45, 25.81 and 26.61%, respectively. After 2 weeks of immersion, the molecular weight of PLA in the composites drastically decreased at faster rate than that of the neat PLA. In comparison, the PLA molecular weight in u-HA/PLA specimens decreased faster than those in the m-HA/PLA and a- HA/PLA specimens.

The possible reason of degradation of PLA chains is the random scissions of the ester linkages in their backbone. Generally, the rate of non-enzymatic degradation of poly(α-hydroxy acid) attributed to the diffusion rate of water and the concentration of OH^- ions which catalyse the hydrolysis of ester bonds of poly(α-hydroxy acid) (Cam *et al.*, 1995; Yuan et *al.*, 2002). Hence, an important factor affecting hydrolysis degradation mechanism of biodegradable polymer via hydrolysis reaction attributed to the uptake of water (Gopferich, 1996).

Table 5.4 Changes in molecular weight of PLA in neat PLA and the composites after immersion in PBS.

Immersion time (weeks)	$\overline{M}_w$			
	PLA	**4A**	**4B**	**4C**
0	1.94×10^5	0.53×10^5	1.24×10^5	1.24×10^5
1	1.19×10^5	0.42×10^5	1.20×10^5	1.16×10^5
2	1.18×10^5	0.42×10^5	1.18×10^5	1.07×10^5
4	0.98×10^5	0.41×10^5	1.15×10^5	0.92×10^5
6	0.95×10^5	0.34×10^5	1.10×10^5	0.91×10^5
8	0.93×10^5	0.30×10^5	1.07×10^5	0.91×10^5

Table 5.5 Percentage of changes in molecular weight of PLA in neat PLA and the composites after immersion in PBS.

Immersion time (weeks)	%Change in $\overline{M}_w$			
	PLA	4A	4B	4C
0	-	-	-	-
1	38.65	20.75	3.22	6.45
2	39.17	20.75	4.84	13.71
4	49.48	22.64	7.25	25.81
6	51.03	35.85	11.29	26.61
8	52.06	43.39	13.71	26.61

As shown in Table 5.4, the molecular weight of PLA in the u-HA/PLA composites decreased faster than those in the neat PLA, a-HA/PLA and m-HA/PLA composites. This was because of the lacking of adhesion between u-HA particles and the PLA matrix indicating by the appearance of gap at interface between u-HA particles and the PLA matrix as shown in SEM micrograph of tensile fracture surface of 20wt% u-HA and 20wt% a-HA composite (Figure 5.7). Hence, phosphate-buffered solution can easily penetrated into the inner site of u-HA/PLA composites though the interface between PLA and u-HA particles and initiate hydrolysis reaction in this composite at a faster rate than it does to other composite systems. On the other hand, the decrease in PLA molecular weight in the composite seemed to be slow down by treating HA surface with a silane coupling agent. This can be explained as follows. Silane-treated HA has more hydrophobic and more compatible to PLA matrix than untreated HA. The incorporated silane-treated HA distribute homogeneously in PLA matrix and provide good adhesion between the two phases as

shown in Figure 5.7 (b). So, PBS solution need long time period to penetrate in and to hydrolyze the silane-treated HA/PLA composites, *i.e.* a-HA/PLA and m-HA/PLA composites.
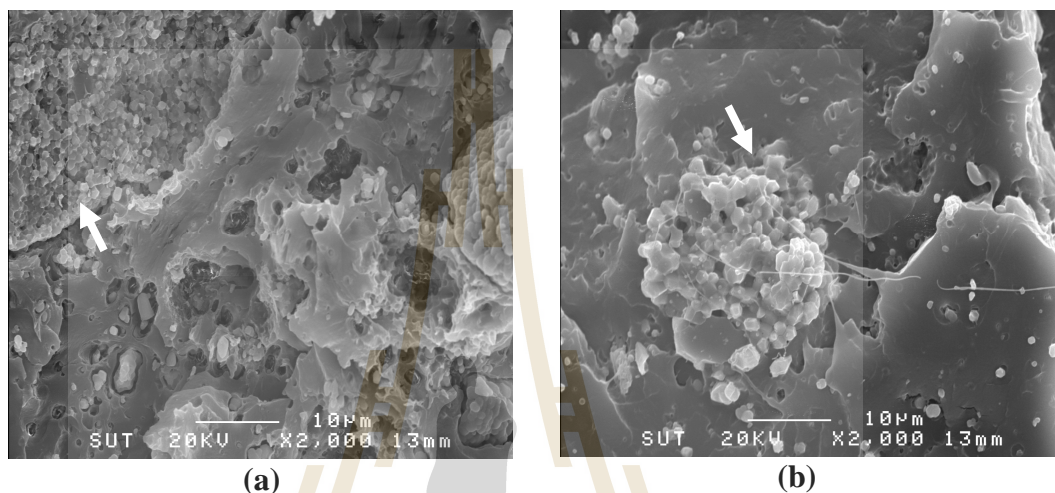

Figure 5.7 SEM micrographs of tensile fracture surfaces of PLA composites at 20wt% of (a) u-HA, (b) a-HA.

5.4.3.5 Change in surface morphologies of the HA/PLA composites

Figure 5.8 and 5.9, respectively, show the SEM micrographs of 40wt% u-HA/PLA and a-HA/PLA composite surfaces at various immersion periods in PBS. As seen, the morphologies of all composites were altered with increasing immersion time, especially those of the u-HA/PLA composite. At the initial time, all composites showed flat composite surfaces. After 2 weeks of immersion, the surface of the composite began to erode because of reactivity between PLA and PBS. After 4 weeks of immersion, the PLA part continued degrading and created the scratch on composite surface, further, some of the cracks became larger. At the immersion time of 8 weeks, the larger hole on the composite surface was observed. This was because

of the degradation of PLA and the release of the degradation products; some of HA particles were exposed out of the composite surface. A large amounts of u-HA particles were observed and accumulated on the u-HA/PLA composite surface. This was due to the faster degradation of PLA in the composite than that of a-HA/PLA and m-HA/PLA composites.
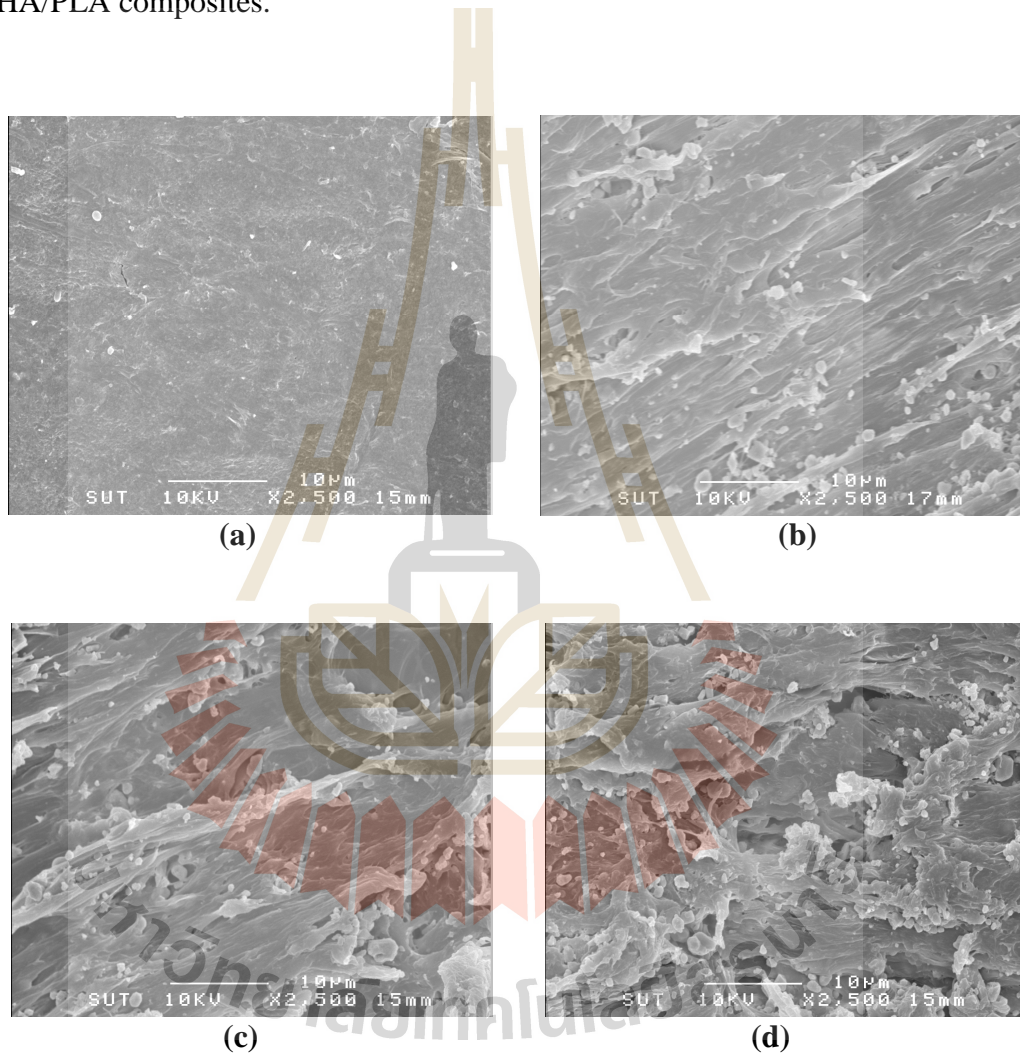

(a)   (b)

(c)   (d)

Figure 5.8 Changes in morphologies of 40wt% u-HA/PLA composites upon immersion in PBS for: (a) 0 week, (b) 2 weeks, (c) 4 weeks and (d) 8 weeks.

(a)

(b)

(c)

(d)
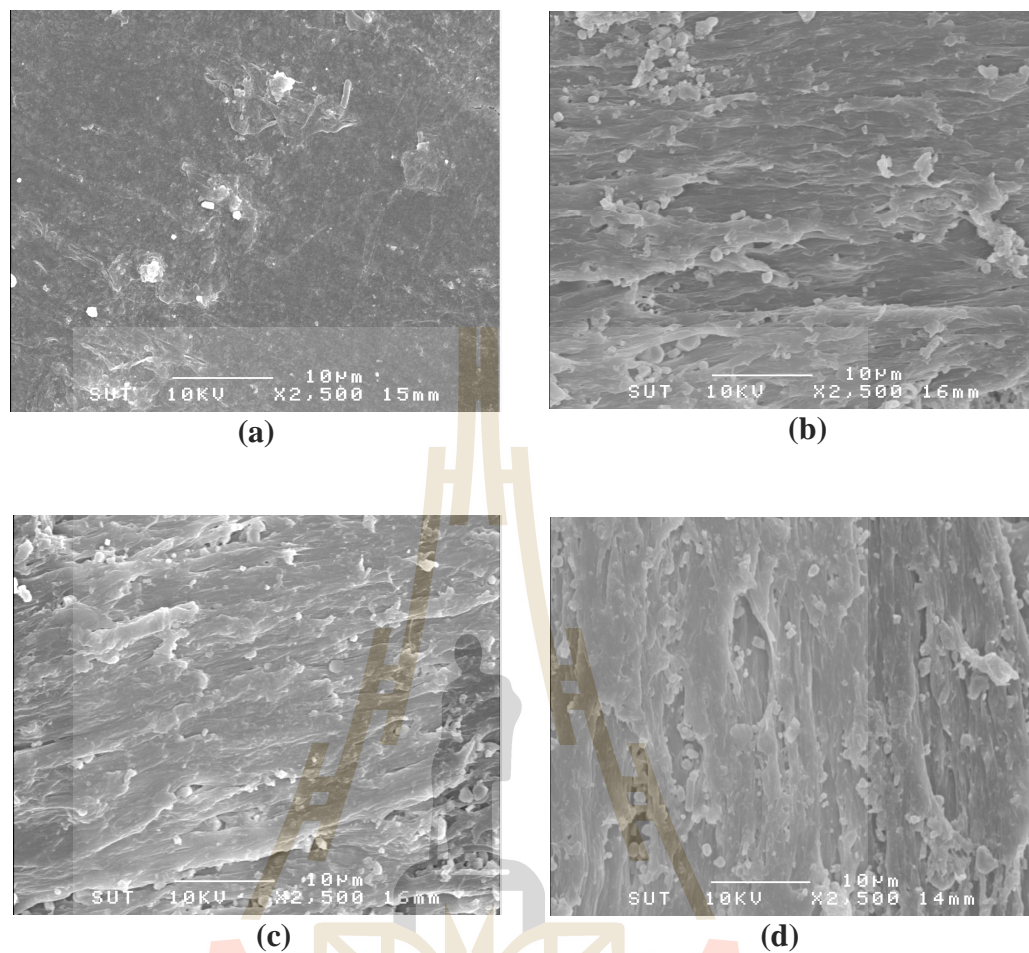
Figure 5.9 Changes in morphologies of 40wt% m-HA/PLA composites upon immersion in PBS for: (a) 0 week, (b) 2 weeks, (c) 4 weeks and (d) 8 weeks.

5.4.4 Investigation of bioactivity of HA/PLA composites

Figure 5.10 (a-d) shows SEM micrographs of the outer surfaces of PLA composites containing 40wt% of u-HA at various immersion period in SBF. At the initial time (Figure 5.10 (a)), a flat composites surface was observed. However, after 3 days of immersion in SBF at 37ºC, the surface of the composite began to degrade while precipitated particles were observed on the composite surface, as

shown in Figure 5.10 (b). Further, after 1 week of immersion, the amounts of the precipitates were obviously increased (Figure 5.10 (c)). After 2 weeks of immersion, the composites specimen surface was covered with the precipitates (Figure 5.10 (d)). The EDX attached to the SEM indicated that the elemental composition in the precipitates were calcium and phosphorus. The precipitated powder was scratched out from the composite surface for further investigation by an XRD and a FTIR spectroscopy.
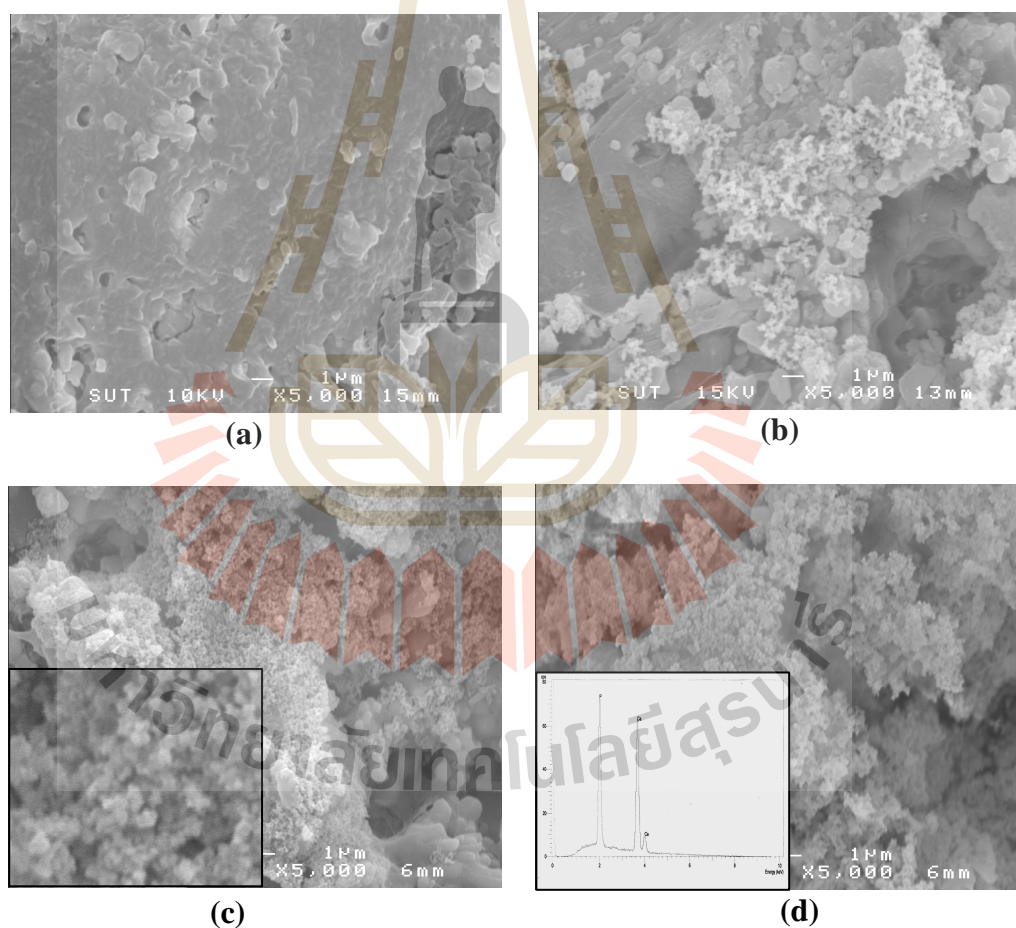

Figure 5.10 SEM micrographs of composite surfaces and the precipitated layer

        formed after immersion in SBF for: (a) 0 week, (b) 3 days,

        (c) 1 week and (d) 2 weeks.

Figure 5.11 displays the XRD pattern of the scratched precipitated powder from the composite surfaces. The scratched powder showed mixed phases of tri-calcium-di-phosphate (TCP) and HA. The characteristic peak of HA at 31.30º was observed and the characteristic peak of TCP at 30.44º was also observed. In addition, the presence of broad peak between 20º and 38.5º indicates the formation of an amorphous phase. Therefore, it can be inferred that the mixture of an amorphous TCB and HA apatite was formed on the HA/PLA composite surface after 3 days of immersion in SBF.
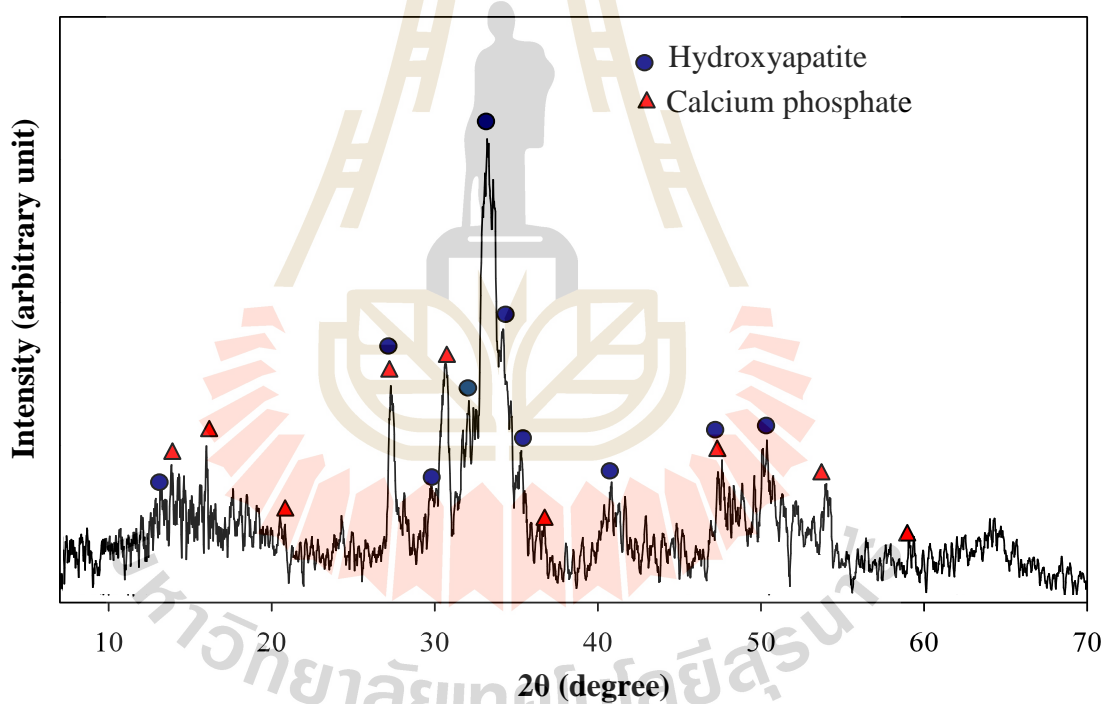
Figure 5.11 XRD pattern of scratched powder from the composite surface after 2 weeks of immersion.

FTIR spectrum of the scratched precipitated powder is shown in Figure 5.12. The peaks at 1085, 1036, 963, 600 and 575 cm^{-1} were assigned to different vibration modes of PO_4^{3-} group in the precipitated powder. Moreover, The stretching and the bending vibration of structural OH groups in the apatite lattice were also observed at 3571 cm^{-1} and 632 cm^{-1}, respectively. According to these results, an amorphous calcium phosphate was formed under this experimental condition (SBF, 37ºC, pH 7.4).

Figure 5.12 FTIR spectrum of the precipitate powder on the composite after 1 week of immersion in SBF at 37ºC.

5.5   Conclusions

The TGA results of HA/PLA composites revealed that thermal properties of HA/PLA composite were crucially depended on surface properties of HA particle. Silane-treated HA/PLA composites showed an 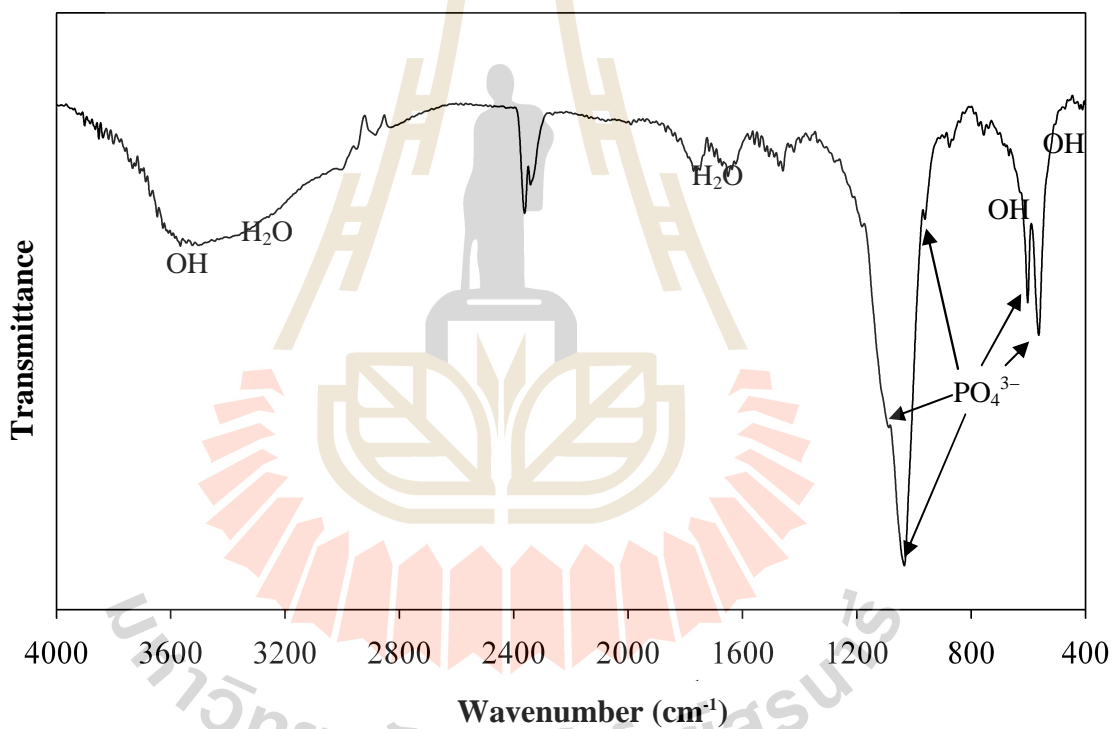increasing in thermal stability as compared with the untreated HA/PLA composites. Moreover, the deposit of silane coupling on HA surface in silane-treated HA/PLA composites delayed the PLA chains scission, which were confirmed by GPC results. Additionally, the *in vitro* degradation behaviors of all HA/PLA composites were investigated. Results showed that the untreated HA/PLA composites exhibited more change in pH stability of PBS, mass, thickness, width, and morphologies than those of silane-treated HA/PLA composites. Moreover, the molecular weight of PLA in the untreated HA/PLA composites were higher changed, after immersion in PBS, than silane-treated HA/PLA composites. The porosity and gap in the composite matrix created by lacking of adhesion between u-HA and PLA matrix led to rapid diffuse of water through the matrix. These was the main reason of the faster degradation of PLA in u-HA/PLA composites. In contrast, silane-treated HA/PLA composite had more adhesion between two phases leading to the less penetrate of water into inner side, therefore, lower degradation of PLA was obtained. Additionally, the bioactive characterization showed the positive result in the formation of a calcium phosphate on the composite surface, after immersion in SBF, which could enhance the interaction between the material and the bone tissue.

5.6   References

Benmarouane, A., Hansena, T., and Lodini, A. (2004). Heat treatment of bovine bone preceding spatially resolved texture investigation by neutron diffraction. **Physica B.** 350: 611-614.

Boccaccini, A. R. and Maquet, V. (2003). Bioresorbable and bioactive polymer/ Biogalss® composites with tailored pore structure for tissue engineering applications. **Compos. Sci. Technol.** 63: 2417-29.

Cam, D., Hyon, S. H., and Ikada, Y. (1995). Degradation of high molecular weight poly(L-lactide) in alkaline medium. **Biomoterials.** 16: 833-843.

Daglilar, S. and Erkan, M. E. (2007). A study on bioceramic reinforced bone cements. **Mater. Lett.** 61: 1456-1459.

Fukushima, K., Tabuani, D., and Camino, G. (2009). Nanocomposites of PLA and PCL based on montmorillonite and sepiolite. **Mater. Sci. Eng. C.** 29: 1433-1441.

Gopferich A. (1996). Mechanisms of polymer degradation and erosion. **Biomaterials.** 17: 103-140.

Gupta, M. and Deshmukh, V. (1982). Thermal oxidative degradation of polylactide acid. Part II: Molecular weight and electronic spectra during isothermal heating. **Colloid. Polym. Sci.** 260: 517-527.

Haberko, K., Bucko, M. M., Brzezinska-Miecznik, J., Haberko, M., Mozgawa, W., Panz, T., Pyda, A., and Zarebski, J.(2006). Natural hydroxyapatite-its behaviour during heat treatment. **J. Euro. Ceram. Soc.** 26: 537-542.

Ignjatovic, N., Suljovrujic, E., Simendic, J., Krakovsky, I., and Uskokovic, D. (2004). Evaluation of hot-pressed hydroxyapatite/poly-L-lactide composite biomaterial characteristics. **J. Biomed. Mater. Res.** 71B: 284-294.

Kang, Y., Xu, X., Yin, G., Chen, A., Liao, L., Yao, Y., Huang, Z., and Liao, X. (2007). A comparative study of the in vitro degradation of poly(L-lactic acid)/b-tricalcium phosphate scaffold in static and dynamic simulated body fluid. **Euro. Polym. J.** 43: 1768-1778.

Kothapalli, C. R., Shaw, M. T., and Wei, M. (2005). Biodegradable HA-PLA 3-D porous scaffolds: Effect of nano-sized filler content on scaffold properties, **Acta Biomater.** 1: 653-662.

Li, H. and Chang, J. (2004). Fabrication and characterization of bioactive wollastonite/PHBV composite scaffolds. **Biomaterials.** 25: 5473-80.

Li, S., Garreau, H., and Vert, M. (1990). Structure-property relationships in the case of the degradation of massive poly(a-hydroxy acids) in aqueous media. Part 3 Influence of the morphology of poly(L-lactic acid). **J. Mater. Sci. Mater. Med.** 1: 198-206.

Li, X., Feng, Q., and Cui, F. (2006). In vitro degradation of porous nano-hydroxyapatite/collagen/PLLA scaffold reinforced by chitin fibres. **Mater. Sci. Eng. C.** 26: 716-720.

Navarro, M., Ginebra, M. P., Planell, J. A., Barrias, C. C., and Barbosa, M. A. (2005). In vitro degradation behavior of a novel bioresorbable composite material based on PLA and a soluble CaP glass. **Acta Biomater.** 1: 411-419.

Wanga, Y. W., Yang, F., Wu, Q., Cheng, Y., Yu, P. H .F., Chen, J., and Chen, G. (2005). Effect of composition of poly(3-hydroxybutyrate-co-3- hydroxyhexanoate) on growth of fibroblast and osteoblast. **Biomaterials.** 26: 755-761.

Wan, Y., Chen, W., Yang, J., Bei, J., and Wang, S. (2003). Biodegradable poly(l-lactide)-poly(ethylene glycol) multiblock copolymer:synthesis and evaluation of cell affinity. **Biomaterials.** 24: 2195–2203.

Ruksudjarit, A., Pengpat, K., Rujijanagul, G., and Tunkasiri, T. (2008). Synthesis and characterization of nanocrystalline hydroxyapatite from natural bovine bone. **Curr. Appl. Phys.** 8: 270-272.

Russias, J., Saiz, E., Nalla, R. K., Gryn, K., Ritchie, R. O., and Tomsia, A. P. (2006). Fabrication and mechanical properties of HA/PLA composites: A study of in vitro degradation. **Mater. Sci. Eng.: C.** 26: 1289-1295.

Shikinami, Y. and Okuno, M. (2001). Bioresorbable devices made of forged composites of hydroxyapatite (HA) powders and poly L–lactide (PLLA). Part II: practical properties of miniscrews and miniplate. **Biomaterials.** 22: 3197-3211.

Sivakumar, M., Kumart, T. S. S., Shantha, K. L., and Rao, K. P. (1996). Development of hydroxyapatite derived fkom Indian coral. **Biomateriols.** 17: 1709-1714.

Stamboulis, A., Hench, L. L., and Boccaccini, A. R. (2002). Mechanical properties of biodegradable polymer sutures coated with bioactive glass. **J. Mater. Sci. Mater. Med.** 13: 843-8.

Stefani, M., Coudane, J., and Vert, M. (2006). In vitro ageing and degradation of PEG/PLA diblock copolymer-based nanoparticles. **Polym. Degrad. Stab.** 91: 2554-2559.

Tsuji, H. and Ikarashi, K. (2004). In vitro hydrolysis of poly(L-lactide) crystalline residues as extended-chain crystallites. Part I: long-term hydrolysis in phosphate-buffered solution at 37ºC. **Biomaterials.** 25: 5449-5455.

Yang, Y., Zhao, Y., Tang, G., Li, H., Yuan, X., and Fan, Y. (2008). In vitro degradation of porous poly(L-lactide-co-glycolide)/β-tricalcium phosphate (PLGA/β-TCP) scaffolds under dynamic and static conditions. **Polym. Degrad. Stab.** 93: 1838-1845.

Yoganand, C. P., Selvarajan, V., Wu, J., and Xue, D. (2009). Processing of bovine hydroxyapatite (HA) powders and synthesis of calcium phosphate silicate glass ceramics using DC thermal plasma torch. **Vacuum.** 83: 319-325.

Yuan, X., Mak, A. F. T., and Yao, K. (2002). Comparative observation of accelerated degradation of poly(l-lactic acid) fibres in phosphate buffered saline and a dilute alkaline solution. **Polym. Degrad. Stab.** 75: 45-53.

Wang, M. and Bonfield, W. (2001). Chemically coupled hydroxyapatite-polyethylene composites:structure and properties. **Biomaterials.** 22: 1311-1320.

CHAPTER VI

CONCLUSIONS

Preparation of biomedical materials from bovine bone is an alternative approach to obtain a suitable bone replacement material with an inexpensive expense. In this study, HA powder was prepared from natural source, *i.e.* bovine bone, and used as a filler for preparing PLA composites. Processing technique and u-HA content were the factors that influenced mechanical properties of u-HA/PLA composites. To form HA/PLA composites, u-HA was incorporated into PLA matrix by either melt-mixing or solution mixing techniques. With increasing u-HA content, tensile strength and impact strength of the composites were decreased while the tensile moduli of the composites were increased. In comparison between two preparation techniques, the composites prepared by melt-mixing technique have higher tensile strength, tensile modulus and impact strength than those prepared by solution-mixing technique. However, the PLA chains in the composites prepared by melt-mixing technique degraded much more than those in the composites prepared by solution-mixing technique as confirmed by GPC results. According to mechanical properties, the melt-mixed process was selected to prepare HA/PLA composite.

To decrease the degradation of PLA chains and increase the adhesion between HA and PLA matrix, the silane coupling agents, *i.e.* APES and MPTS, were selected to modify HA surface. Tensile strength, tensile modulus, elongation at break and impact strength of the PLA composites can also be improved by modifying u-HA surface with either APES or MPTS. The enhancement of mechanical properties of

silane-treated HA/PLA composites was caused by the good dispersion of silane-treated HA in PLA matrix and the good interfacial interaction between the two phases. However, the mechanical properties of silane-treated HA/PLA composites still need to be further enhanced or adjusted in order to meet requirement for a specific medical application. The TGA results of HA/PLA composites revealed that thermal properties of HA/PLA composite were crucially dependent on surface properties of HA particle. Silane-treated HA/PLA composites showed an increasing in thermal stability as compared with the untreated HA/PLA composites. Moreover, the deposit of silane coupling on HA surface in silane-treated HA/PLA composites delayed the PLA chains scission, which were confirmed by GPC results.

Additionally, the *in vitro* degradation behaviors of all HA/PLA composites were investigated. Results showed that the untreated HA/PLA composites exhibited more change in pHof PBS, mass, thickness, width, and morphologies than the silane-treated HA/PLA composites. Moreover, the molecular weights of PLA in the untreated HA/PLA composites decreased faster than those of silane-treated HA/PLA composites after immersion in PBS. The porosity and gap in the composite matrix created by lacking of adhesion between u-HA and PLA matrix led to rapid diffuse of water through the matrix. These was the main reason of the faster degradation of PLA in u-HA/PLA composites. In contrast, silane-treated HA/PLA composite had more adhesion between two phases leading to the less penetration of water into inner side, therefore, lower degradation of PLA was obtained. Additionally, the bioactive characterization showed the positive result in the formation of calcium phosphate compound on the composite surface, after immersion in SBF, which could enhance the interaction between the material and the bone tissue. In addition, the results from

in vitro cytotoxicity test suggested a potential of using bovine bone based HA/PLA composite as a biomaterial.

REFERENCES

Agrawal, C. M., Athanasiou, K. A., and Heckman, J. D. (1997). Biodegradable PLA-PGA polymers for tissue engineering in orthopadics. **Mater. Sci. Forum.** 250: 115-129.

Arami, H., Mahajerani, M., Mazloumi, M., Khalifehzadeh, R., Lak, A., and Sadrnezhaad, S. K. (2009). Rapid formation of hydroxyapatite nanostrips via microwave irradiation. **J. Alloy. Compd.** 469: 391-394.

Benmarouane, A., Hansena, T., and Lodini, A. (2004). Heat treatment of bovine bone preceding spatially resolved texture investigation by neutron diffraction. **Physica B**. 350: 611-614.

Bleach, N. C., Nazhat, S. N., Tanner, K. E., Kellomaki, M., and Tormala, P. (2002). Effect of filler content on mechanical and dynamic mechanical properties of particulate biphasic calcium phosphate-polylactide composites. **Biomaterials.** 23: 1579-1585.

Boccaccini, A. R. and Maquet, V. (2003). Bioresorbable and bioactive polymer/ Biogalss® composites with tailored pore structure for tissue engineering applications. **Compos. Sci. Technol.** 63: 2417-29.

Cam, D., Hyon, S. H., and Ikada, Y. (1995). Degradation of high molecular weight poly(L-lactide) in alkaline medium. **Biomoterials.** 16: 833-843.

Chandrasekhar, R. K., Montgomery, T. S., and Wei, M. (2005). Biodegradable HA-PLA 3-D porous scaffolds: Effect of nano-sized filler content on scaffold properties. **Acta Biomater.** 1: 653-662.

Coutand, M., Cyr, M., Deydier, E., Guilet, R., and Clastres, P. (2008). Characteristics of industrial and laboratory meat and bone meal ashes and their potential applications. **J. Hazard. Mater.** 150: 522-532.

Daglilar, S. and Erkan, M. E. (2007). A study on bioceramic reinforced bone cements. **Mater. Lett.** 61: 1456-1459.

Daglilar, S., Erkan, M. E., Gunduz, O., Ozyegin, L. S., Salman, S., Agathopoulos, S., and Oktar, F. N. (2007). Water resistance of bone-cements reinforced with bioceramics. **Mater. Lett.** 61: 2295-2298.

Deng, X., Hao, J., and Wang, C. (2001). Preparation and mechanical properties of nanocomposites of poly(D,L-lactide) with Ca-deficient hydroxyapatite nanocrystals. **Biomaterials.** 22: 2867-2873.

Dueka, E. A. R., Zavaglia, C. A. C., and Belangero, W. D. (1999). *In vitro* study of poly(lactic acid) pin degradation. **Polymer.** 40: 6465-6473.

Dupraz, A. M. P., Wijn, J. R., Meer, S. A. T., and Groot, K. (1996). Characterization of silane-treated hydroxyapatite powders for use as filler in biodegradable composites. **J. Biomed. Mater. Res.** 30: 231-238.

Dupraz, A. M. P., Wijn, J. R., Meer, S. A. T., and Groot, K. (1996). Characterization of silane-treated hydroxyapatite powders for use as filler in biodegradable composites. **J. Biomed. Mater. Res.** 30: 231-238.

Edwin P. P. **Silane coupling agents.** 2nd ed. New York: Plenum Press; 1991. p. 144-149.

Fathi, M. H., Hanifi, A., and Mortazavi, V. (2008). Preparation and bioactivity evaluation of bone-like hydroxyapatite nanopowder. **J. Mater. Proc. Technol..** 202: 536-542.

Fukushima, K., Tabuani, D., and Camino, G. (2009). Nanocomposites of PLA and PCL based on montmorillonite and sepiolite. **Mater. Sci. Eng. : C.** 29: 1433-1441.

Furukawa, T., Matsusue, Y., Yasunaga, T., Shikinami, Y., Okuno, M., and Nakamura, T. (2000). Biodegradation behavior of ultra-high-strength hydroxyapatite/ poly(L-lactide) composite rods for internal fixation of bone fractures. **Biomaterials.** 21: 889-898.

Furuzono, T., Sonoda, K., and Tanaka, J. (2001). A hydroxyapatite coating covalently linked onto a silicone implant material. **J. Biomed. Mater. Res.** 56: 9-16.

Gay, S., Arostegui, S., and Lemaitre, J. (2009). Preparation and characterization of dense nanohydroxyapatite/PLLA composites. **Mater. Sci. Eng. C.** 29: 172-177.

Gopferich, A. (1996). Mechanisms of polymer degradation and erosion. **Biomaterials.** 17: 103-140.

Gupta, M. and Deshmukh, V. (1982). Thermal oxidative degradation of polylactide acid. Part II: Molecular weight and electronic spectra during isothermal heating. **Colloid. Polym. Sci.** 260: 517-527.

Hasegawa, S., Ishii, S., Tamura, J., Furukawa, T., Neo, M., Matsusue, Y., Shikinami, Y., Okuno, M., and Nakamura, T. (2006). A 5-7 year *in vivo* study of high-strength hydroxyapatite/poly(L-lactide) composite rods for the internal fixation of bone fractures. **Biomaterials.** 27: 1327-1332.

Haberko, K., Bucko, M. M., Miecznik, J. B., Haberko, M., Mozgawa, W., Panz, T., Pyda, A., and Zarebski, J. (2006). Natural hydroxyapatite-its behaviour during heat treatment. **J. Euro. Ceram. Soc.** 26: 537-542.

Hiljanen-Vainio, M., Heino, M., and Seppala, J. V. (1998). Reinforcement of biodegradable poly(ester-urethane) with fillers. **Polymer.** 39: 865-872.

Horst, A. R., Robert, L. C., Suzanne, G. E., and Antonios, G. M. (1995). Degradation of polydispersed poly(L-lactic acid) to modulate lactic acid release **Biomaterials.** 16: 441-447.

Ignjatovic, N., Suljovrujic, E., Simendic, J. B., Krakovsky, I., and Uskokovic, D. (2001). A study of HAp/PLLA composite as a substitute for bone powder using FT-IR spectroscopy. **Biomaterials.** 22: 271-275.

Ignjatovic, N., Suljovrujic, E., Simendic, J., Krakovsky, I., and Uskokovic, D. (2004). Evaluation of hot-pressed hydroxyapatite/poly-L-lactide composite biomaterial characteristics. **J. Biomed. Mater. Res.** 71B: 284-294.

Ignjatovic, N., Tomic, S., Dakic, M., Miljkovic, M., Plavsic, M., and Uskokovic, D. (1999). Synthesis and properties of hydroxyapatite/poly-L-lactide composite biomaterials. **Biomaterials.** 20: 809-16.

Ignjatovic, N. and Uskokovic, D. (2004). Synthesis and application of hydroxyapatite/polylactide composite biomaterial. **App. Surf. Sci.** 238: 314-319.

Jamshidi, K., Hyon, S. H., and Ikada, Y. (1988). Thermal characterization of polylactides. **Polymer.** 29: 2229-2234.

Kang, Y., Xu, X., Yin, G., Chen, A., Liao, L., Yao, Y., Huang, Z., and Liao, X. (2007). A comparative study of the *in vitro* degradation of poly(L-lactic acid)/β-tricalcium phosphate scaffold in static and dynamic simulated body fluid. **Eur. Polym. J.** l43: 1768-1778.

Kasuga, T., Ota, Y., Nogami, M., and Abe, Y. (2001). Preparation and mechanical properties of polylactic acid composites containing hydroxyapatite fibers. **Biomaterials.** 22: 19-23.

Kothapalli, C. R., Shaw, M. T., and Wei, M. (2005). Biodegradable HA-PLA 3-D porous scaffolds: Effect of nano-sized filler content on scaffold properties. **Acta Biomater.** 1: 653-662.

Li, H. and Chang, J. (2004). Fabrication and characterization of bioactive wollastonite/PHBV composite scaffolds. **Biomaterials.** 25: 5473-80.

Li, S., Garreau, H., and Vert, M. (1990). Structure-property relationships in the case of the degradation of massive poly(a-hydroxy acids) in aqueous media. Part 3 Influence of the morphology of poly(L-lactic acid). **J. Mater. Sci. Mater. Med.** 1: 198-206.

Li, X., Feng, Q., and Cui, F. (2006). *In vitro* degradation of porous nano hydroxyapatite/collagen/PLLA scaffold reinforced by chitin fibres. **Mater. Sci. Eng. C.** 26: 716-720.

Lin, P. L., Fang, H. W., Tseng, T., and Lee, W. H. (2007). Effects of hydroxyapatite dosage on mechanical and biological behaviors of polylactic acid composite materials. **Mater. Lett.** 61: 3009-3013.

Liu, Q., Wijn, J. R., Groot, K., and Blitterswijk, C. A. (1998). Surface modification of nano-apatite by grafting organic polymer. **Biomaterials.** 19: 1067-1072.

Lorprayoon, C. (1989). Synthesis of calcium hydroxyapatite and tricalcium phosphate from bone ash. **Ion. Polym. Order. Polym. Hi. Perf. Mater. Biomater.** 329-336.

Mathieu, L. M., Bourban, P. E., and Manson, J. A. E. (2006). Processing of homogeneous ceramic/polymer blends for bioresorbable composites. **Comp. Sci. Technol.** 66: 1606-1614.

Navarro, M., Ginebra, M. P., Planell, J. A., Barrias, C. C., and Barbosa, M. A. (2005). *In vitro* degradation behavior of a novel bioresorbable composite material based on PLA and a soluble CaP glass. **Acta Biomater.** 1: 411-419.

Nejati, E., Firouzdor, V., Eslaminejad, M. B., and Bagheri, F. (2009). Needle-like nano hydroxyapatite/poly(L-lactide acid) composite scaffold for bone tissue engineering application. **Mater. Sci. Eng. C.** 29: 942-949.

Ooi, C. Y., Hamdi, M., and Ramesh, S. (2007). Properties of hydroxyapatite produced by annealing of bovine bone. **Ceram. Int.** 33: 1171-1177.

Perego, G., Cella, G. D., and Bastioli, C. (1996). Effect of molecular weight and crystallinity on poly(lactic acid) mechanical properties. **J. Appl. Polym. Sci.** 59: 37-43.

Ruksudjarit, A., Pengpat, K., Rujijanagul, G., and Tunkasiri, T. (2008). Synthesis and characterrization of nanocrystalline hydroxyapatite from natural bovine bone. **Curr. Appl. Phys.** 8: 270-272.

Russias, J., Saiz, E., Nalla, R. K., Gryn, K., Ritchie, R. O., and Tomsia, A. P. (2006). Fabrication an mechanical properties of HA/PLA composites:A study of *in vitro* degradation. **Mater. Sci. Eng.** 26: 1289-1295.

Ruksudjarit, A., Pengpat, K., Rujijanagul, G., and Tunkasiri, T. (2008). Synthesis and characterization of nanocrystalline hydroxyapatite from natural bovine bone, **Curr. Appl. Phys.** 8: 270-272.

Russias, J., Saiz, E., Nalla, R. K., Gryn, K., Ritchie, R. O., and Tomsia, A. P. (2006) Fabrication and mechanical properties of HA/PLA composites: A study of *in vitro* degradation. **Mater. Sci. Eng. : C.** 26: 1289-1295.

Shikinami, Y. and Okuno, M. (2001). Bioresorbable devices made of forged composites of hydroxyapatite (HA) particles and poly-L-lactide (PLLA): Part I. Basic characteristics. **Biomaterials.** 20: 859-877.

Shikinami, Y. and Okuno, M. (2001). Bioresorbable devices made of forged composites of hydroxyapatite (HA) powders and poly L–lactide (PLLA). Part II: practical properties of miniscrews and miniplate. **Biomaterials.** 22: 3197-3211.

Shinzato, S., Nakamura, T., Kokubo, T., and Kitamura, Y. (2001). Bioactive bone cement: Effect of silane treatment on mechanical properties and osteoconductivity. **J. Biomed. Mater. Res.** 55:, 277-284.

Signori, F., Coltelli, M. B., and Bronco, S. (2009). Thermal degradation of poly(lactic acid) (PLA) and poly(butylenesadipate-co-terephthalate) (PBAT) and their blends upon melt processing. **Polym. Degrad. Stab.** 9: 74-82.

Sivakumar, M., Kumart, T. S. S., Shantha, K. L., and Rao, K. P. (1996). Development of hydroxyapatite derived fkom Indian coral. **Biomateriols** 17: 1709-1714.

Stamboulis, A., Hench, L. L., and Boccaccini, A. R. (2002). Mechanical properties of biodegradable polymer sutures coated with bioactive glass. **J. Mater. Sci. Mater. Med.** 13: 843-8.

Stefani, M., Coudane, J., and Vert, M. (2006). In vitro ageing and degradation of PEG/PLA diblock copolymer-based nanoparticles. **Polym. Degrad. Stab.** 91: 2554-2559.

Suganuma, J. and Alexander, H. (1993). Biological response of intramedullary bone to poly-L-lactic acid. **J. Appl. Biomater.** 15: 13-27.

Tadakasu, M. and Toru, M., (1998). Crystallization behavior of poly(L-lactide). **Polymer.** 39: 5515-5521.

Takayama, T., Todo, M., and Takano, A. (2008). The effect of bimodal distribution on the mechanical properties of hydroxyapatite particle filled poly(L-lactide) composites. **J. Mech. Behav. Biomed. Mater.** 2: 105-112.

Todo, M., Park, S. D., Arakawa, K., and Takenoshita, Y. (2006). Relationship between microstructure and fracture behavior of bioabsorbable HA/PLLA composites. **Compostes: Part A.** 37: 2221-2225.

Tsuji, H. and Ikarashi, K. (2004). *In vitro* hydrolysis of poly(-lactide) crystalline residues as extended-chain crystallites. Part I: long-term hydrolysis in phosphate-buffered solution at 37°C. **Biomaterials.** 25: 5449-5455.

Verheyen, C. C. P. M., Klein, C. P. A. T., Blieckhogervorst, J. M. A., Wolke, J. G. C., Blitterswijn, C. A., and Groot, K. (1993). Evaluation of hydroxylapatite/ poly (L-lactide)composites: physico-chemical properties. **J. Mater. Sci. Mater. Med.** 4: 58-65.

Wachsen, O., Platkowski, K., and Reichert, K. H. (1997). Thermal degradation of poly-L-lactide -studies on kinetics, modelling and melt stabilisation. **Polym. Degrad. Stability.** 57: 87-94.

Wan, Y., Chen, W., Yang, J., Bei, J., and Wang, S. (2003). Biodegradable poly(l-lactide)-poly(ethylene glycol) multiblock copolymer:synthesis and evaluation of cell affinity. **Biomaterials.** 24: 2195-2203.

Wang, M., Joseph, R., and Bonfield, W. (1998). Hydroxyapatite-polyethylene composites for bone substitution: effects of ceramic particle size and morphology. **Biomaterials.** 19: 2357-66.

Wang, M., Deb, S., and Bonfield, W. (2000). Chemically coupled hydroxyapatite-polyethylene composites: processing and characterization. **Mater. Lett.** 44: 119-124.

Wang, M. and Bonfield, W. (2001). Chemically coupled hydroxyapatite-polyethylene composites:structure and properties. **Biomaterials.** 22: 1311-1320.

Wanga, Y. W., Yang, F., Wu, Q., Cheng, Y., Yu, P. H .F., Chen, J., and Chen, G. (2005). Effect of composition of poly(3-hydroxybutyrate-co-3- hydroxyhe-xanoate) on growth of fibroblast and osteoblast. **Biomaterials.** 26: 755-761.

Wen, J., Li, Y., Zuo, Y., Zhou, G., Li, J., Jiang, L., and Xu, W. (2008). Preparation and characterization of nano-hydroxyapatite/silicone rubber composite **Mater. Lett.** 62: 3307-3309.

Yang, Y., Zhao, Y., Tang, G., Li, H., Yuan, X., and Fan, Y. (2008). In vitro degradation of porous poly(L-lactide-co-glycolide)/β-tricalcium phosphate (PLGA/β-TCP) scaffolds under dynamic and static conditions. **Polym. Degrad. Stab.** 93: 1838-1845.

Yoganand, C. P., Selvarajan, V., Wu, J., and Xue, D. (2009). Processing of bovine hydroxyapatite (HA) powders and synthesis of calcium phosphate silicate glass ceramics using DC thermal plasma torch. **Vacuum.** 83: 319-325.

Yuan, X., Mak, A. F. T., and Yao, K. (2002). Comparative observation of accelerated degradation of poly(l-lactic acid) fibres in phosphate buffered saline and a dilute alkaline solution. **Polym. Degrad. Stab.** 75: 45-53.

Zhang, S. M., Liu, J., Zhou, W., Cheng, L., and Guo, X. D. (2005). Interfacial fabrication and property of hydroxyapatite/polylactide resorbable bone fixation composites. **Curr. Appl. Phys.** 5: 516-518.

Zheng, X., Zhou, S., Li, X., and Weng, J. (2008). Shape memory properties of poly(D,L-lactide)/hydroxyapatite composites. **Biomaterials.** 27: 4288-4295.

Zhongkui, H., Peibiao, Z., Chaoliang, H., Xueyu, Q., Aixue, L., Li, C., Xuesi, C., and Xiabin, J. (2005). Nano-composite of poly(L-lactide) and surface grafted hydroxyapatite: Mechanical properties and biocompatibility. **Biomaterials.** 26: 6296-6304.

APPENDIX A

PUBLICATION

CHARACTERIZATION OF SILANE-TREATED NATURAL HYDROXYAPATITE/POLY (LACTIC ACID) NANOCOMPOSITES

Suriyan Rakmae[1,2], Yupaporn Ruksakulpiwat[1,2], Wimonlak Sutapan[1,2] and Nitinat Suppakarn[1,2*]

[1] Suranaree University of Technology /Institute of Engineering /School of Polymer Engineering, Nakhon Ratchasima, 30000 Thailand

[2] Center of Excellence for Petroleum, Petrochemical, and Advanced materials /Chulalongkorn University, Bangkok, 10330 Thailand

*E-mail:nitinat@sut.ac.th, Tel: +66-44-224439

Abstract: In this work, bovine bone based HA was prepared by thermal treatment and then incorporated into PLA matrix. The 3-aminopropyltriethoxysilane (APES) and 3-methacryloxypropyltrimethoxysilane (MPTS) were used to modify HA surface in order to improve the compatibility between HA and PLA matrix. FTIR spectrum of untreated HA revealed that the obtained HA was a highly crystalline carbonated hydroxyapatite. SEM micrograph showed that the obtained HA after calcination at 1100°C was composed of agglomerated hydroxyapatite particles. The agglomeration of particles was reduced by treating HA surface with silane coupling agent. Tensile modulus of all HA/PLA composites increased with increasing HA content. This was in contrast to the tensile and impact strength of the composites which decreased with increasing HA content. In addition, mechanical properties of HA/PLA composites can be improved by treating HA surface with a silane coupling agent.

Introduction

Hydroxyapatite (HA) has been investigated as a biomaterial and used in various medical applications, *e.g.* spacers and bone graft substitutes in orthopaedic and maxillofacial applications. This is because of its excellent biocompatibility and its osteoconductivity [1, 2]. HA can be synthetically prepared or derived from natural sources, *e.g.* coral, bovine bone. However, the major drawbacks of using HA as a biomaterial are its brittleness and the difficulty of processing. One attempt to solve these problems is mixing HA with a flexible and bioresobable polymer.

Many kinds of bioresorbable polymers have been developed and used in medical applications. Among those polymers, poly (lactic acid) (PLA) is a good candidate due to its biodegradability and nontoxic byproducts yielded after degradation [3]. A composite between PLA and HA is a good alternative for using as a biomaterial since it is combining strength and stiffness of HA with flexibility and resorbability of PLA. However, the major drawbacks found in HA/PLA composites are the agglomeration of HA and the failure at the interface between HA and the polymeric matrix. These lead to the decreasing in mechanical properties of HA/PLA composites. Therefore, an improvement of the interfacial adhesion between particles and matrix has become an important

area of studies of HA/PLA composites [4, 5]. The HA surface can be treated with a coupling agent, such as organofunctional silanes, by which the interfacial adhesion between filler and polymer matrix is effectively improved [6].

In recent years, natural HA has been attracting much attention since it is natural and less expensive sources for producing HA [7, 8]. In addition, there are high volumes of bovine bone as a livestock waste in Thailand. So, this work attempted to produce natural HA powders from bovine bones and to use the powder as a filler for PLA. The bovine bone based HA was treated with silane coupling agents, *i.e.* 3-aminopropyl triethoxysilane and 3-methacryloxypropyltrimethoxy silane. The properties of untreated HA and silane-treated HA were characterized. In addition, effects of filler characteristics and filler content on morphological and mechanical properties of HA/PLA composites were determined.

Materials and Methods

Materials: PLA (4042D) was purchased from NatureWorks, LLC. Bovine bones were supplied by Limeiseng Co., Nakhon Ratchasima. 3-aminopropyl triethoxysilane (APES) and 3-methacryloxypropyl trimethoxysilane (MPTS) were purchased from Optimal Tech Co., Ltd. and Aldrich, respectively.

Preparation of HA powders: Bovine bones were burned in open air and were then ground into powders, using a ball milling machine. Then the HA powders were heat treated at 1100°C for 3 h, call HA. After that, the powders were modified by either APES or MPTS. The content of silane used was 2.0 wt% based on weight of HA powders. To prepare silane solution, the APES was dissolved in an aqueous solution whereas MPTS was dissolved in 30 vol% of alcoholic solution. The pH of each silane solution was adjusted to 3.5 using acetic acid. HA powders were soaked in each silane solutions and left under agitation at room temperature for 3 h. Then the silane-treated powders were washed and dried at 80°C overnight in an oven.

Preparation of HA/PLA composites: HA/PLA composites were prepared through melt-compounding technique using an internal mixer (HAAKE/Rheomix). PLA and HA were mixed at 170°C with 70 rpm for 10

min. The weight ratios of HA/PLA were 9/1, 8/2, 7/3, and 6/4. Each HA/PLA composite was left at room temperature for 24 h. then it was ground into small pieces. To prepare composite specimens for mechanical tests, the ground HA/PLA composite was heated in dumbbell-shaped and rectangular-shaped molds from room temperature to 180°C and maintained at that temperature for 10 min. Subsequently, it was hot-pressed vertically for 5 min at 180°C under a pressure of 2000 psi and cooled to room temperature.

Characterization of HA powders: Functional groups of the untreated and silane-treated HA powders were identified by a Fourier transform infrared spectrometer (FTIR) (BIO-RAD/FTS175C, KBr pellet technique). The spectrum was recorded in the 400-4000 cm^{-1} region with 2 cm^{-1} resolution. The thermal behaviors of silane-treated and untreated HA powders were determined by thermogravimetric analyzer (TGA) (TA Instrument/SDT2960). The powders were heated from room temperature to 600°C at a rate of 20 °C/min under a nitrogen atmosphere. In addition, a scanning electron microscopy (SEM) (Jeol/JSM-6400) operating at 15-20 kV was used to reveal microstructure of the HA powders.

Characterization of HA/PLA composites: A scanning electron microscopy (SEM) (Jeol/JSM-6400) operating at 20 kV was used to visualize tensile fracture surfaces of the HA/PLA composites. All samples were coated with a thin layer of gold before examining. Tensile properties of HA/PLA composites were investigated according to ASTM method D638-03 using a universal testing machine (Instron/5569). Moreover, Izod impact strength of unnotched HA/PLA specimens were determined according to ASTM D256 using an impact testing machine (Atlas/BPI).

Results and Discussion

Characterization of HA powders: The FTIR spectrum of bovine bone based HA is shown in Figure 1. The peaks at 3420 and 1630 cm^{-1} were attributed to the vibration bending mode of adsorbed water. Two absorption bands at 602 and 571 cm^{-1} were ascribed to the bending modes of PO_4^{3-}. The peaks at 1092 and 1053 cm^{-1} were assigned to the stretching vibration of PO_4^{3-}. The stretching vibration band of OH^- and the OH^- bending vibration were observed at 3570 cm^{-1} and 632 cm^{-1}, respectively [8-9]. The peaks appeared at 1412 and 1459 cm^{-1} were related to CO_3^{2-} groups. The appearance of carbonate functional group on FTIR spectrum of the obtained powders could be explained as follows: 1) carbon was adsorbed from atmosphere during heating process and substituted the PO_4^{3-} groups of the HA or 2) the carbon from the organics did not pyrolyze completely and may instead dissolve into the hydroxyapatite crystal. As a result, the FTIR spectrum revealed that the powders obtained from bovine bone were carbonated hydroxyapatite with highly crystalline structure.

Figure 2 shows FTIR spectra of the silane-treated HA powders. The additional peaks compared to the FTIR spectrum of untreated HA were observed around

2850-2950 cm^{-1}. The peaks were attributed to C–H stretching of carbon chains of APES and MPTS on HA surfaces [10]. Additionally, MPTS-treated HA showed the peak of C=O stretching vibration of MPTS molecules at 1712 cm^{-1}.
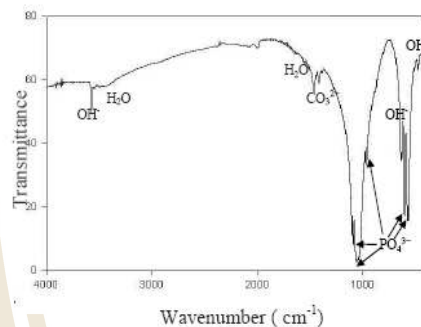

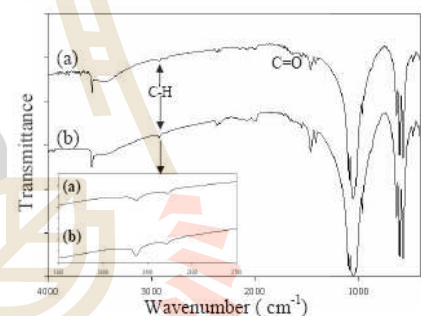Figure 1. FTIR spectrum of bovine bone based HA (sintered at 1100 °C).

Figure 2. FTIR spectra of silane-treated HA : MPTS treated HA(a), APES treated HA(b).

SEM micrographs of untreated HA and silane-treated HA are shown in Figure 3 (a-d). The micrographs in Figure 3 (a) shows the agglomeration of HA powders. The micrograph at higher magnification revealed that the untreated HA powders were composed of particles with irregular shape as shown in Figure 3 (b). On the other hand, the micrographs of silane-treated HA in Figure 3 (c) and (d) show the smaller size of agglomerated HA powders compared to those of untreated HA. The results indicated that silane treatment tended to reduce particle agglomeration. To prepare HA/PLA composites, the less HA powder agglomeration would lead to better processability and enhance mechanical properties of the composites.

The thermal behaviors of silane-treated and untreated HA were determined by TGA. As shown in Figure 4, the untreated HA displayed higher weight loss than silane-treated HA. This implied that treating HA surface with a silane coupling agent slightly increased thermal stability of HA.
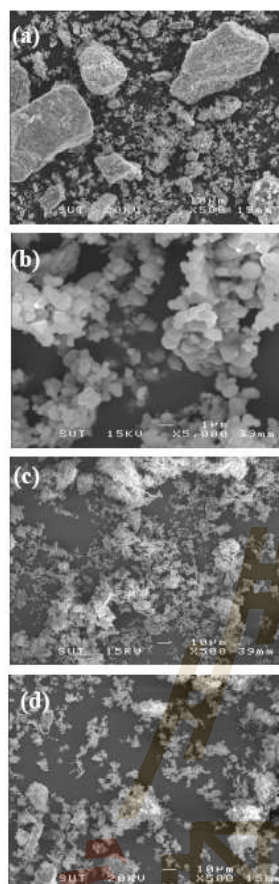
Figure 3. SEM micrographs of HA powders: untreated HA at low magnification (X 500) (a), untreated HA at high magnification (X 5000) (b), APES treated HA (X 500) (c) and MPTS treated HA (X 500) (d)
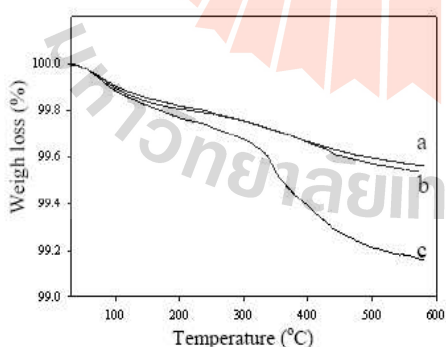

Figure 4. TGA curves of HA powders: MPTS treated HA (a), APES treated HA (b) and untreated HA (c)

Characterization of HA/PLA composites: Tensile strength, tensile modulus and impact strength of

HA/PLA composites at various HA contents are illustrated in Figure 5 (a-c). Tensile strength and impact strength of the composites were decreased with increasing HA content. In contrast, tensile modulus of the composites was increased with increasing HA content. The increase of the tensile modulus implied that HA is a reinforcing filler for PLA matrix.
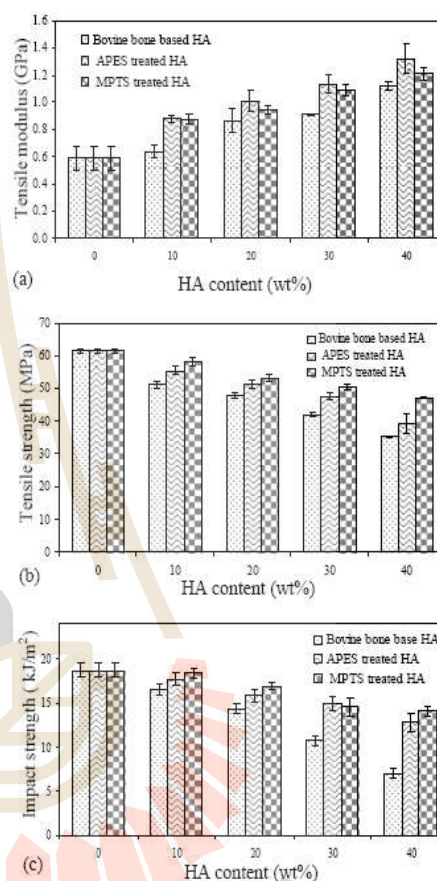

Figure 5. Tensile modulus (a), Tensile strength (b) and Impact strength (c) of HA/PLA composites at various HA contents

In comparison, the composites containing silane-treated HA had higher tensile strength, tensile modulus and impact strength than those containing untreated HA. This was probably attributed to good adhesion between two phases and good dispersion of silane-treated HA powders in PLA matrix. In addition, the composites containing MPTS treated HA exhibited the highest tensile strength and impact strength while those containing APES treated HA showed the highest tensile modulus.

The SEM micrographs of tensile fracture surfaces of the HA/PLA composites containing 20 wt% of HA are presented in Figure 6 (a-c). The agglomeration of HA powders were observed in HA/PLA composite

with untreated HA powders, as shown in Figure 6(a). In addition, a gap at the interface between untreated HA and PLA matrix was observed. From figure 6 (b-c), on the other hand, the microstructure of PLA composite containing silane-treated HA illustrated more homogenous distribution of HA powders in the PLA matrix. However, some HA agglomeration was still observed. This result was consistent with the morphology of silane-treated HA as shown in Figure 3 (c-d). Moreover, the micrograph shown in Figure 6 (b-c) elucidated that the gap between silane-treated HA and PLA interface became smaller than that between untreated HA and PLA interface. This implied that treating HA surface with a silane coupling agent can improve interfacial adhesion between PLA and HA.
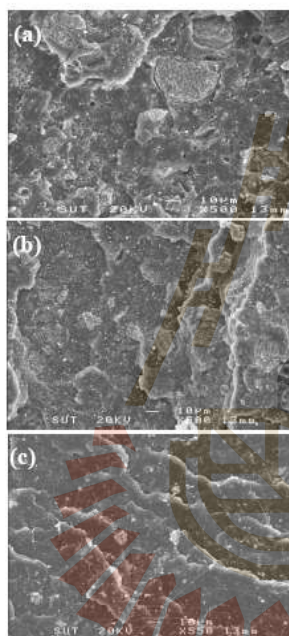

Figure 6. SEM micrographs of tensile fracture surfaces of HA/PLA composites at 20 wt% content of HA: untreated HA (a), APES-treated HA (b) and MPTS-treated HA (c)

Conclusions

In this study, HA powders were prepared from natural source, *i.e.* bovine bone. The results from FTIR revealed that the obtained HA was a highly crystalline carbonate hydroxyapatite. HA surface treatment and HA content were the key factors that influenced mechanical properties of HA/PLA composites. SEM micrographs revealed the good distribution of silane-treated HA in PLA matrix and good adhesion between the HA powders and the polymer matrix. Tensile strength and impact strength of the composites were decreased with increasing HA content while the tensile modulus of the composites was increased with increasing HA content. In comparison, the composites containing silane-treated HA had higher tensile strength, tensile modulus and impact strength than those containing the untreated HA composites. In addition, the composites containing MPTS treated HA exhibited the highest tensile strength and impact strength while those containing APES treated HA showed the highest tensile modulus.

Acknowledgements

References

[1] S. Hasegawa, S. Ishii, J. Tamura, T. Furukawa, M. Neo, Y. Matsusue, Y. Shikinami, M. Okuno and T. Nakamura, *Biomaterials*. **27** (2006), pp.1327-1332.
[2] Y. Shikinami, Y. Matsusue and T. Nakamur, *Biomaterials*. **26** (2005), pp. 5542-5551.
[3] H. Tsuji and K. Ikarashi, *Biomaterials*, **25** (2004), pp. 5449-5455.
[4] N. Ignjatovic, E. Suljovrujic, J.B. Simendic, I. Krakovsky and D. Uskokovic, *Biomaterials*. **22** (2001), pp. 271-275.
[5] C.R. Kothapalli, M.T. Shaw, and M. Wei, *Acta Biomater*. **1** (2005), pp. 653-662.
[6] H. Arami, M. Mahajerani, M. Mazloumi, R. Khalifehzadeh, A. Lak and S.K. Sadrnezhaad, *J. Alloy Compd*. **469** (2009), pp.391-394.
[7] A. Ruksudjarit, K. Pengpat, G. Rujijanagul and T. Tunkasiri, *Curr. Appl. Phys*. **8** (2008), pp. 270-272.
[8] C.Y. Ooi, M. Hamdi and S. Ramesh, *Ceram. Int*. **33** (2007), pp. 1171-1177.
[9] M.H. Fathi, A. Hafini and V. Mortazavi, *J. Mater. Process. Technol*. **202** (2008), pp. 536-542.
[10] T. Furuzono, K. Sonoda and Junzo Tanaka1, *J. Biomed. Mater. Res*. **56** (2001), pp. 9-16.

BIOGRAPHY

Mr. Suriyan Rakmae was born on January 23, 1981 in Chiangrai Province, Thailand. He graduated from Maejo University in 2004 with the Bachelor of Science in Chemistry (2nd class honors). During his undergraduate study, he has taken a position of leader of chemistry club, Maejo University. After graduation, he has been employed as a pharmaceutical chemist at Better Pharma Co., Ltd., Betagro group, for 3 years. He then pursued his Master's degree in Polymer Engineering at school of Polymer Engineering, Institute of Engineering, Suranaree University of technology. During his master's degree study, he presented one paper entitled of **"Characterization of Silane-treated Natural Hydroxyapatite/Poly(lactic acid) nanocomposites"** in Pure and Applied Chemistry International Conference 2009 (PACCON2009) in Phitsanulok, Thailand.